Mental retardation-related protease neurotrypsin in spinogenesis, synaptic plasticity, and learning

Dissertation

zur Erlangung des akademischen Grades

doctor rerum naturalium (Dr. rer. nat.)

genehmigt durch die Fakultät für Naturwissenschaften
der Otto-von-Guericke-Universität Magdeburg

von M.Sc. Maura Ferrer Ferrer

geb. am 3.4.1989 in Girona, Spanien

Gutachter: Prof. Dr. Alexander Dityatev

Prof. Dr. Victor Tarabykin

eingereicht am: 1.10.2018

verteidigt am: 16.5.2019

SUMMARY

Maura Ferrer Ferrer, M.Sc.

"Mental retardation-related protease neurotrypsin in spinogenesis, synaptic plasticity and learning"

Several studies implicate the role of extracellular proteases in synaptic plasticity, learning, and memory (Gundelfinger et al., 2010; Tsilibary et al., 2014). Neurotrypsin (NT), a neuronal trypsin-like serine protease, has been recognized to play an essential role in cognitive brain function because a 4-nucleotide deletion, which results in an earlier stop codon, is associated with severe mental retardation in humans (Molinari et al., 2002). Moreover, it has been recently shown that $Cln1^{-/-}$ mice, a mouse model of a neurodegenerative lysosomal storage disease, in which NT activity is suppressed due to upregulation of its inhibitor serpina1, have substantially reduced agrin-22 levels (the specific product of neurotrypsin-dependent cleavage of agrin) and this may be related with the synaptic dysfunction present in the disease (Peng et al., 2015). In the adult central nervous system (CNS), NT mRNA is highly expressed in the hippocampus, the cerebral cortex and the amygdala (Gschwend et al., 1997). In the developing mouse brain, postnatal NT mRNA is strongly expressed in cortex and hippocampus, reaching its peak of expression during neural development and correlating with periods of synaptogenesis (Wolfer et al., 2001). By electron microscopy, NT was localized at the presynaptic terminals of human cortical synapses (Molinari et al., 2002). Live imaging studies on cultured hippocampal neurons revealed that neurotrypsin is recruited and released from synapses in an activity-dependent manner (Frischknecht et al., 2008). Interestingly, proteolytic activity of NT requires synchronous activation of NMDA receptors (Matsumoto-Miyai et al., 2009). This illustrates that NT is released from the presynaptic terminals in its inactive form and it is activated in the extracellular space by a postsynaptic NMDAR-dependent mechanism. The unique known substrate for NT is the extracellular matrix (ECM) molecule agrin (Reif et al., 2007). Particularly, synaptic agrin is cleaved by NT at two sites α and β, yielding a 110 kDa N-terminal fragment, a 90 kDa internal fragment, and a 22 kDa C-terminal fragment (Stephan et al., 2008). In NT knockout mice, no proteolytic fragments of agrin can be detected, suggesting agrin to be exclusively processed by NT in the CNS (Reif et al., 2007). Activity-dependent exocytosis of NT from presynaptic terminals and cleavage of agrin induces the formation of dendritic filopodia in the context of NMDA receptor-dependent plasticity. This is supported by the finding that in NT-deficient mice no activity-dependent generation of dendritic filopodia could be observed. However, activity-dependent formation of filopodia could be rescued in the NT-deficient mice by application of agrin-22 but not agrin-90 (Matsumoto-Miyai et al., 2009). Agrin-22 induces dendritic filopodia through its binding and inhibiting the neuronal alpha3 Na+/K+ ATPase (α3NKA) (Hilgenberg et al., 2006a). Taken together, these results qualify neurotrypsin-dependent agrin cleavage as a coincidence detector for correlated activity of the presynaptic and postsynaptic neuron, with a possible involvement in synapse formation and thus, Hebbian learning. In this thesis, we investigated the putative involvement of neurotrypsin in functional synaptic plasticity, different types and phases of learning, social behaviour, and spinogenesis and spine morphology in naïve conditions and upon learning. The results revealed impairments of specific forms of long-term potentiation, behaviour and striking differences in spines in NT-deficient mice compared to their WT littermates. Moreover, we could rescue the spine loss in NT knockout mice by injecting an adeno-associated virus (AAV) expressing agrin-22 and thus form a basis for a search of mechanistic treatments that would restore plasticity and behaviour in these mutants.

ZUSAMMENFASSUNG

Maura Ferrer Ferrer, M.Sc.

"Mental retardation-related protease neurotrypsin in spinogenesis, synaptic plasticity and learning"

Verschiedene Studien implizieren die Rolle von extrazellulären Proteasen in der synaptischen Plastizität, im synaptischen Lernen sowie der synaptischen Erinnerung (Gundelfinger et al., 2010; Tsilibary et al., 2014). Der neuronalen, Trypsin-ähnlichen Serinprotease Neurotrypsin (NT) wird eine wichtige Rolle in der kognitiven Gehirnfunktion zugeschrieben, weil eine 4-Nukleotid-Mutation, welche ein früheres Stopcodon zur Folge hat, mit schwerwiegenden geistigen Behinderungen bei Menschen in Verbindung gebracht wird (Molinari et al., 2002). Zudem wurde kürzlich veröffentlicht, dass CIn1$^{-/-}$-Mäuse, ein Maus-Modell neurodegenerativer, lysosomaler Speicherkrankheiten, in denen die Neurotrypsin-Aktivität durch die Hochregulierung des Hemmstoffs Serpina1 unterdrückt wurde, eine stark reduzierte Konzentration von Agrin-22 (das Produkt von Neurotrypsin-abhängiger Zellteilung von Agrin) zeigen. Dies kann mit der synaptischen Funktionsstörung der Krankheit zusammenhängen (Peng et al., 2015). Im zentralen Nervensystem von Erwachsenen (ZNS) wird NT-mRNA hauptsächlich im Hippokampus, der Großhirnrinde und der Amygdala ausgeschüttet (Gschwend et al., 1997). Im sich entwickelnden Gehirn einer Maus wird NT-mRNA verstärkt in der Großhirnrinde und im Hippokampus exprimiert, wobei die NT-mRNA-Expression während der neuralen Entwicklung am höchsten ist. Außerdem korreliert die NT-mRNA-Expression mit den Phasen der Synaptogenese (Wolfer et al., 2001). Mit Hilfe von Elektronenmikroskopie wurde NT an den presynaptischen Enden von menschlichen, kortikalen Synapsen lokalisiert (Molinari et al., 2002). Live-Imaging-Studien an kultivierten Hippokampus-Neuronen zeigten dabei, dass NT von den Synapsen in einer aktivitätsabhängigen Art und Weise erneuert und ausgeschüttet wird (Frischknecht et al., 2008). Die proteolytische Aktivität von NT erfordert interessanterweise die synchrone Aktivierung von NMDA-Rezeptoren (Matsumoto-Miyai et al., 2009). Demnach wird NT von den presynaptischen Enden in seiner inaktiven Form abgegeben und erst im extrazellulären Raum von einem postsynaptischen, NMDAR-abhängigen Mechanismus aktiviert. Das einzig bekannte Substrat für NT ist Agrin, ein Molekül der extrazellulären Matrix (ECM) (Reif et al., 2007). Synaptisches Agrin wird von NT an den zwei Seiten a und b geteilt, woraus ein N-terminales Fragment (110 kDa), ein internes Fragment (90 kDa) und ein C-terminales Fragment (22 kDa) entstehen (Stephan et al., 2008). In NT-Knockout-Mäusen können keine proteolytischen Fragmente von Agrin nachgewiesen werden, was eine exklusive Verarbeitung Agrins von NT im ZNS vermuten lässt (Reif et al., 2007). Aktivitätsabhängige Exozytose von NT in presynaptischen Nervenenden und die Teilung von Agrin führen zur Entstehung dendritischer Filopodien im Kontext der NMDA-Rezeptor-abhängigen Plastizität. Gestützt wird dies durch den Befund, dass in NT-Knockout-Mäusen keine aktivitätsabhängige Bildung von dendritischen Filopodien beobachtet werden konnte. Die aktivitätsabhängige Bildung von Filopodien konnte bei diesen Mäusen jedoch durch die Verwendung von Agrin-22 wiederhergestellt werden, wohingegen Agrin-90 keine Wirkung erzielte (Matsumoto-Miyai et al., 2009). Agrin-22 erzeugt dendritische Filopodien durch seine Bindung und Hemmung von neuronaler alpha3-Na^+/K^+-ATPase (a3NKA) (Hilgenberg et al., 2006a). Zusammenfassend qualifizieren diese Ergebnisse Neurotrypsin-abhängige Agrin-Zellteilung als einen Koinzidenzdetektor für die korrelierende Aktivität des presynaptischen und des postsynaptischen Neurons mit einer möglichen Mitwirkung bei der Synapsen-Entstehung und somit des Hebbschen Lernens. In dieser Doktorarbeit untersuchten wir die vermeintliche Mitwirkung von Neurotrypsin in der funktionalen, synaptischen Plastizität, den verschiedenen Typen und Phasen des

Lernens, dem sozialen Verhalten sowie der Genese und der Morphologie von Dornfortsätzen sowohl unter naiven Bedingungen als auch im Lernprozess. Die Ergebnisse zeigten Beeinträchtigungen von speziellen Formen der Langzeitpotenzierung, des Verhaltens sowie starke Unterschiede der Dornfortsätze bei Mäusen mit einem NT-Defizit verglichen mit ihren WT-Wurfgeschwistern. Darüber hinaus konnten wir den Dornfortsatz-Verlust bei NT-Knockout-Mäusen mittels Injektionen von Adeno-assoziierten Viren (AAV), welche Agrin-22 ausschütten, retten und somit eine Grundlage für die Suche nach mechanistischen Verfahren für die Wiederherstellung der Plastizität und des Verhaltens in diesen Mutationen legen.

LIST OF ABBREVIATIONS

α3NKA	α3-subtype of the Na^+/K^+-ATPase
AAV	Adeno-associated virus
ACSF	Artificial cerebrospinal fluid
ADAMTS	A disintegrin and metalloproteinase with thrombospondin motifs
AMPAR	α-amino-3-hydroxy-5-methyl-4-isoxazoleproprionic acid receptor
ANOVA	Analysis of variances
bp	Base pair
CA1	*Cornus ammonis 1*
CA3	*Cornus ammonis 3*
CaM	Calmodulin
CaMK	Ca^{2+} /calmodulin kinase
CaMKII	Calcium/calmodulin-dependent protein kinase II
CaMKKα	CaM kinase kinase α
CaN	Calcineurin
CC-	Neurtral context
CC+	Conditioned context
CFC	Contextual fear conditioning
CLN1	Ceroid lipofuscinosis neuronal-1
CNS	Central nervous system
CREB	Transcription factor cyclic AMP-responsive element binding protein
CS	Conditioned stimulus
df	Degrees of freedom
DG	*Dentate gyrus*
ECM	Extracellular matrix
fEPSP	Field excitatory post synaptic potential
Fig.	Figure
GAG	Glycosaminoglycan
GSK-3β	glycogen synthase kinase-3β
h	Hours

Hz	Hertz
ICAM5	Intercellular cell adhesion molecule 5
IgCAM	Immunoglobulin-like cell adhesion molecules
INCL	Infantile neuronal ceroid lipofuscinosis
IQ	Intelligence quotient
KO	Knock-out
LTD	Long-term depression
LTP	Long-term potentiation
mA	Milliampere
MAPK	Mitogen-activated protein kinase
min	Minutes
ml	Milliliters
mM	Millimolar
MMP9	Matrix metalloprotease 9
mPFC	Medial prefrontal cortex
MR	Mental retardation
ms	Millisecond
mTOR	Mammalian target of rapamycin
mV	Millivol
NA	Numerical aperture
NCX	Plasma-membrane sodium/calcium exchanger
nl	Nanoliter
NMDAR	N-methyl-D-aspartate receptor
NMJ	Neuromuscular junction
NOR	Novel object recognition
NT	Neurotrypsin
ºC	Degrees Celcius
p	Probability of error
P	Postnatal day
PBS	Phosphate-buffered saline
PI3K	Phosphoinositide 3-kinase
PKA	Protein kinase A

PKC	Protein kinase C
PKM	Protein kinase M
PPT1	Palmitoyl-protein thioesterase-1
PRSS12	Serine protease 12, gene enconding for neurotrypsin
PSD	Postsynaptic density
PSD95	Postsynaptic density protein 95
RM	Repeated measures
s	Seconds
SEM	Standard error of mean
SRCR	Scavenger receptor cysteine-rich
TBS	Theta-burst stimulation
tPA	Tissue plasminogen activator
TRKB	Phosphoinositide 3-kinase
TVA	Tierversuchantrags
UCS	Unconditioned stimulus
VGCCs	Voltage-gated Ca^{2+} channels
VGLUT1	Vesicular glutamate transporter 1
WT	Wild-type
µm	Micrometer

TABLE OF CONTENTS

1. INTRODUCTION

1.1. Learning, memory and synaptic plasticity

1.1.1. A historical broad brushstroke

Learning and memory are two of the most fascinating capabilities of our mind. Learning is the biological process of acquiring new knowledge and memory is the process of retaining and reconstructing that knowledge over time (reviewed in Kandel et al., 2014).

The theory that adjustments in the efficacy and strength of synapses could mediate the storage of information acquired during learning has a long history. Hypothetical theories about the formation of neuronal connections in the brain and the circumstances in which such formation might occur date back to Ramón y Cajal and, in the mid-twentieth century, to Hebb and Konorski (Takeuchi et al., 2013).

The first insights about the cellular theory of memory storage as an anatomical change in the functional connections between nerve cells, later called synapses (Foster and Sherrington, 1897), come from Santiago Ramón y Cajal (1852-1934), considered nowadays as the father of neuroscience for many scientists. The neuroanatomist is known for many significant discoveries, but he is best known for being the first scientist to prove that independent neurons are the building blocks of the central nervous system. Ramón y Cajal used the Golgi silver impregnation method, discovered by Camillo Golgi (1843-1926), to visualize the morphology and architecture of neurons and their circuits throughout the brain. This protocol stained only a fraction of the nervous system cells and they appeared black under a light microscope. With his meticulous drawings (**Fig. 1.1**), Ramón y Cajal could illustrate the functional organization of circuits by looking at the anatomical arrangements of the constituting network and popularize and confirm the now-accepted Neuron Doctrine, that postulates, that the nervous system is organized by many independent neurons, which build the circuits of the nervous system (Jones, 1994; Llinás, 2003; Takeuchi et al., 2013).

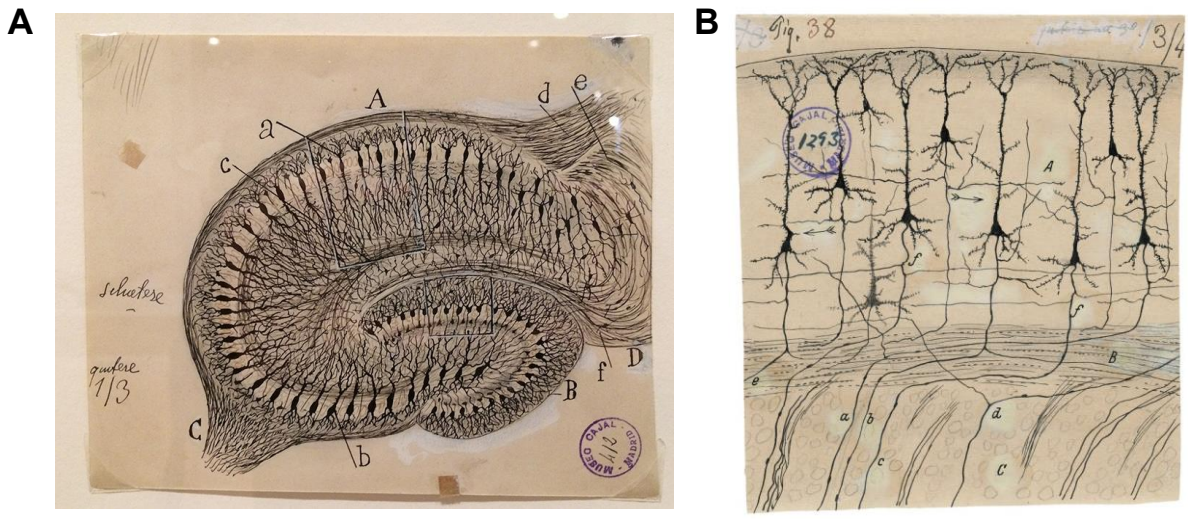

Fig. 1.1 | Santiago Ramón y Cajal hand drawings showing neuronal structures and their connections. (A) The hippocampus. **(B)** Pyramidal neurons of the central cortex and their axon pathways. *Pictures from the exhibition at Ciutat de les Arts i les Ciències, València (Spain).*

Later, in 1949, Donald Hebb (1904-1985) published *The Organization of Behavior*, in which he proposed the algorithm of synapse modification as the coincident activation of pre- and postsynaptic neurons (Hebb, 1949). A similar concept was proposed by Jerzy Konorski (1903-1973) as he was wondering how pre-existing connections between neurons could be changed by conditioning. In his monograph, *Conditioned reflexes and neuron organization* (1948), he expounded the idea that morphological changes in neuronal synaptic connections should constitute the substrate of learning. In the same book, he introduced for the first time the term "synaptic plasticity" as the ability of neurons to modulate the strength of their synapses as a result of use and process, in a malleable way, incoming information to produce behaviours that change (Zielinski, 2006).

Twenty years later, in 1973, Tim Bliss and Terje Lømo reported the discovery of what we know nowadays as "long-term potentiation" (or LTP). They described that tetanization of the perforant pathway in the hippocampal formation of anesthetized rabbit resulted in a significant increase in the excitatory postsynaptic potentials in postsynaptic neurons (Bliss and Lømo, 1973), which further supported Hebb's theories. Later on, the same phenomenon was showed in anesthetized and freely moving mice and rats.

However, it has been demonstrated that plasticity in the brain reaches far beyond a simple change in synaptic strength. In a broad sense, neural plasticity refers to the ability of neurons to change in structure and function in response to alterations in their environment. Most research attention has usually focused on functional aspects of synaptic plasticity and their

contribution to learning and memory mechanisms. Functional synaptic plasticity properties, by quickly changing synaptic strength, allow fast adaptations of network activity which are critical for information processing. Nevertheless, studies in the last decade have determined the importance of the associated structural rearrangements. These morphological changes are tightly regulated by activity and have the potential to continuously modify the organization of synaptic networks and thereby, allow a more significant and stable rewiring of synaptic networks on a longer timescale (Bernardinelli et al., 2014; Butz et al., 2009).

1.1.2. Mechanisms of activity-dependent structural plasticity

The connectivity of neural networks is continuously regulated and adjusted to properly adapt to new environmental influences by several activity-dependent mechanisms. There are, at least, two types of process to adapt synaptic efficacies (both functionally and structurally): Hebbian synaptic plasticity and homeostatic synaptic plasticity (reviewed in Fauth and Tetzlaff, 2016). Hebbian synaptic plasticity is a mechanism through which coincident pre- and postsynaptic activity leads to long-lasting changes in synaptic function. Homeostatic plasticity refers to a global form of plasticity that restrains cellular and circuit excitability to physiological levels (reviewed by Forrest et al., 2018).

In contrast to functional plasticity mechanisms that change synaptic strength without changing the anatomical connectivity between neurons, structural plasticity includes changes in spine and filopodia densities, axonal and dendritic branching patterns and synapse numbers among others, such as alterations in astroglial processes and extracellular matrix in the perisynaptic areas. Spines are very dynamic structures with a striking capacity to undergo structural changes in both adult and young brain. Spines can form *de novo*, grow, shrink and be maintained or eliminated, depending on the optimal situation of each neuronal circuit (Caroni et al., 2012). Synapse dynamics are guided by the dendritic spines dynamics. Accordingly, structural plasticity depends on the spines morphology and their sizes and shapes (Nägerl et al., 2008; Tønnesen et al., 2011, 2014). Several experiments provide evidence that the spine dendritic volume tightly correlates with the synaptic efficacy and the distribution of functional AMPA receptors of the corresponding synapse (Knott et al., 2006; Matsuzaki et al., 2001; Zito et al., 2009). Consequently, experimental findings show that LTP induces spine enlargement (Fifková and Van Harreveld, 1977; reviewed in Yuste and Bonhoeffer, 2001) whereas long-term depression (LTD) causes spine shrinkage (Oh et al., 2012; Okamoto et al., 2004; Zhou et al., 2004). Hereby, synaptic and structural adjustments are regulated by signalling cascades, which are triggered by the same signals (Matsuzaki et al., 2004; Zhou et al., 2004).

One can distinguish between reactive structural plasticity, which occurs after surgical or pharmacological interventions and spontaneous or experience-dependent structural plasticity, which exists physiologically throughout life in the brain (reviewed in Butz et al., 2009). It is beyond the scope of this introduction to give an extensive view of reactive structural plasticity mechanisms. Therefore, I will focus on spontaneous and experience-dependent structural plasticity mechanisms, which occurs normally during development or in the adult brain.

1.1.2a Molecular mechanisms regulating activity-mediated stabilization of dendritic spines

Accumulating evidence over the last decade, reveal that synaptic networks are also structurally plastic and that connectivity is remodelled over the lifespan, through mechanisms of synapse formation, stabilization, and elimination. This has generated the idea of structural plasticity, which can include several morphological changes that result in functional consequences. These include both structural rearrangements at pre-existing synapses and formation or elimination of synapses, neuronal processes or neurons (reviewed by Caroni et al., 2012).

An outstanding aspect of excitatory and inhibitory synapses is their high level of structural variability and the plasticity and dynamics of their morphologies (Bourne and Harris, 2008; Kasai et al., 2010a). This phenomenon is activity-dependent, and spine head and sizes correlate with synaptic strengths (Matsuzaki et al., 2004), presynaptic properties (Tokuoka and Goda, 2008) and the synapse persistence (Holtmaat et al., 2005). Thus, the morphological features of synapses determine their level of functionality and stability.

The first evidence that the induction of synaptic plasticity could influence the shape and size of dendritic spines come from electron microscopy studies (Yuste and Bonhoeffer, 2001). Later, two-photon imaging and glutamate uncaging experiments elucidated a correlation between increased synaptic strength and an enlargement of the spine head (Matsuzaki et al., 2004). This enlargement could imply several functional modifications at the synapse, like changes in receptor expression that are thought to be responsible for the increase in synaptic strength (Malinow and Malenka, 2002), the mobilization of subcellular resources to potentiated synapses (Ostroff et al., 2002) and a more global set of modifications that support the stabilization of the synapse (De Roo et al., 2008). Several studies have featured the importance of synapse stabilization for behavioural learning (Holtmaat et al., 2005; Roberts et al., 2010; Xu et al., 2009; Yang et al., 2009). This research provides evidence that the

stabilization of specific subpopulations of spines could represent a structural basis for memory storage.

However, many studies support the idea that there is an overlap between the molecular pathways involved in all aspects of synapse and spine stability (**Fig. 1.2**), underlining the link between induction of plasticity and synapse stability.

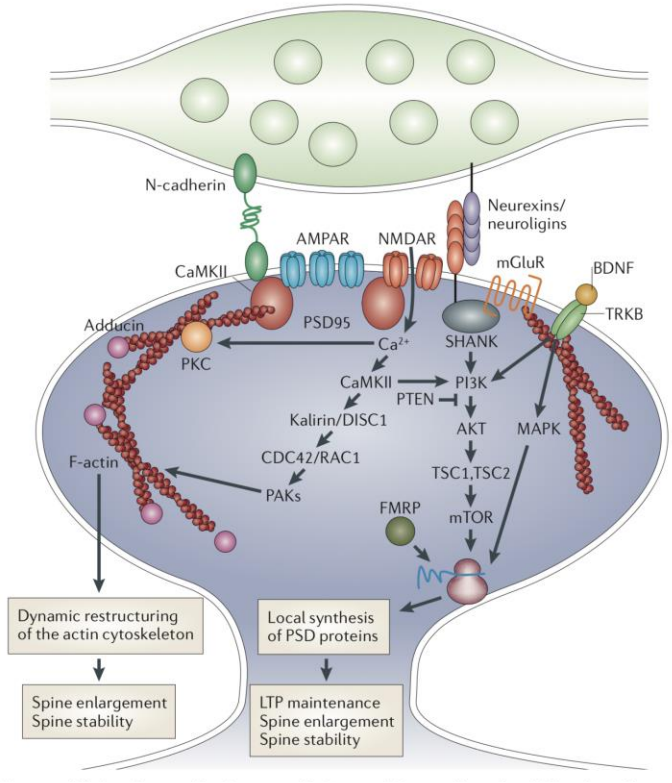

Fig. 1.2 | Molecular mechanisms regulating activity-dependent stabilization of dendritic spines. *Caroni et al., 2012*.

Phosphorylation mechanisms showed to play an important role in these processes. Both calcium/calmodulin-dependent protein kinase II (CaMKII) and protein kinase C (PKC) have been tightly involved in LTP maintenance and behavioural learning (reviewed in Lisman et al., 2012; Sacktor, 2011). CaMKII activity indicated to be necessary for activity-dependent spine enlargement (Yamagata et al., 2009), and PKC contributed to spine stabilization *in vivo* (Bednarek and Caroni, 2011). However, more recently, Volk and colleagues (2013) showed that PKC was not required for LTP maintenance and memory, as both conventional and conditional PKC/PKM (a brain-specific isoform of PKC) knockout mice showed normal synaptic transmission and LTP at Schaffer collateral–CA1 synapses, and had no deficits in several hippocampal-dependent learning and memory tasks (Volk et al., 2013). This suggests

that pharmacological inhibition of PKC/PKM used in most of the previous studies may have additional effects that could have led to the former controversial results.

Another mechanism crucial for spine stabilization requires the local regulation of protein synthesis, which comprises different signalling cascades (such as the mitogen-activated protein kinase (MAPK) and phosphoinositide 3-kinase (PI3K) pathways) downstream of receptor tyrosine kinase B (TRKB; also known as NTRK2) activation, the mammalian target of rapamycin (mTOR signalling complex and the translation of mRNAs that encode proteins such as ARC (activity-regulated cytoskeleton-associated protein) or CaMKII. A disruption in these signalling pathways, in protein synthesis or in ARC translation have been associated with compromised LTP maintenance and spine enlargement (reviewed in Caroni et al., 2012).

Additionally, actin regulatory proteins and pathways have been strongly implicated in spine stabilization and control of the spine actin cytoskeleton. Blockage of actin polymerization resulted in LTP maintenance impairment and changes in spine size (Bramham, 2008; Cingolani and Goda, 2008; Honkura et al., 2008). Further evidence for the role of the cytoskeleton in spine stability comes from studies in Rho GTPases signalling and several upstream and downstream modulators of this cascade. Interference in this pathway has been associated with LTP and spine enlargement disruption (Hayashi-Takagi et al., 2010; Xie et al., 2007).

Finally, one essential mechanism, through which synapse stability is affected, is by changes in the organization of the postsynaptic density (PSD). Expression of PSD95 (postsynaptic density protein 95) and/or AMPA receptors increases synaptic strength and stability (Ehrlich et al., 2007; Ripley et al., 2011). In addition, several cell adhesion molecules have been associated with spine stability, including neuroligin 1 and N-cadherin among others (Mendez et al., 2010; Wittenmayer et al., 2009).

During the formation of the PSD, NMDA receptors and PSD95 are recruited to nascent synapses. NMDA receptors are present in mobile clusters that are rapidly recruited to new sites of axodendritic contact (Washbourne et al., 2002), but do not co-localize with PSD95 in dendrites before synaptogenesis. PSD95 binds to NMDAR receptors in mature PSDs (Kornau et al., 1995). Adhesion between neurexin-1b (Nrx1b) and neuroligin-1 (Nlg1) induces recruitment of PSD95 at excitatory synapses (Giannone et al., 2013). Recently, it was shown that unphosphorylated ephrin-B3 interacts directly with PSD95 and stabilizing it at synapses (Hruska et al., 2015).

Experiments have also evinced that activity also destabilizes existing synapses (Holtmaat et al., 2005; De Roo et al., 2008). Motor training resulted in high ratios of spine formation and elimination (Xu et al., 2009; Yang et al., 2009) and, more recently, Lai and colleagues (2012) showed that spine elimination and formation caused by fear conditioning and extinction, respectively, occur in a cue- and location-specific manner (Lai et al., 2012).

Interestingly, activity-mediated spine dynamics might be regulated locally. Experiments have shown that induction of plasticity is facilitated in the proximity of potentiated spines and *de novo* spine formation preferentially occurs in the vicinity of activated spines (Harvey et al., 2008; Kleindienst et al., 2011; De Roo et al., 2008). Nevertheless, in some cases, the effect may be more global and differentially affect spine formation and elimination, leading to changes in spine density (Hofer et al., 2009). For example, in motor learning experiments, the increase in spine formation and elimination cancelled each other out, generating no apparent changes in spine density (Xu et al., 2009; Yang et al., 2009). Conversely, environmental enrichment greatly promoted spine formation, resulting in an increase in the absolute spine number (Bednarek and Caroni, 2011). Overall, these findings suggest that the rewiring observed under behaviour learning tasks represents a structural correlate of learning. However, the temporal sequences of events and the regulatory mechanisms connecting learning and structural plasticity to long-term memory are not fully elucidated.

1.1.2b Plasticity of spine structure: local signaling and cytoskeletal reorganization

The spine structure is maintained by a network of actin cytoskeleton. Long- and short-branched filamentous actin (F-actin) are connected through multiple actin-binding proteins (ABPs), building a highly branched structure (Hotulainen and Hoogenraad, 2010). Thus, dynamic remodelling of actin networks within dendritic spines is crucial for activity- dependent structural changes of spines (Honkura et al., 2008; Okamoto et al., 2004). F-actin is formed by polymerization of monomeric globular actin (G-actin). These two forms of actin go through a cycle named tread-milling: ATP-bound G-actin is added to the fast- growing end (plus end) and ADP-bound G-actin is dissociated from the other side (minus end) of F-actin. The balance between actin polymerization and de-polymerization is essential for structural plasticity of dendritic spines (Hotulainen and Hoogenraad, 2010).

Strong excitatory synaptic inputs trigger postsynaptic Ca^{2+} elevation through NMDA receptors and/or voltage-gated Ca^{2+} channels (VGCCs) in the activated spine (Sabatini et al., 2002).

Ca^{2+} build-up in spines induces downstream signalling cascades for long-term synaptic plasticity including LTP. Ca^{2+} binds to calmodulin (CaM), a Ca^{2+}-binding protein and Ca^{2+} bound CaM (Ca^{2+}/CaM) subsequently activates Ca^{2+}/CaM-dependent kinases and phosphatases such as CaMKII and calcineurin (CaN). Upon Ca^{2+}/CaM binding, active CaMKII can undergo autophosphorylation, which results in an activity independent of Ca^{2+}/CaM binding function of the kinase. This Ca^{2+}/CaM-independent activation, could persist for a long time after Ca^{2+} decays. Short CaMKII activation triggers downstream signalling molecules including small GTPase proteins. The activity of these downstream signals lasts more than tens of minutes, reorganizing actin cytoskeleton over this time period (reviewed by Nakahata and Yasuda, 2018). The activation of these small GTPase proteins (RhoA, Cdc42, Rac1 and Ras) are all activated by CaMKII, and required for structural LTP (Bosch et al., 2014; Harvey et al., 2008). RhoA activation controls spine remodelling through the activation of downstream effectors such as Rho-associated protein kinase (ROCK). Activated ROCK phosphorylates LIMK, which further phosphorylate ADF/cofilin (Arber et al., 1998). Cdc42 and Rac1 promote actin polymerization through activating WASP and WAVE, respectively. The activated WASP and WAVE bind to and upregulate Arp2/3 complex, which induces actin nucleation and thus spine enlargement (Hlushchenko et al., 2016). Cdc42 and Rac1 also stabilizes actin cytoskeleton by inhibiting ADF/cofilin-mediated actin depolymerization through downstream effectors p21-activated kinase (PAK)-LIMK pathway and the PAK-phosphatases slingshot (SSH) pathway (Bosch et al., 2014). Recent studies suggest that Copine-6, a Ca^{2+}-binding molecule is another upstream regulator of the Rac1-PAK-LIMK pathway (**Fig. 1.3;** Burk et al., 2017; Reinhard et al., 2016).

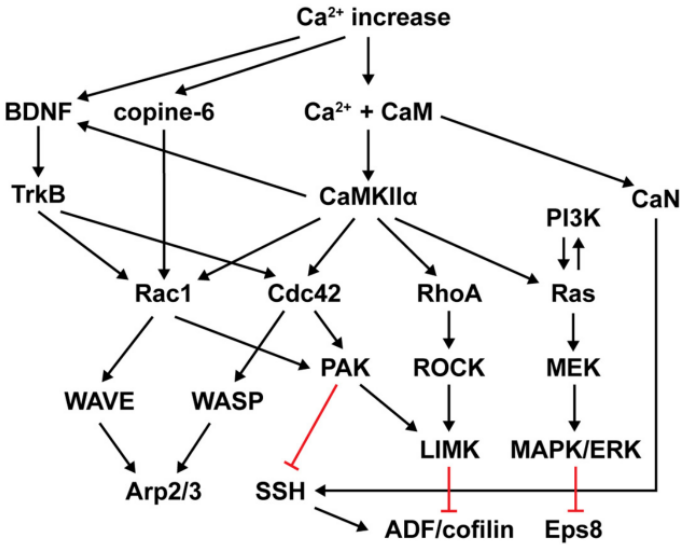

Fig. 1.3 | Signaling pathways controlling actin binding proteins (ABPs) in dendritic spines. Black arrows represent downstream activation and red lines represent downstream inhibition. *Adapted from Nakahata and Yasuda, 2018*.

1.1.2c Evidence for Hebbian structural plasticity

LTP induction by a strong neuronal activation is associated with an enhancement of the synaptic efficacy of existing synapses (Malenka and Bear, 2004) but also an increase of synapse number and filopodia density (Chang and Greenough, 1984). In agreement with these observations, several studies have reported an increase of dendritic spines after LTP induction (Engert and Bonhoeffer, 1999; Moser et al., 1994; Trommald et al., 1996). This increase in spine density after LTP provides evidence for a putative interaction between Hebbian synaptic plasticity and Hebbian structural plasticity. More recently, it was shown that LTP-inducing stimuli stabilize newly formed spines and that this mechanism is NMDA receptor-dependent (Hill and Zito, 2013). Similarly, experimental results showed that blocking the signals inducing LTP (e.g., by blocking NMDA receptors) inhibits the observed increase in dendritic spine density (Engert and Bonhoeffer, 1999; Maletic-Savatic et al., 1999; Toni et al., 1999). Likewise, at the presynaptic site, an LTP-inducing stimulus increases the number of axonal boutons (Nikonenko et al., 2003).

Like dynamics yielded by an LTP-stimulus, experimental research indicated that the induction of an LTD-stimulus (by low frequency) triggers a separation of pre- and postsynaptic terminals (Bastrikova et al., 2008) and a loss of dendritic spines (Nägerl et al., 2004; Wiegert and Oertner, 2013). In agreement with these findings, experimental data showed that the prevention of LTD by blockage of NMDA receptors impeded the structural effects (Nägerl et al., 2004; Yu et al., 2013). Like for LTP-induced dynamics, also the axonal boutons are affected by low-frequency stimulation (LTD) as it dramatically increases the turnover of presynaptic boutons (De Paola et al., 2006; Stettler et al., 2006), resulting in a reduction of synaptic contacts (Becker et al., 2008).

Overall, stimulation protocols inducing Hebbian synaptic plasticity modify and have an effect on stability and number of synaptic contacts. In short, a strong activation triggers synaptogenesis while a low activation results in a loss of synapses (**Fig. 1.4A,C**).

1.1.2d Evidence for homeostatic structural plasticity

Like for synaptic plasticity, also structural changes exhibit homeostatic dynamics, i.e., a decrease of connectivity with high neuronal activity and an increase with low activity. These homeostatic dynamics are observed under persistent altered neuronal activity and, hence, at slower timescales. Essentially, these structural changes seem to compensate for the altered activity and regulate it back to an intermediate level (**Fig. 1.4B,C**). Similar to Hebbian structural plasticity, homeostatic structural changes are driven by the dynamics of dendritic spines and presynaptic boutons (reviewed in Butz et al., 2009; Fauth and Tetzlaff, 2016). Experiments reported that blockage of NMDA receptors results in an increase in spine protrusions (Chen et al., 2015; Yu et al., 2013) or inhibition of spine elimination (Bock and Braun, 1999). Nonetheless, newly formed spines usually host silent synapses needing synaptic plasticity to be converted into functional synapses (Nakayama, 2005). Conversely, prolonged depolarization of neurons results in a loss of dendritic spines (Drakew et al., 1996; Muller et al., 1993). In addition, it was reported that cultured hippocampal neurons exposed to NMDA lead to spine loss in a time- and concentration-dependent manner by the destabilization of the spine actin scaffold (Halpain et al., 1998). Intriguingly, Hebbian synaptic plasticity can induce competitive effects between newly formed and up-scaled pre-existing spines simultaneously, which destabilizes the recently formed synapses, and, hence, prolongs the recovery of the system (Vlachos et al., 2013).

Furthermore, changes in the number of spines are calcium level-dependent (Kirov and Harris, 1999; Kirov et al., 2004; Tian et al., 2010). However, the detailed relation between calcium, activity and spine dynamics is complex as the calcium levels are also controlled by cell adhesion molecules and other signals (reviewed in Fauth and Tetzlaff, 2016).

In summary, the changes in neuronal activity cause two different directions of structural plasticity (**Fig. 1.4**). On a fast timescale (minutes to hours), the dynamics of dendritic spines go along with the change in neuronal activity in a Hebbian manner. On a slower timescale (hours to days), dendrites and dendritic spines homeostatically counterbalance changes in activity and regulate it back to an intermediate level.

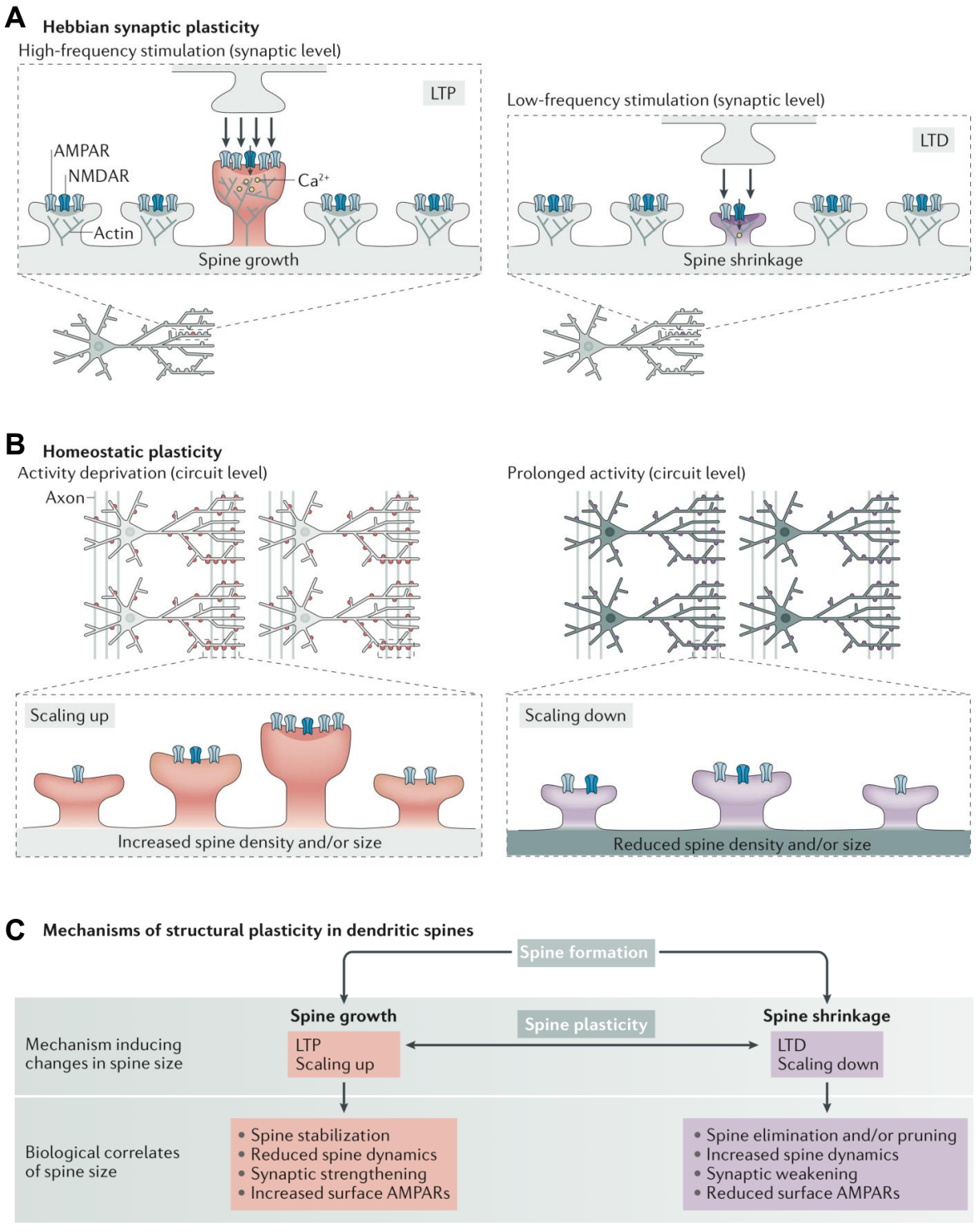

Fig. 1.4 | Mechanisms of structural plasticity. (A) Hebbian synaptic plasticity mechanisms. High-frequency synaptic activity associated with high calcium entry causes long-term potentiation (LTP), which induces spine growth, an enlargement of the postsynaptic density (PSD) and actin polymerization and promotes the surface expression of AMPA receptors (AMPARs). Low-frequency synaptic activity associated with modest calcium entry through NMDA receptors (NMDARs) causes long-term depression (LTD), which induces shrinking of the spine and PSD, actin depolymerisation and a reduction of surface AMPAR expression. **(B)** Proposed mechanisms of homeostatic synaptic plasticity. Synaptic scaling is a form of

homeostatic plasticity that allows neurons to modify their overall synaptic input (excitability) in response to changes in circuit activity. Activity deprivation causes neurons to scale up, proportionally strengthening synapses by increasing surface AMPAR expression to increase overall synaptic input. Prolonged circuit activity causes neurons to scale down, proportionally reducing synaptic strength by removal of surface AMPARs. **(C)** Summary of mechanisms that can regulate spine development and plasticity. *Adapted from Forrest et al., 2018*.

1.1.3. Role of extracellular matrix remodelling in learning and synaptic plasticity

In the higher vertebrate brain, the balance between structural stabilization and remodelling of neuronal networks and synapses is modified throughout life. The developing brain is characterized by high structural plasticity. The extracellular matrix (ECM) has been seen as an essential element for guaranteeing the structural stability of neuronal tissue. However, several studies described that ECM undergoes significant changes during brain maturation. Interestingly, ECM appearance closely matches the closure of critical periods in different brain regions, supporting the hypothesis that brain's ECM transform juvenile into adult plasticity restricting the potential for neuronal reorganization. The adult brain has developed an efficient manner to structurally stabilize neuronal circuits formed during experience-dependent learning, which is a crucial process for long-term memory storage and memory recalls. In the juvenile brain, periods of high structural plasticity allow the formation of brain networks by experience (reviewed in Frischknecht and Happel, 2016).

Research evidence that endogenous ECM-modulating enzymes have an important influence on synaptic function in both developing and adult brain. These enzymes may function by modifying extracellular milieu by digesting the ECM or by generating proteolytic fragments that may act as a signalling neoepitopes (reviewed by Frischknecht and Happel, 2016). A large group of such enzymes are the metalloproteases of the ADAMTS (a disintegrin and metalloproteinase with thrombospondin motifs) family. Among ADAMTS members expressed in the brain are ADAMTS1, 4, 5, 8, 9 and 15, which cleave lecticans, including aggrecan, brevican, versican and neurocan. Nevertheless, lecticans are not the exclusive target of ADAMTS as they showed to cleave also phosphacan (Tauchi et al., 2012) and reelin (Hisanaga et al., 2012; Krstic et al., 2012). Several studies suggest that ADAMTS are upregulated after CNS injury and disease as they may be required for the activation of plasticity mechanisms (reviewed by Ferrer-Ferrer and Dityatev, 2018).

The most studied extracellular protease is the matrix metalloprotease 9 (MMP9). Activity-dependent expression of MMP9 regulates synaptic plasticity, learning and memory. Either genetic or pharmacological inhibition of MMP9 impairs late phase of LTP at various pathway.

At the behavioural level, blocking of MMP9 function resulted in disrupted appetitive and spatial memory formation (reviewed by Kaczmarek, 2016).

MMP9 induces elongation and thinning of the spines (reviewed in Dziembowska and Wlodarczyk, 2012; Michaluk et al., 2011; Stawarski et al., 2014). Moreover, it was elucidated that elongation and spine thinning are controlled by integrin β1 signalling and this results in changes in the decay time of miniature synaptic currents (Michaluk et al., 2011). However, on the other hand, physiologically and locally MMP9 promotes conversion of small spines to larger (Szepesi et al., 2014; Wang et al., 2008a). This apparent paradox can be explained as full function of MMP9 requires first its activity, followed by subsequent inhibition by TIMP1 (Kaczmarek, 2016).

MMP9 also showed to increase the lateral mobility of NMDARs (Michaluk et al., 2009). Recently, it was discovered that increasing glycogen synthase kinase-3β (GSK-3β) activity caused higher activity of extracellularly acting MMP9 and this resulted in an increase in the number of thin spines (Kondratiuk et al., 2017). Another example of MMP9-mediated proteolysis was discovered by Conant and colleagues (2011) as they described that the full-length intercellular cell adhesion molecule 5 (ICAM5) was cleaved by MMP9 and detected shortly after LTP induction (Conant et al., 2011). Furthermore, this ICAM5 ectodomain produced by MMP9 cleavage increased AMPA mini excitatory postsynaptic current (mEPSC) frequency and this reflected a recruitment of the GluA1 AMPAR subunit to the membrane (Lonskaya et al., 2013).

Similarly, the brain-specific serine protease neurotrypsin is activated in a NMDAR-dependent manner and requires coincident pre- and postsynaptic activation to cleave its specific target, the heparan sulfate proteoglycan agrin. Proteolytic cleavage of agrin results in release of a 22kDa fragment of agrin that induces the formation of new dendritic filopodia in acute hippocampal slices (Matsumoto-Miyai et al., 2009). More detailed literature of neurotrypsin and its cleavage will be elucidated in 1.2. and 1.3. as it is the main focus of this dissertation.

Altogether, this suggests that proteolysis of ECM molecules not only changes the structural rigidity but also activates instructive signal molecules that locally modulate synaptic functions.

1.2. Neurotrypsin in learning and structural synaptic plasticity

1.2.1. Trypsin family of serine proteases

Several research studies demonstrate that trypsin and trypsin-like family of serine proteases play crucial roles in regulating neural development and synaptic plasticity in the brain. The most comprehensively characterized components of this family belong to the thrombin-like proteases (comprising thrombin, tissue plasminogen activator (tPA), and plasmin) and trypsin-like proteases (including trypsin, neurotrypsin, and neuropsin). Serine proteases are secreted as zymogens (inactive proenzymes) that requires proteolysis to remove the pro-peptide from the enzyme to become active. These enzymes degrade ECM molecules, other serine proteases, or protease-activated receptors (reviewed by Tsilibary et al., 2014; Wlodarczyk et al., 2011).

Tissue plasminogen activator is a serine protease that converts plasminogen to plasmin and it is predominantly implicated in thrombolysis. However, more recent evidence shows that tPA plays also physiological and pathological roles in the brain. tPA is expressed in several brain regions and it is synthesized and released by neurons, glia, and endothelial cells. It was shown that tPA is released by the presynaptic terminals of cerebral cortical neurons following membrane depolarization (Echeverry et al., 2010). tPA is negatively regulated by endogenous serine protease inhibitors called serpins (Tsilibary et al., 2014). tPA is constituted of five functional domains through which it interacts with different substrates, binding proteins, and receptors. Depending on the study, endogenous tPA was reported as deleterious or beneficial for neurons. Although it is challenging to integrate these discoveries, some studies suggest that tPA is neuroprotective at low levels, but neurotoxic at higher levels. Certainly, the target involved is essential in the effect of tPA. In general, the pro-survival effects of tPA are independent of its proteolytic activity involving EGF receptors, annexin II, PI3 kinase-, AMPK-, mTor-HIF-1α-dependent signaling pathways. In the adult, the neurotoxic effects of tPA appeared to be dependent on its proteolytic activity, targeting either plasminogen, NMDARs, components of the extracellular matrix such as MMPs, inflammatory mediators, and/or other proteases (Chevilley et al., 2015). It was demonstrated that tPA regulates neuronal plasticity and is involved in emotions, learning and memory formation (Calabresi et al., 2000; Huang et al., 1996; Pawlak et al., 2002; Samson and Medcalf, 2006). Indeed, tPA-deficient mice exhibit a deficit in spatial navigation tasks, fear conditioning, cerebellar motor learning among other learning paradigms (Huang et al., 1996; Norris and Strickland, 2007; Pawlak et al., 2002). Not surprisingly, these mice have impaired LTP (Huang et al., 1996). In addition, it was also

demonstrated that the tPA/plasmin system is involved in synaptogenesis and spine formation (Bennur et al., 2007; Mataga et al., 2002; Oray et al., 2004; Pawlak et al., 2005).

Neuropsin hydrolyzes the ECM molecules by its active site serine, regulating learning and memory in the CNS (Wang et al., 2008b). Neuropsin is mainly expressed in the forebrain, showing high expression patterns in the projection neurons of CA1 and CA3 regions of the hippocampus and magnocellular neurons of the lateral and basolateral amygdala complex (Chen et al., 1995). Neuropsin is synthesized as a zymogen (proneuropsin), which is then secreted and stored in the extracellular space in its inactive form. Conversion to active neuropsin has indicated to be neuronal activity- (Shimizu et al., 1998) and NMDAR-dependent (Matsumoto-Miyai et al., 2003). In the brain, there are four documented protein targets for neuropsin: ECM protein fibronectin (Shimizu et al., 1998), cell adhesion molecule L1 (Matsumoto-Miyai et al., 2003), membrane tyrosine kinase receptor EphB2 (Attwood et al., 2011), and neuregulin-1 (Tamura et al., 2012). Experiments in neuropsin-deficient mice or in which neuropsin function was inhibited revealed a strong impairment in the early-phase, but not the late-phase LTP in the Schaffer collateral pathway of the hippocampus (Ishikawa et al., 2008; Tamura et al., 2006). In agreement with these observations, neuropsin-deficient mice showed a striking reduction in E-LTP in the lateral-basal pathway of the amygdala while the basal synaptic transmission remained unaffected (Attwood et al., 2011). Indeed, this protease showed to be important for several hippocampus- and amygdala-dependent learning tasks (reviewed in Tsilibary et al., 2014). Hirata and colleagues (2001) examined the importance of neuropsin in neuronal morphology and spinogenesis. They described that neuropsin-deficient mice have shorter dendritic processes in the pyramidal cells in the hippocampus than their wild-type littermates. In addition, they found a significant reduction in the number of asymmetric synapses in neuropsin$^{-/-}$ mice (Hirata et al., 2001).

1.2.2. Presynaptic release of neurotrypsin and its activation

Neurotrypsin is a nervous system-specific serine protease, which is expressed predominantly in the neurons of the cerebral cortex, the hippocampus and the lateral amygdala, brain structures involved in learning and memory. Furthermore, neurotrypsin expression is also significantly high in the motoneurons of the brain stem and spinal cord (Gschwend et al., 1997; Iijima et al., 1999; Wolfer et al., 2001). Immuno-electron analysis of adult human brain sections revealed a strong neurotrypsin immunoreactivity in the presynaptic nerve ending of cortical synapses. The most intense immunoreactivity was observed over the presynaptic membrane lining the synaptic cleft. In addition, gold-labeled secondary antibodies revealed a high

immunoreactivity in a subpopulation of presynaptic vesicles situated in close proximity to the presynaptic membrane (Molinari et al., 2002). In mature neurons, neurotrypsin was detected in transport vesicles along axons and in both intracellular and extracellular pools at synapses. Live imaging studies on cultured hippocampal neurons expressing neurotrypsin fused with enhanced green fluorescent protein or its pH-sensitive variant superecliptic pHluorin, elucidated that neurotrypsin is released from presynaptic terminals in an activity-dependent manner. Particularly, they observed that short depolarization resulted in neurotrypsin exocytosis at the synapse and once externalized, neurotrypsin remained at its synaptic release site for several minutes before it disappeared (Frischknecht et al., 2008). Taken together, the activity-dependent recruitment, exocytosis and transient persistence of neurotrypsin at the synapse, suggest a spatially- and temporally-restricted proteolytic action of neurotrypsin, supporting its mechanism as an adaptive response to changes in the context of learning and memory.

Interestingly, proteolytic activity of neurotrypsin does require synchronous activation of NMDA receptors (Matsumoto-Miyai et al., 2009). This illustrates that neurotrypsin is released from the presynaptic terminals in its inactive form and it is activated at the extracellular space by a postsynaptic NMDA receptor-dependent mechanism. Nonetheless, the exact mechanism of neurotrypsin activation remains unknown. However, the zymogen activation site at the N-terminal of the protease comprises the furin-type proprotein convertase recognition sequence “RRQKR” (Reif et al., 2008). Indeed, it was later shown that neurotrypsin is activated by this mechanism *in vitro,* as a proprotein convertase inhibitor dec-RVKR-CMK prevented the activation of neurotrypsin in HEK-293T cells and a sequence mutation at the zymogen activation site abolished the proteolytic cleavage of neurotrypsin (Gisler et al., 2013).

1.2.3. Agrin as neurotrypsin substrate at the synapse

Sequence alignments and structure modelling of the catalytic domain indicated a trypsin-like substrate specificity of the protease. Up to date, the only known substrate of neurotrypsin is the proteoglycan agrin. In particular, synaptic agrin is subjected to proteolytic cleavage by neurotrypsin at two sites, α and β, yielding a 110 kDa N-terminal fragment, a 90 kDa internal fragment, and a 22 kDa C-terminal fragment (**Fig. 1.5**) (Reif et al., 2007; Stephan et al., 2008). Interestingly, these fragments were not present in tissue from neurotrypsin-deficient mice, demonstrating that agrin cleavage by neurotrypsin occurs *in vivo*, and, furthermore, agrin cleavage strictly depends on neurotrypsin (Reif et al., 2007). Moreover, Stephan et al., 2008 revealed that neurotrypsin-dependent cleavage of agrin is more pronounced at synapses

when compared with other subcellular fractions. It was suggested that neurotrypsin processes preferentially highly glycosylated forms of agrin (Stephan et al., 2008). Indeed, Gisler and colleagues (2013) showed that the glycosaminoglycan (GAG) side chains enhanced agrin cleavage more likely due to increased zymogen activation of neurotrypsin by proprotein convertases. In addition, they described that neurotrypsin binds to agrin on the cell surface via heparin sulfate side chains, which is the major GAG in agrin (Gisler et al., 2013). Altogether, the present study describes the heparin-binding site present in one of the splicing agrin variants (*Y* splicing site in **Fig. 1.5**) as a potentially key regulatory factor of the neurotrypsin-agrin axis in the CNS.

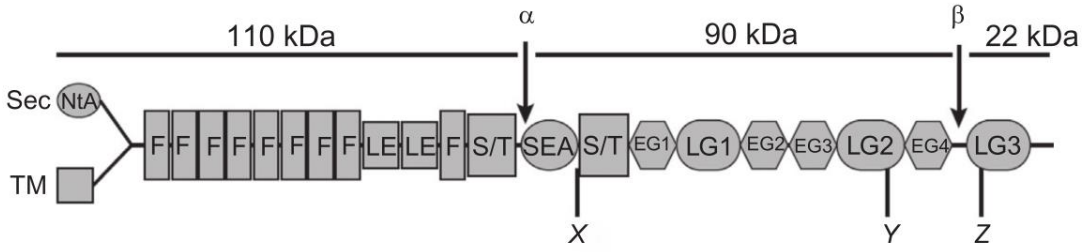

Fig. 1.5 | Schematic representation of agrin. Alternative splicing results in several transmembrane (TM) or secreted (Sec) agrin variants and variable inserts of several amino acids at the x, y, and z splicing sites. Neurotrypsin cleaves agrin at two sites (α and β, arrows) generating fragments of 110, 90, and 22 kDa. NtA, N-terminal agrin domain; TM, transmembrane domain; F, follistatin-like domains; LE, laminin-epidermal growth factor (EGF)-like domains; S/T, serine–threonine-rich region; SEA, sperm protein, enterokinase, and agrin domain; EG, EGF-like domains; LG, laminin- globular domains. *Adapted from Tsilibary et al., 2014*.

1.2.4. Mechanisms downstream of agrin cleavage by neurotrypsin

The α3-subtype of the Na^+/K^+-ATPase (α3NKA) was identified as a neuronal agrin receptor in the brain, and it was found that its Na^+/K^+-pumping function was inhibited by agrin binding, hence suggesting a depolarizing role of agrin on CNS neurons. In particular, the authors showed that agrin inhibition of the α3NKA activity led to membrane depolarization and increased action potential frequency in both cortical neurons and acute cortical slices. The α3NKA is a member of the NKA family selectively expressed in neurons and the authors showed that agrin acts as an endogenous ouabain-like molecule that targets specifically to this subunit (Hilgenberg et al., 2006), presumably by displacing the NKA β-subunit and exploiting the ouabain binding pocket (Tidow et al., 2010a). In a previous study, ouabain

induced hyperexcitability in hippocampal neurons, causing changes in both intrinsic membrane properties and synaptic transmission (Vaillend, 2002).

Evidence that agrin receptor exists comes from earlier biochemical studies describing that C-terminal agrin triggers c-Fos expression in cortical neurons (Hilgenberg et al., 1999) and increases CREB phosphorylation in cultured hippocampal neurons (Ji et al., 1998). Several studies suggest that these two processes are involved in synaptic plasticity and memory formation (Kaczmarek, 1993; Kandel, 2001). Hilgenberg and Smith (2004) described also that activation of the agrin receptor results in a tyrosine kinase-dependent increase in intracellular Ca^{2+} that engages both CaMKII and MAPK signal pathways, which serves as the triggering event for many of agrin's effects on neurons (Hilgenberg and Smith, 2004). Interestingly, before finding that the α3NKA is the neuronal receptor for agrin, Hoover et al., 2003 already elucidated that a receptor for agrin is concentrated at the synaptic sites using different agrin fragments as affinity probes (Hoover et al., 2003a). O'Connor and coauthors showed that agrin expression is activity-dependent (O'Connor et al., 1995). Intriguingly, signalling by the α3NKA shares some similitudes with agrin-induced AChR clustering in muscle, most remarkably its Ca^{2+} dependence and sensitivity to inhibition of tyrosine kinase activity (Hilgenberg et al., 2006, see 1.2.6 for further information).

Interestingly, agrin-15, a shorter agrin fragment that acts as a competitive agrin antagonist, disrupted endogenous agrin-α3NKA interactions, resulting in a depressed action potential frequency, providing evidence that endogenous neuronal agrin increases excitatory synaptic signalling through its binding to and inhibition of α3NKA (Hilgenberg et al., 2006).

Earlier studies from Bouron and Reuter (1996) indicated that functional coupling between the α3NKA and the plasma-membrane sodium/calcium exchanger (NCX) plays a role in neurotransmitter release and vesicle cycling (Bouron and Reuter, 1996). In agreement with these observations, Böse et al., 2000 described that ablation of agrin expression in neurons is associated with a decrease in synaptic vesicle cycling in cultured hippocampal neurons (Bose et al., 2000).

1.2.5. Neurotrypsin and Hebbian-like induction of filopodia in the hippocampus

Activity-dependent exocytosis of neurotrypsin from presynaptic boutons and cleavage of agrin were found to be crucial for the formation of dendritic filopodia in the context of NMDAR-

dependent plasticity. Matsumoto-Miyai and colleagues (2009) showed that the activity-dependent formation of filopodia is suppressed in hippocampal neurons from juvenile (4- to 6-week-old) neurotrypsin-deficient mice. Moreover, they found that administration of C-terminal agrin-22 but not agrin-90 or agrin-110 in hippocampal slices (see **Fig. 1.5**), induced a significant increase of filopodia on secondary apical dendrites of CA1 pyramidal neurons, reaching the filopodia density levels observed in wild-type mice. Therefore, they concluded that the C-terminal agrin was only effective in the form of agrin-22 and thus, the β-cleavage was crucial to generate filopodia response associated with LTP via neurotrypsin-dependent agrin cleavage.

Furthermore, they demonstrated that presynaptic release of neurotrypsin depends on action potential firing and P/Q/N-type calcium channels, while neurotrypsin-dependent agrin cleavage requires activation of the postsynaptic neuron (Matsumoto-Miyai et al., 2009). Therefore, neurotrypsin-dependent cleavage of agrin could represent a coincident detector for correlated activity of the pre- and postsynaptic neuron. Because dendritic filopodia are thought to be important precursors of new spines and synapses (Jontes and Smith, 2000; Yuste and Bonhoeffer, 2004, **Fig. 1.6**), these results suggest that the neurotrypsin-dependent agrin cleavage at the synapse may be instrumental for Hebbian learning and involved in the activity-dependent regulation of synaptogenesis and remodelling of neuronal circuits in the CNS.

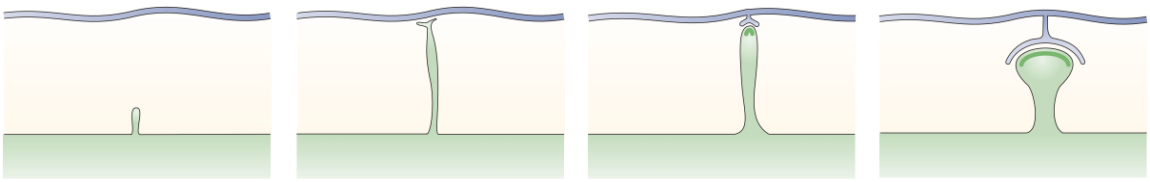

Fig. 1.6 | Schematic representation of the filopodial spinogenesis model. This diagram illustrates how a dendritic filopodium captures an axonal terminal and becomes a spine. *Adapted from Yuste and Bonhöffer., 2004*.

1.2.6. Agrin signalling at the neuromuscular junction (NMJ)

Agrin has been shown to be essential for the development of the NMJ. Neuromuscular junctions are excitatory chemical synapses formed between nerve terminals of spinal cord

motor neurons and skeletal muscle fibers that use acetylcholine (ACh) as the neurotransmitter (reviewed in Nishimune, 2018). The known molecular mechanisms of agrin function at the NMJ and in the CNS are fundamentally distinct. At the NMJ, agrin is secreted from nerve terminals and binds to the postsynaptic site through the muscle-specific receptor tyrosine kinase (MuSK) and its co-receptor the low-density lipoprotein receptor-related protein 4 (LRP4) (Glass et al., 1996; Kim et al., 2008). This signalling triggers cytosolic proteins Dok-7 and Rapsyn to accumulate AChR (Apel et al., 1995, 1997; Inoue et al., 2009; Okada et al., 2006) and it promotes the formation, maturation, and maintenance of the synaptic specialization by protecting it from a synapse-dispersing activity (Kummer et al., 2006).

MuSK-deficient mice showed devastating defects in both presynaptic and postsynaptic differentiation and died at birth because of apnea (DeChiara et al., 1996). In myasthenia gravis, transmembrane proteins, AChRs, and MuSK become targets of autoantibodies (reviewed in Nishimune, 2018). Mice lacking agrin failed to maintain neuromuscular junctions, whereas neuromuscular synapses differentiated largely in the absence of Ach (Gautam et al., 1996; Misgeld et al., 2005). In line with this, transgenic overexpression of neurotrypsin in motoneurons led to NMJ disassembly and thus muscle fibre denervation, which was followed by degeneration and eventually the loss of the affected muscle fibres. Neurotrypsin, which is the unique agrin-cleaving protease in the CNS, was excluded as the physiological agrin-cleaving protease at the NMJ, as NMJ maturation was normal in neurotrypsin-deficient mice (Bolliger et al., 2010).

1.3. Impact of neurotrypsin on learning and memory

1.3.1. LTP in neurotrypsin knockout mice

Activity-dependent synaptic plasticity is considered as a cellular mechanism underlying learning and memory. Several molecules and mechanisms were outlined since the LTP discovery. In the last two decades, ECM molecules and their receptors became recognized as crucial players in synaptic modifications (Dityatev et al., 2010), which support induction and consolidation of diverse forms of neuronal plasticity. The ECM has to be remodeled by extracellular proteases, including neurotrypsin (Gundelfinger et al., 2010). The exact role of neurotrypsin in functional synaptic plasticity is not yet defined and subject of this thesis. Because activation of NMDARs and postsynaptic Ca2+ influx are crucial for LTP induction (Malenka and Nicoll, 1999), and neurotrypsin activation appeared to be NMDAR-dependent, Matsumoto-Miyai and colleagues (2009) investigated whether neurotrypsin may play a role in

LTP expression. They tested LTP in acute hippocampal slices of 4- to 6-week old wild-type and neurotrypsin-deficient mice. Interestingly, TBS-induced LTP was not impaired in neurotrypsin-deficient mice, indicating that neurotrypsin was not essential for LTP expression (**Fig. 1.7A**). However, it is extremely intriguing that LTP-induced generation of filopodia was abolished in neurotrypsin-deficient mice (Matsumoto-Miyai et al., 2009, **Fig. 1.7B**).

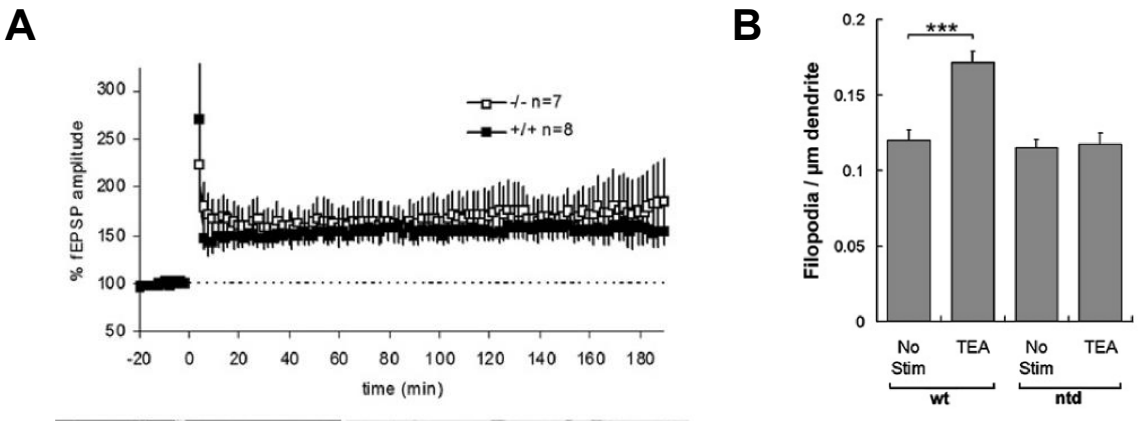

Fig. 1.7 | LTP is intact, but LTP-associated formation of filopodia is abolished in neurotrypsin-deficient mice. LTP and LTP-associated promotion of dendritic filopodia were assessed in hippocampal slices of 4- to 6-week-old neurotrypsin-deficient mice. **(A)** LTP was studied by stimulation of the Schaffer collaterals and electrophysiological recordings of Schaffer collateral-CA1 synaptic responses. Test stimuli were delivered at 30 s intervals and LTP was induced by delivering four 1 s 100 Hz trains at 30 s intervals. Comparison of LTP in the hippocampal CA1 area of neurotrypsin-deficient (white squares) and wild-type (black squares) mice. Data are shown as mean ± SEM. The results indicate that neurotrypsin-deficient mice have normal LTP. **(B)** Comparison of filopodia formation after TEA stimulation (a chemical LTP inducer which also induces normal LTP to both wild-type and neurotrypsin-deficient mice) in wild-type (wt) and neurotrypsin-deficient mice (ntd). Error bars indicate SEM. *Adapted from Matsumoto-Miyai et al., 2009*.

Krámar et al., 2012 reported that a second theta-burst stimulation (TBS2) applied at least 60 minutes after the first TBS (TBS1) doubled the level of potentiation (**Fig. 1.8A**) and induced actin polymerization in more synapses, as compared to TBS1 (**Fig. 1.8B**), supporting the idea that a new population of synapses was potentiated by TBS2. This spaced form of LTP is accompanied by filopodia generation and their conversion into functional synapses and has the potential to be impaired in mice lacking neurotrypsin.

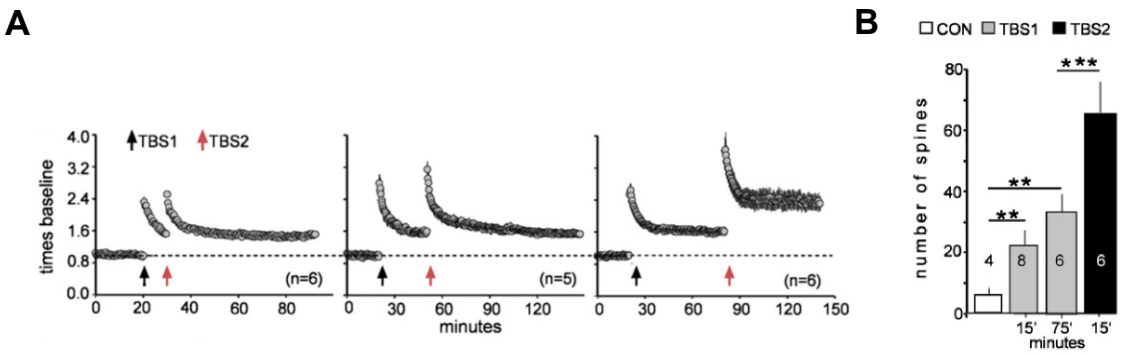

Fig. 1.8 | Timing determines the efficacy of a second theta train in eliciting additional potentiation and expanding the pool of F-actin-enriched spines. (A) A second theta burst train (TBS2) does not produce additional potentiation when applied 10 min (*Left*) or 30 min (*Center*) post-TBS1 but is effective when applied after a 60 min delay (*Right*). Y-axis: fold change in the slope of field (f)EPSP relative to the pre-TBS1 baseline: means ± SEMs. **(B)** Counts of densely phalloidin-positive spines in slices collected 15 or 75 min after TBS1 (grey bars) or 15 min after TBS2 delayed by 60 min (black bar). *Adapted from Krámar et al., 2012*.

1.3.2. Memory assessment in neurotrypsin knockout mice

Behavioural testing has been extensively used to achieve a better comprehension of learning and memory. Formation of lasting memories is critically dependent on the formation and structural reorganization of synapses, requiring a synchronized adjustment of pre- and postsynaptic structures, including the cytoskeleton, several membrane receptors, and the ECM. Indeed, the dynamic arrangement of cell surface molecules, including integrins, cadherins, and IgCAMs has been strongly implicated in memory formation (Dityatev et al., 2008; Senkov et al., 2006). Moreover, several studies revealed that reorganization of the ECM is critical for the formation and stability of different forms of memory (Dityatev et al., 2010). Neurotrypsin may also play such a role. This is because neurotrypsin regulates the generation of new dendritic filopodia upon coincident pre- and postsynaptic activation (Matsumoto-Miyai et al., 2009), which is a first step to the formation of new spine synapses, and as such may be crucial for memory formation (Yuste and Bonhoeffer, 2004).

In all behavioural tests, the responses of the experimental subjects towards a stimulus or an environment are measured. These responses are subsequently analyzed and interpreted as the presence or absence of a successful learning and/or memory recollection episode. However, those responses do not rely exclusively on the learning and memory capabilities of the experimental subjects, but also on its general health status, reflexes, motor skills, emotional condition, anxiety and all physiological conditions that may affect the behaviour of

the experimental subject. Hence, several aspects such as anxiety-like behaviour, innate fear response, and social interactions should be considered before performing a memory behavioural test. A large set of rodent behavioural tasks are used to examine these features before testing learning and memory abilities, and thus to better understand their influence on the performance in cognitive tests.

1.3.2a Open-field

The open field test was first introduced in 1934 as a measure of emotional behaviour in rats (Hall, 1934). However, it was later proved to be equally applicable in mice (Christmas and Maxwell, 1970). During the test, the experimental subject is exposed to an unknown environment (an arena) and its escape is blocked by surrounding walls (Walsh and Cummins, 1976). Anxiety in this test is triggered by agoraphobia, due to the brightly lit and, unprotecting and novelty of the environment, which is also very large considering the animal's usual home cage. Rodents typically spend a significantly higher amount of time exploring the periphery of the arena, frequently in contact with the walls, than the unprotected central area. Mice that spend significantly more time exploring the unprotected central area exhibit anxiolytic-like baseline behaviour. Thus, this test allows to systematically assess anxiety levels, novel environment exploration, general locomotor activity, and stereotypical behaviour and provides an initial screening for general well-being of the rodents (Prut and Belzung, 2003).

1.3.2b Pavlovian fear conditioning

Associative learning is an adaptive process that grants an organism to learn to anticipate actions and events by learning. Ivan Pavlov described it firstly nine decades ago (Pavlov, 1927). Pavlovian fear conditioning is a form of associative learning that has been extensively studied in many species (Kim and Jung, 2006). In fear conditioning tests, the dependent measure is the freezing response that follows pairing of an unconditioned stimulus (UCS) such as a foot shock, with a conditioned stimulus (CS), such as a particular context or an auditory cue. These tests are a commonly used paradigm to investigate memory and emotional learning in rodents as they evoke robust associative learning (Johansen et al., 2011; Maren et al., 2013). Fear conditioning tests induce fear responses in the experimental subjects with two types of CS, cued and contextual, each engaging different brain areas. Contextual fear memory has indicated to be hippocampus- and amygdala-dependent and cued fear memory is hippocampus-independent but amygdala-dependent (Kim and Fanselow, 1992). Here,

animals are trained to associate a foot shock with either a context (contextual fear conditioning) or/and a tone (cued fear conditioning). During contextual fear conditioning, animals must first form a representation of the context. After it has been encoded, context representations can be associated with other events, such an aversive foot shock, UCS. Therefore, in a contextual fear conditioning test, the experimental subjects first encode a representation of the context and then associate it with the UCS. Cued fear conditioning procedure is similar to contextual conditioning, but instead of the context, a tone or light is used as a cue to induce the conditioning of the animal. In both tests, memory is evaluated by comparing the freezing behaviour of the subject under the conditioned condition (memory recall) *vs.* the non-conditioned or habituation session (previous to foot shocks) (Davis, 1997; Lavond et al., 1993).

Gogolla and colleagues (2009) showed that enzymatic removal of a particular part of the ECM, the perineuronal nets, leads to the instability of fear memories (Gogolla et al., 2009). Recently, it was described that mice deficient in the extracellular matrix glycoprotein tenascin-C ($TNC^{-/-}$) showed normal learning and memory in the contextual fear conditioning paradigm but impaired extinction of conditioned fear responses (Morellini et al., 2017). Endogenously expressed extracellular proteases of different families have also been involved in these processes. Essentially, it is believed that these proteases break connections and thus allow flexibility for reorganization of synaptic structures. Distinctly, tissue plasminogen activator has been involved in fear memory and spatial learning (Pawlak et al., 2005; Qian et al., 1998).

1.3.2c Novel object recognition

The novel object recognition (NOR) test is one of the most popular tests for assessing rodents' ability to identify previously presented stimuli (Ennaceur and Delacour, 1988). The NOR test consists of two sessions of 10 min. In the first session, also called training session, the animal is placed in an arena with high walls lacking polarizing spatial cues, in which two identical objects are placed and the experimental subject can explore them freely. After a specific period of time (inter-trial interval), which depends on the type of memory (short- or long-term memory) under study, the memory session (or memory recall) takes place. In the memory session, the animal is again placed in the NOR arena, but one of the objects is changed for a new one. Afterwards, the time exploring each object (familiar and novel) is measured. Because rodents are interested in novelty, significant longer exploration of the new object compared to the exploration of the familiar object is interpreted as recognition of the familiar object (Vogel-Ciernia and Wood, 2015). However, despite its wide usage, the underlying

neuronal circuitry and mechanisms supporting NOR are still under investigation. Particularly, the role of rodent hippocampus in object memory remains under consideration due to controversial findings across temporary and permanent hippocampal lesions studies and current evidence that the perirhinal cortex may support this memory. Several studies reviewed by Cohen and Stackman (2015), described that the hippocampus plays a critical role for the retention of this type of memory when the interval between sessions is longer than 10 min (Cohen and Stackman, 2015). Thus, the non-conditioned nature of the novel object recognition test presents another tool to test hippocampal-dependent memory if the delay between sessions is longer than 10 minutes.

1.3.2d Sociability

Social interactions are fundamental to many species, including mice. Under natural circumstances, mice prefer to spend time investigating and exploring another mouse, thus demonstrating a sociability (Hartmann et al., 2012; Masana et al., 2014). Alterations in social behaviour are symptoms of several neuropsychiatric and neurological diseases such as autism spectrum disorders, anxiety disorders, depression, bipolar disorders, and schizophrenia (reviewed by Zimprich et al., 2017). A widely used method to measure sociability, also named social affinity or social approach behaviour, is the three-chamber sociability test (Moy et al., 2004). The procedure consists of two phases: the adaptation to the three-chamber apparatus (habituation phase) and the test (sociability phase), each lasting 10 min. In the habituation phase, the experimental subject is familiarized with the empty apparatus. During this phase, the side preference can be measured and used to control that there are no basal preferences for a certain chamber. During the sociability phase, the experimental mouse has the free choice to explore the central chamber, the “non-social” chamber, which contains an empty cylinder, and the “social” chamber, which contains a cylinder with an unfamiliar mouse (stimulus mouse) inside. The tendency to approach or avoid the compartment with the stimulus mouse provides a measure of sociability (reviewed in Zimprich et al., 2017).

1.3.3. Truncating neurotrypsin mutation in autosomal recessive non-syndromic mental retardation and neurotrypsin-related diseases in the CNS

Moderate to severe mental retardation (MR), which is defined as intelligence quotient (IQ) score below 50 (IQ<50), affects 0.3 to 0.8% of the population and its prevalence increases up

to 2% if mild MR is included (50<IQ<70) (Roeleveld and Zielhuis, 1997). There are several causes of MR and they include environmental factors or teratogens, metabolic diseases impairing neuronal function, and chromosomal abnormalities (Stromme, 2000). Conversely, MR with seemingly normal brain development and no other clinical symptoms like non-syndromic mental retardation represents the most common cognitive dysfunction. As the condition is so heterogeneous and there is a lack of large pedigrees for its genetic analysis, this form of mental retardation is still poorly understood (Molinari et al., 2002). Molinari et al., 2002 described that a 4-nucleotide deletion in the neuronal serine protease neurotrypsin gene was associated with autosomal recessive non-syndromic mental retardation. They investigated an Algerian family with four healthy children and four mentally retarded children, which were homozygous for a 4-base pair (bp) deletion in exon 7 of the PRSS12 gene. This 4-nucleotide deletion resulted in a frameshift and led to a premature stop codon, 147 nucleotides downstream of the deletion. As a consequence, the third SRCR domain of neurotrypsin was shortened and ill-folded and the fourth SRCR and the protease domain were eliminated (**Fig. 1.9B**). Restriction analyses revealed co-segregation of the mutation with the disease in all affected individuals, and that both parents were heterozygous. Interestingly, these children had normal psychomotor development in their first 2 years but became mentally retarded thereafter. The same 4-nucleotide deletion was detected in another child, apparently unrelated to the previous family, but originating from the same area of Eastern Algeria (Molinari et al., 2002).

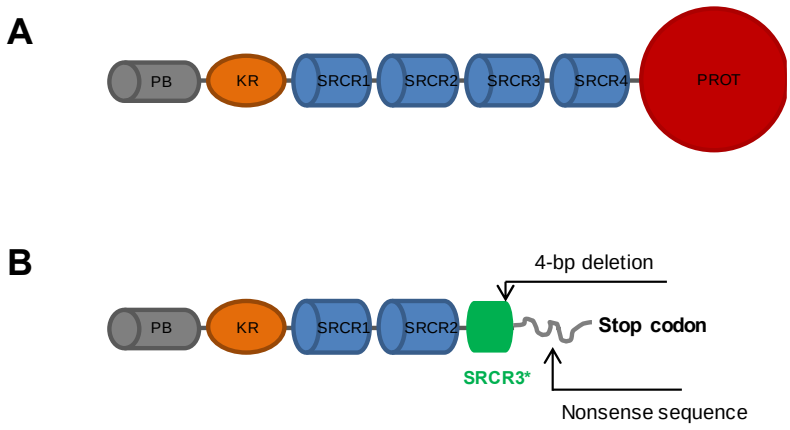

Fig. 1.9 | Schematic representation of neurotrypsin domains. (A) Scheme of neurotrypsin; PB, proline-rich basic segment; KR, kringle domain; SRCR1-4, scavenger receptor cysteine-rich domain; PROT, serine protease domain. **(B)** Representation of truncated neurotrypsin after 4-base pair deletion in exon 7 of PRSS12 gene: the deletion causes a frameshift resulting in a nonsense sequence producing an ill-folded SRCR-3 domain and an earlier stop codon.

There is also another devastating disease in which neurotrypsin function in the brain is disrupted. This pathology, named infantile neuronal ceroid lipofuscinosis (INCL), is a neurodegenerative lysosomal storage disease caused by mutations in the ceroid lipofuscinosis neuronal-1 gene (CLN1) (Vesa et al., 1995), which is encoding palmitoyl-protein thioesterase-1 (PPT1) (Camp et al., 1994). Cln1-deficient ($Cln1^{-/-}$) brains, which mimic INCL, and postmortem brain tissue from INCL patients show higher oxidative stress levels. Recently, Peng and coauthors (2015) revealed that $Cln1^{-/-}$ mice oxidative stress in the brain is due to upregulation of the transcription factor CCAAT/enhancer-binding protein-δ, which stimulates expression of serpina1, which is an inhibitor of neurotrypsin. Moreover, they described that the high levels of serpina1 in $Cln1^{-/-}$ brains resulted in a reduced production of agrin-22. Treatment of these mice with an antioxidant thioesterase-mimetic small molecule, N-tert (Butyl) hydroxylamine (NtBuHA), increased agrin-22 levels. Since agrin-22 has an essential role in synaptic homeostasis, the authors believe that this abnormality, at least in part, contributed to synaptic dysfunction in $Cln1^{-/-}$ mice (Peng et al., 2015).

2. OBJECTIVES

As explained above, neurotrypsin is a nervous system-specific serine protease, which is stored in presynaptic terminals and, in association with presynaptic action potential (AP) firing, is secreted to the extracellular space in an inactive form (Frischknecht et al., 2008). Its activation requires an NMDAR-dependent postsynaptic mechanism (Matsumoto-Miyai et al., 2009). Activated neurotrypsin cleaves agrin and releases a 22 kDa fragment (Stephan et al., 2008) which inhibits the neuronal α3-subtype of the Na^+/K^+-ATPase (α3NKA) (Hilgenberg et al., 2006a) and induces the formation of new dendritic filopodia (Matsumoto-Miyai et al., 2009).

However, this is the valid model for neurotrypsin-dependent agrin cleavage *in vitro*. Relatively little is known about the relevance of neurotrypsin-dependent mechanisms *in vivo*. The general objective of this thesis is to study the influence of the neurotrypsin proteolysis dependent signalling pathway on learning and memory formation from the cellular to the systemic level. The specific objectives are as follow:

- Evaluate the relevance of neurotrypsin-dependent mechanisms for functional synaptic plasticity.
- Identify memory processes and phases sensitive to disruption of neurotrypsin.
- Examine the putative involvement of neurotrypsin in social behaviour.
- Study how neurotrypsin affects spinogenesis and spine morphology in naïve conditions and upon learning.

3. MATERIALS AND METHODS

3.1. Animals

All experiments and behavioural procedures were conducted in accordance with animal research ethics standards defined by German law and approved by the Ethical Committee on Animal Health and Care of the State of Saxony-Anhalt (TVA 2502-2-1159 and 42502-2- 1343).

Mice constitutively lacking the exons 10 and 11 from the neurotrypsin gene ($NT^{-/-}$) (Reif et al., 2007) and their wild-type littermates ($NT^{+/+}$) were backcrossed to C57BL/6J mice for > 9 generations. $NT^{-/-}$ and $NT^{+/+}$ mice for experiments were obtained by mating male and female $NT^{+/-}$ mice. NT mice were kindly provided by Dr. Renato Frischknecht from Leibnitz-Institut für Neurobiologie (LIN) in Magdeburg. Heterozygous neurotrypsin ($NT^{+/-}$) mice were crossbred with Thy1-EGFP-$M^{+/-}$ mice, which were purchased from Jackson Laboratory (https://www.jax.org/strain/007788). $NT^{+/+}$/Thy1-EGFP-$M^{+/?}$ and $NT^{-/-}$/Thy1-EGFP-$M^{+/?}$ mice for experiments were obtained by mating male and female $NT^{+/-}$/Thy1-EGFP-$M^{+/-}$ mice.

C57BL/6J, NT, Thy1-EGFP-M and NT/Thy1-EGFP-M mice were bred at the animal facility of DZNE Magdeburg. For electrophysiological experiments, we used $NT^{-/-}$ and $NT^{+/+}$ 4-week-old mice from both sexes. For behavioural experiments, we used males $NT^{-/-}$, $NT^{+/+}$, $NT^{-/-}$/Thy1-EGFP-$M^{+/-}$ and $NT^{+/+}$/Thy1-EGFP-$M^{+/?}$ 3- to 5-week-old mice. For immunohistochemistry and spine imaging, we used $NT^{-/-}$/Thy1-EGFP-$M^{+/-}$ and $NT^{+/+}$/Thy1-EGFP-$M^{+/?}$ 3- to 4-week-old mice from both sexes. For viral injections, we used $NT^{-/-}$/Thy1-EGFP-$M^{+/?}$ P7 mice from both sexes.

Mice were kept in a reverse light-dark cycle (12:12 hours, light on at 9:00 pm) with food and water *ad libitum* and were transferred weekly into fresh cages. All experiments were carried out during the dark phase of the cycle, i.e. when mice are active.

For behavioural and spine imaging experiments, mice were individually housed at least 3 days prior to the start of the experiments. For electrophysiological experiments, mice were housed in groups of 3-4 mice per home cage. All behavioural tests were analysed manually twice and the mean values were plotted in graphs. Behavioural analysis was performed by an experimenter blinded to group identity. After the open field test, few mice of both genotypes were discarded for subsequent cognitive behavioural tasks, as they were not properly habituated to the arena, showing signs of nervousness, anxiety and agitation. Most likely, due to its young age. Number of mice used for each experiment are detailed in figure legend. From these numbers, only outliers were removed. Outliers were excluded from graphs and subsequent statistical analysis using the GraphPad outlier calculator software

(https://www.graphpad.com/quickcalcs/Grubbs1.cfm). For spine imaging experiments (see Results 4.3), mice from the same litter were randomly allocated into three experimental groups (naïve, CFC, extinction). For viral injections (see Results 4.4), mice from the same litter were randomly allocated into two experimental groups (AAV-Ag15 or AAV-Ag22). Injections were performed as following: 1 mouse injected with AAV-Ag15 – 1 mouse injected with AAV-Ag22 – etc., Postnatal day 7 mice were randomly picked up by its tail from the nest.

3.2. Electrophysiological recordings in hippocampal slices *(in collaboration with Jenny Schneeberg)*

3.2.1. Preparation of acute brain slices

Acute hippocampal slices were prepared from $NT^{-/-}$ and $NT^{+/+}$ 4-week-old mice. Each mouse was killed by cervical dislocation, followed by decapitation. The brain was removed from the skull and transferred into ice-cold artificial cerebrospinal fluid (ACSF), saturated with carbogen (95% O_2/5% CO_2) containing (in mM) 250 sucrose, 25.6 $NaHCO_3$, 10 glucose, 4.9 KCl, 1.25 KH_2PO_4, 2 $CaCl_2$, and 2.0 $MgSO_4$ (pH 7.3). Both hippocampi were dissected out and sliced transversally (400 µm) using a tissue chopper with a cooled stage (custom-made by LIN, Magdeburg, Germany). Slices were kept at room temperature in carbogen-bubbled ACSF (95% O_2/5% CO_2) containing 124 mM NaCl instead of 250 mM sucrose for at least 2 h before the start of recording.

3.2.2. Extracellular recordings of spaced LTP

Recordings were performed in the same solution in a submerged chamber that was continuously superfused at 32°C with carbogen-bubbled ACSF (1.2 ml/min). Recordings of field excitatory postsynaptic potentials (fEPSPs) were performed in CA1a and CA1c with a glass pipette filled with ACSF to activate synapses in CA1b *stratum radiatum*. The resistance of the pipette was 1-4 MΩ. Stimulation pulses were applied to Schaffer collaterals via a monopolar, electrolytically sharpened and lacquer-coated stainless-steel electrode located approximately 300 µm closer to the CA3 subfield than the recording electrode. Basal synaptic transmission was monitored at 0.05 Hz and collected at 3 pulses/min. The spaced LTP protocol was performed as previously described (Kramár et al., 2012). LTP was induced by applying 5x theta-burst stimulation (TBS) with an interval of 20 s. One TBS consisted of a single train of 10 bursts (4 pulses at 100 Hz) separated by 200 ms and a width of the single

pulses of 0.2 ms. To induce the spaced LTP, we applied two trains of TBS (TBS1/TBS2) separated by 1h. The stimulation strength was set to provide baseline fEPSPs with slopes of approximately 50% of the subthreshold maximum. The data were recorded at a sampling rate of 10 kHz and then filtered (0-5 kHz) and analysed using IntraCell software (custom-made, LIN Magdeburg, Germany).

3.3. Behavioural tests

All experiments were done under uniform illumination (30 lux) and all behaviour was video recorded using a USB video camera and analysed using ANY-maze software (ANY-maze, version 4.99, Stoelting Co., Wood Dale, IL). All recorded movies were analysed by a trained observer blinded to the groups.

3.3.1. Open field

The open field test apparatus was made out of white polyacrylics and consisted of a white square arena (50 x 50 x 30 cm, **Fig. 3.1**). Experimental subjects were carried to the testing room in their home cages at least 30 minutes before the beginning of the experiment. Mice were placed in the centre of the open field and allowed to freely explore it for 10 min. First 5 minutes were used for analysis of the following behavioural parameters: time spent in the inner area (central zone, blue square in **Fig. 3.1**) and in the outer area (periphery) of the open field arena, locomotor activity (total travelled distance), average speed, immobility time, grooming activity (including washing or mouthing of forelimbs, hind paws, face, body and genitals) and number of defecations (number of faecal boli produced). Before the start of each session and between animals, the open field test apparatus was carefully wiped with a 70% alcohol solution.

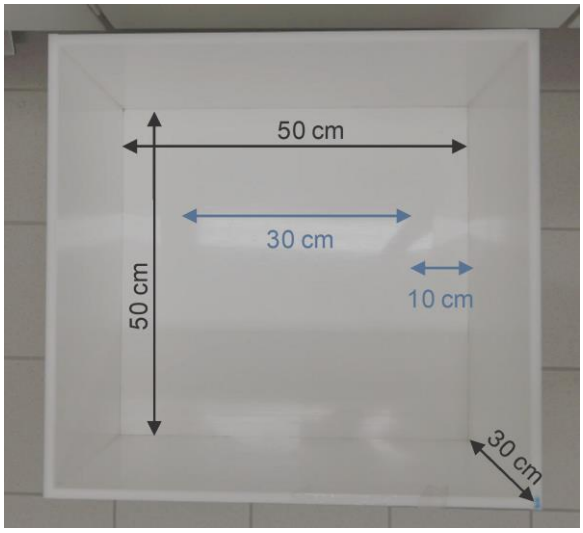

Fig. 3.1 | Open field test apparatus. Blue area marks out the central area (30 x 30 cm). Outer area (periphery) consists of 10 cm ring close to walls.

3.3.2. Spaced contextual fear conditioning

A spaced contextual fear conditioning paradigm was performed as previously described (Senkov et al., 2006) with small modifications of the protocol to split the learning session (training session) into two sessions separated by 1 h. Before CFC training, mice were handled and habituated to the experimental room and conditions in a neutral context (home cage) during 3 days for 5 min each day. During the training day (day 0, d0), CFC was performed as follows: mice were placed into a neutral context (CC-) for 5 min (the first min was taken as the baseline, see **Fig. 4.3D**). Two hours later, mice were placed into a conditioned context (CC+) for 2.5 min and 3x medium intensity foot shocks were applied (0.5 mA, 1 s) with an interval of 30 s. This procedure was repeated 1 h later (spaced learning): mice were placed again into a conditioned context (CC+) for 2.5 min and 3x medium-intensity foot shocks were applied (0.5 mA, 1 s) with an interval of 30 s. The protocol included 1-min exploration of CC+ (the freezing level during this time was taken as the baseline, see **Fig. 4.3D**) then first shock, after 30 s second shock, and again after 30 s the third shock. Mice were then given another 30 s in CC+ before being removed. The conditioned context (CC+) was a chamber (20 × 20 × 30 cm) with contrast black-and-white chess-like pattern on the walls and a metal grid on the floor. The neutral context (CC−) was the same chamber, but with grey walls and grey plastic floor. Memory retrieval was performed at d2 and for that mice were placed in CC+ for 5 min to assess the retention of contextual memory. Subsequently, 9x memory extinction sessions were performed in 3 consecutive days (d5-d7, 3x sessions per day). In each session, mice were placed in CC+ for 5 min. At d9, mice were placed again in CC+ for 5 min (second memory

retrieval) and freezing was assessed to evaluate fear memory extinction (see **Fig. 4.3A** for scheme and timeline of the experimental set-up). For CFC, we used a computerized fear conditioning system (Ugo Basile, Gemonio, Italy). Before the start of each session and prior to bringing the next animal, the fear conditioning apparatus was carefully wiped with a 75% alcohol solution (CC+) and with another cleaning solution with a different smell (CC-), to facilitate discrimination between both contexts. The total freezing time was manually calculated as the percentage of 5 min when animals show no movement except for breathing. In the spaced CFC test, the discrimination ratio was calculated as follows: [freezing time in CC+ – freezing time in CC-] / [freezing time in CC+ + freezing time in CC-] x 100%.

3.3.3. Contextual fear conditioning

A classical Pavlovian contextual fear conditioning (CFC) paradigm was used. Before CFC training, mice were handled and habituated to the experimental room and conditions in a neutral context (home cage) during 3 days for 5 min each day. CFC was performed at day 0 (d0) as follows: mice were placed into a conditioned context (CC+) for 5 min and 3x medium intensity foot shocks were applied (0.5 mA, 1 s) with an interval of 1 min. The protocol included 2-min exploration of CC+ (the freezing level during this time was taken as the baseline, see **Fig. 4.4C**), then the first shock, after 1 min the second shock, and again after 1 min the third shock. Mice were then given another minute in CC+ before being removed. The conditioned context (CC+) was a chamber (20 × 20 × 30 cm) with contrast black-and-white chess-like pattern on the walls and a metal grid on the floor. 24 h later, on d1, mice were placed in CC+ for 5 min to assess the retention of contextual memory (retrieval session). Subsequently, 9x memory extinction sessions were performed in 3 consecutive days (3x sessions per day). In each session, mice were placed in CC+ for 5 min. At d5, mice were placed again in CC+ for 5 min (second retrieval session) and freezing was assessed to evaluate fear memory extinction (see **Fig. 4.4A** for scheme and timeline of the experimental set-up).

Also for this protocol, we used a computerized fear conditioning system (Ugo Basile, Gemonio, Italy). Before the start of each session and between animals, fear conditioning apparatus was carefully wiped with a 75% alcohol solution. The total freezing time was calculated as the percentage of 5 min. In the CFC test, the discrimination ratio was calculated as follows: [freezing time in CC+ – freezing time in CC-] / [freezing time in CC+ + freezing time in CC-] x 100%.

3.3.4. Novel object recognition

The same apparatus (50 x 50 x 30 cm) used for the open field test was used in the novel object recognition test. Experimental subjects were carried to the testing room in their home cages at least 30 minutes before the beginning of the experiment. The test was performed using a standard protocol (Leger et al., 2013) that included two phases: a familiarization/encoding phase and a test/retrieval phase. Mice were habituated to the apparatus 2 days before familiarization for 10 minutes each day. During familiarization, mice were placed for 10 minutes in the arena and were allowed to freely explore two identical objects positioned in the centre of the arena, separated by 25 cm. During retrieval phase, one familiar object and one novel object were placed in the centre of the arena and mice were allowed to explore the apparatus for 10 minutes (see **Fig. 4.5A** for scheme and timeline of the experimental set-up). In the same trial, objects were counterbalanced between mice, and between trials, different sets of objects were used. The interval between the encoding and retrieval phases was 24 hours. Before the start of each session and prior to bringing the next animal, the novel object recognition test apparatus was carefully wiped with a 70% alcohol solution. The exploration time for each object and the total exploration time were manually estimated. Exploration was considered when the orientation of the animal's snout was at a distance <2 cm toward the object, and the time spent sniffing and directly touching the object. Novelty detection was evaluated by calculating the discrimination ratio as follows: [novel object time – familiar object time] / [novel object time + familiar object time] x 100%.

3.3.5. Three-chamber sociability test

Sociability levels were assessed using the three-chamber sociability test. The three-chamber apparatus (60 x 30 x 30 cm, **Fig. 3.2**) was made out of white polyacrylics and had connecting doors between chambers as shown in **Fig. 4.6A** and **Fig. 3.2**. The test was performed using a standard protocol (Kaidanovich-Beilin et al., 2011): mice were habituated to the apparatus for 10 minutes 2 hours before the test. Subsequently, one stimulus mouse was placed inside a small cage in one end of the compartments and an empty cage was placed in the opposite compartment. The mouse performing the test was allowed to explore the whole apparatus for 10 minutes. The exploration times spent at the cage containing the stimulus mouse and at the empty cage were estimated. The time spent sniffing and directly touching the mouse and the empty cage was considered as exploration time. As active social interaction is difficult to track automatically and hard to distinguish from just spending time close to the social partner, the analysis to score the social interaction was done manually. In the three-chamber sociability

test, the discrimination ratio was calculated as follows: [stimulus mouse time – empty cage time] / [stimulus mouse time + empty cage time] x 100%. Before the start of each session and prior to bringing the next animal, the three-chamber sociability test apparatus was carefully wiped with a 70% alcohol solution and stimulus mice were changed every two sessions to avoid anxiety and stress.

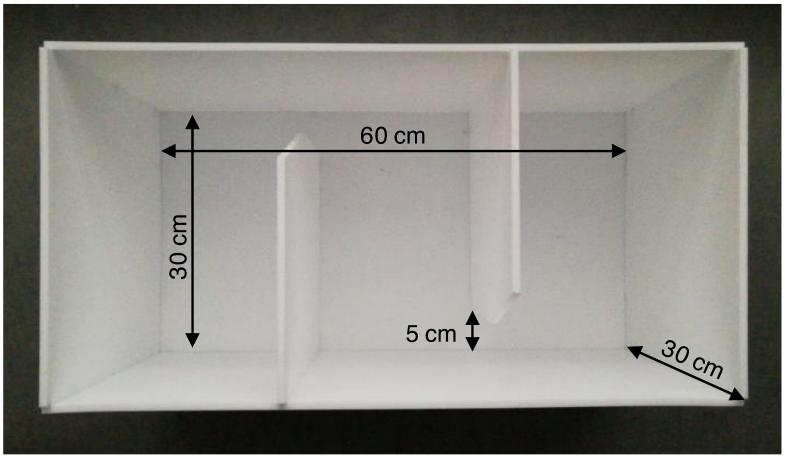

Fig. 3.2 | Three-chamber sociability test apparatus.

3.4. Spine analysis

3.4.1. Sample collection, perfusion and tissue processing

Mice were individually anaesthetized with 3-5% Isoflurane (Baxter, Germany) and transcardially perfused with 0.1 M phosphate buffer solution (PBS, pH 7.4) followed by 4 % formaldehyde diluted in 0.1 M phosphate buffer solution for 15 min. Brains were removed, post-fixed for 24 h in 4% formaldehyde-PBS at 4°C. The brains were then transferred to a sucrose solution (1 M in 0.1 M NaH2PO4 buffer) until the solution had infiltrated into the whole brain (~48 h) in order to cryoprotect the tissue. Finally, the brains were frozen in 100% 2-methylbutan at -80ºC and cryo-sectioned in 50-μm-thick coronal sections. Floating sections were kept in cryoprotective solution (1 part of ethylenglycol, 1 part of glycerin, 2 parts of PBS, pH 7.4). All sections were washed 3x in 0.1 M phosphate buffer solution (PBS, pH 7.4) for 10 min with gentle shaking. Subsequently, sections were shorty washed in bi-distilled water to remove salts from PBS and mounted on SuperFrost glasses with Fluoromount (Sigma F4680).

3.4.2. Spine imaging and deconvolution

Images were acquired using a confocal laser-scanning microscope (LSM 700, Carl Zeiss, Germany) and Zen software (Carl Zeiss, Jena, Germany). Spine imaging was performed on segments of hippocampal CA1 secondary proximal dendrites, which express EGFP in NT/Thy1-EGFP-M mice. Z-stacks were taken using an oil 63x objective (NA = 1.4) with a Z-step of 0.21µm, and 2.6x optical zoom. The following voxel size was used: 0.0644 x 0.0644 x 0.2065 µm. Deconvolution of images was performed using Huygens deconvolution software (Scientific Volume Imaging) (**Fig. 3.3**). The images were deconvolved using the "Classic Maximum Likelihood Estimation (CMLE)" algorithm implemented in Huygens software (Scientific Volume Imaging), set with 50 iterations, a quality threshold of 0.01 and an SNR (signal-to-noise ratio) value of 25. A theoretical point spread function was used.

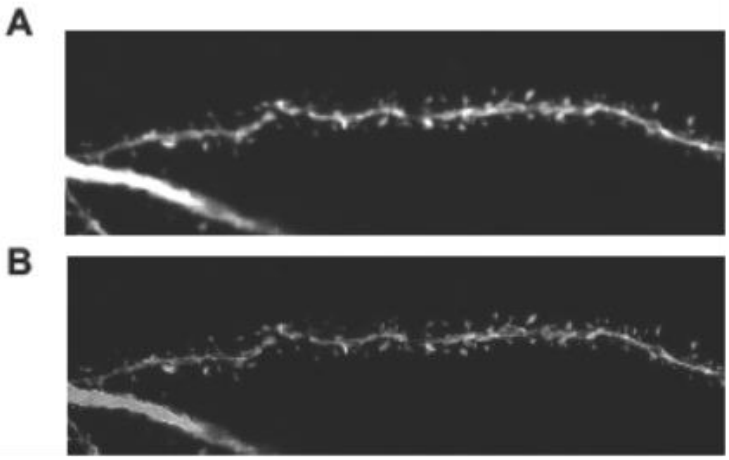

Fig. 3.3 | CA1 secondary proximal apical dendrite before and after deconvolution. (A) Representative image from a CA1 apical dendrite before deconvolution. **(B)** Representative image from a CA1 apical dendrite after deconvolution with Huygens deconvolution software.

3.4.3. Spine density and morphology analysis

To identify, classify, and count dendritic spines, images were morphometrically analysed using NeuronStudio software (CNIC, Mount Sinai School of Medicine, New York, NY, USA, **Fig. 3.4**) and a custom-written Excel worksheet template to count the parameters provided by the NeuronStudio software. Analysis was done by an experimenter blinded to group identity. Spines along the dendrites were assessed using standard parameters for the distinction of stubby, filopodia-like/thin, and mushroom-type spines, as previously described (Rodriguez et

al., 2008; Sigler et al., 2017). Parameters were kept as suggested (Rodriguez et al., 2008). Briefly, NeuronStudio classifies spines into either stubby, thin, or mushroom. This classification scheme makes use of each spine's head to neck diameter ratio, length to head diameter ratio, and head diameter to determine its proper type. “Neck ratio”: spines with head to neck diameter ratio greater than 1.1 were considered thin or mushroom. “Thin ratio”: spines that do not meet the neck ratio value and have a length to spine to head diameter above 2.5 are classified as thin, otherwise as stubby. “Mushroom size”: spines that meet the neck ratio value and have a head diameter equal or greater than 0.35 μm are labelled as mushroom, otherwise as stubby. Only protrusions with a clear connection of the head of the spine to the shaft of the dendrite were counted as spines. In addition, visual examination was also used to detect false ‘‘spine calls’’. This systematic approach was chosen to account for possible changes in spine distribution along dendrites. **Fig. 3.5** shows examples of each spine type in $NT^{+/+}$/Thy1-EGFP-$M^{+/?}$ and $NT^{-/-}$/Thy1-EGFP-$M^{+/?}$ mice.

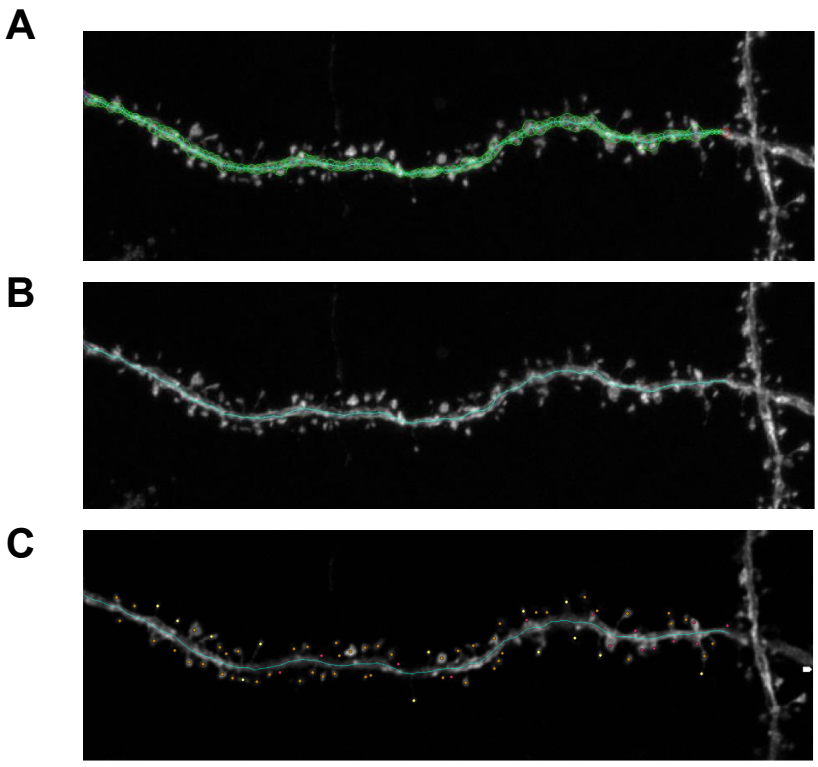

Fig. 3.4 | Spine analysis using NeuronStrudio software. (A) Semi-automatic tracing of the dendrite shaped as hollow ellipses. **(B)** Semi-automatic tracing of the dendrite shaped as solid lines, which we used for visualization of the dendrite trace. **(C)** Semi-automatic dendritic spine detection. This image shows the same dendritic segment from A and B after spine detection and classification (pink dots for stubby spines, orange dots for mushroom spines, and yellow dots for thin spines).

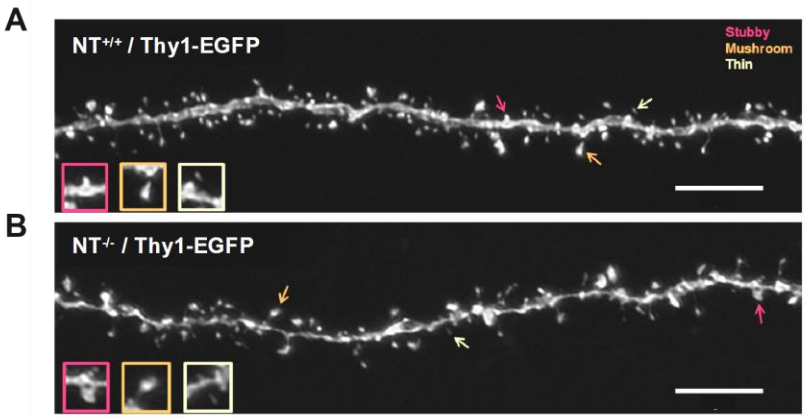

Fig. 3.5 | Representative spine morphology examples in NT$^{+/+}$/Thy1-EGFP-M$^{+/?}$ and NT$^{-/-}$/Thy1-EGFP-M$^{+/?}$ mice. (A) Representative image of CA1 secondary apical dendrite from a NT$^{+/+}$/Thy1-EGFP-M$^{+/?}$ mouse. Scale bar, 5 µm. **(B)** Representative image of CA1 secondary apical dendrite from a NT$^{-/-}$/Thy1-EGFP-M$^{+/?}$ mouse. Scale bar, 5 µm.

3.5. Agrin-expression constructs and generation of adeno-associated viral (AAV) particles *(in collaboration with Dr. Rahul Kaushik)*

Full-length (GeneID:11603) agrin constructs were obtained from Dharmacon (Accession: BC150703). The DNA sequence corresponding to C-terminus 22 kDa of agrin was used to induce spinogenesis and filopodia as previously described (Matsumoto-Miyai et al., 2009), while C-terminus 15 kDa sequence was used as a control as described previously (Hilgenberg et al., 2006b). The cDNA was amplified using primers (sequences of the primers can be found in **Table 3.1**) and cloned into AAV vector where the gene was expressed under the synapsin promoter and the red fluorescent protein scarlet was used as the fluorescent reporter (Bindels et al., 2016). In order to secrete agrin fragments into the extracellular environment, we additionally cloned a secretion signal sequence from protein Receptor Tyrosine Phosphatase Sigma (RPTP-σ) at the N-terminus of agrin sequence as described previously (Aricescu et al., 2006) to secrete it extracellularly. AAV particles were produced as previously described (McClure et al., 2011) with minor modifications. Briefly, HEK 293T cells were transfected using the calcium phosphate method with equimolar mixture of the expression plasmid, pHelper plasmid and RapCap plasmid DJ. After 48 h of transfection, cells were lysed using freeze-thaw and treated with benzonase at a final concentration of 50 units/ml for 1 h at 37°C. The lysate was centrifuged at 8000g at 4°C. The supernatant was collected and filtered with 0.2 micron filter. Filtered supernatant was passed through pre-equilibrated Hitrap Heparin columns (Cat no. 17-0406-01; Ge HealthCare Life science), followed by a wash with wash Buffer 1 (20 mM Tris, 100 mM NaCl, pH 8.0; filtered sterile).

Columns were additionally washed with wash Buffer 2 (20 mM Tris 250 mM NaCl, pH 8.0; filtered sterile). Viral particles were eluted with elution buffer (20 mM Tris 500 mM NaCl, pH 8.0; filtered sterile). Amicon ultra-4 centrifugal filter (100000 molecular weight cutoff) were used to exchange the elution buffer with sterile PBS. Finally, viral particles were filtered through 0.22 µm syringe filter (Sigma-Aldrich, product no. Z741696-100EA), aliquoted and stored at -80°C until required.

Intern. Nr.	Name	Sequence
315	AAV_Syn_Agrin-22_Scarlet_WPRE_EcoR1_Fw	5'-TAAGCAGAATTCGCCACCATGTCAGTGGGGGACCTAGAAACAC-3'
316	AAV_Syn_Agrin-22/Agrin-15_Scarlet_WPRE_Xho1_Rev	5'-TAAGCACTCGAGGAGAGTGGGGCAGGGTCTTAG-3'
317	AAV_Syn_Agrin-15_Scarlet_WPRE_EcoR1_Fw	5'-TAAGCAGAATTCGCCACCATGTGGATTGGAAAGGTTGGAGAACG-3'
318	AAV_Syn_Sec(CPTX)_Agrin-22_Scarlet_WPRE_Age1_Fw	5'-TAAGCAACCGGTTCAGTGGGGGACCTAGAAACAC-3'
319	AAV_Syn_Sec(CPTX)_Agrin-22 and Agrin-15_Scarlet_WPRE_Xba1_Rev	5'-TAAGCATCTAGACATATGGTCGACGAGCTCG-3'
320	AAV_Syn_Sec(CPTX)_Agrin-15_Scarlet_WPRE_Age1_Fw	5'-TAAGCAACCGGTTGGATTGGAAAGGTTGGAGAACG-3'

Table 3.1 | Plasmids used for amplification of agrin constructs

3.6. AAV intrahippocampal injections

$NT^{-/-}$/Thy1-EGFP-$M^{+/-}$ mice of both genders were anesthetized at postnatal day P7 with 3% Isoflurane (Baxter, Germany) delivered as a mixture with O_2 through a Vaporizer (Matrx VIP 3000, Midmark, Versailles, USA) and a custom-made mouse breathing mask suitable for P7 mouse size. The cranial skin was locally disinfected and incised, the skull was exposed by a displacement of the skin and muscles, and a small hole was drilled into the skull at the injection site. The craniotomy was performed on both hemispheres using stereotaxic information with respect to external landmarks on the skull, such as lambda and bregma, and to other distinct landmarks like characteristic blood vessels of the bone and the brain (Xiong et al., 2017) (**Fig. 3.6**), which had to be adapted to the smaller size of the young skull and brain. The following coordinates were used to target the CA1 area: ML: 1 mm; DV: 1.2mm. 500nl of viral

suspension (1.84 x 10^{11} particles/ml) were injected per hemisphere using a pulled glass micropipette (World Precision Instruments, WPI, glass capillaries with product no. 4878) and a Nanoliter injector (WPI, Nanoliter2010). To prevent backflow, the micropipette was left in the brain for 5 min before pulling up. The scalp was closed and sutured, and then the animals were allowed to recover on a heated pad. P7 pups were separated from the mother for maximum 3 h to prevent their rejection.

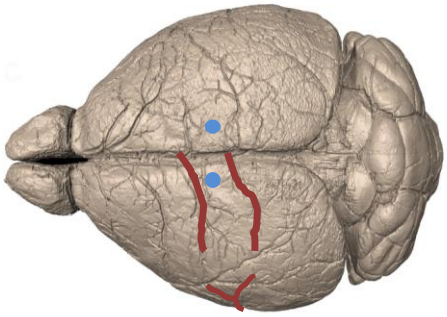

Fig. 3.6 | Schematic representation of characteristic blood vessels used as landmarks for CA1 injections in P7 mice. Blue dots show injection sites, coordinates: ML: 1 mm; DV: 1.2mm. *Adapted from Xiong et al., 2017*.

3.7. Immunohistochemistry

Sample collection, animal perfusion and tissue processing were performed as in 3.4.1. For immunohistochemistry, 40 μm free-floating sections were washed in PBS (3x 10 min, at room temperature (RT) with gentle shaking) and incubated for 1 h (at RT with gentle shaking) in a blocking and permeabilizing solution containing 5% normal goat serum (NGS, Gibco, 16210-064), 0.5% Triton X-100 (Sigma Aldrich, T9284) and 0.1% Tween-20 (Roth, 9127.1) in PBS. Subsequently, slices were treated for 24 h (at 4ºC with gentle shaking) with the primary antibody (see **Table 3.2**) in PBS containing 5% NGS, 0.5% Triton X-100 and 0.1% Tween-20. The slices were then washed 3x 10 min at RT in PBS containing 0.1% Triton X-100 and 0.1% Tween-20 (washing buffer) and incubated on a shaker for 3 hours at RT with the secondary antibody (see **Table 3.2**). Afterwards, slices were washed 3x 10 min at RT with washing buffer and 1x 10 min at RT with PBS and mounted on SuperFrost glasses with Fluoromount (Sigma F4680).

Images were acquired using a confocal laser-scanning microscope (LSM 700, Carl Zeiss, Germany) and Zen software (Carl Zeiss, Jena, Germany). Images were processed using ImageJ 1.46 software (NIH, USA).

3.7.1. Mouse antibodies

The following antibodies were used for immunohistochemistry with the protocol detailed in 3.7.:

Primary antibodies	Catalogue number and supplier	Dilution and incubation time
Mouse monoclonal anti-Sodium Potassium ATPase Alpha 3	XVIF9-G10; Novus Biologicals	1:250, 24 h 4ºC
Guinea pig anti-VGLUT1	135304; Synaptic Systems	1:1000, 24 h 4ºC
Mouse anti-PSD95	Ab2723; Abcam	1:500, 24 h 4ºC
Secondary antibodies		
Alexa Fluor 488 Goat anti-Mouse	A11029; Life Technologies	1:800, 3 h RT
Alexa Fluor 488 Goat anti-Guinea pig	A11073; Life Technologies	1:800, 3 h RT
Alexa Fluor 405 Donkey anti-Guinea pig	SAB4600230; Sigma Aldrich	1:500, 3 h RT

Table 3.2 | Antibodies and conditions used for immunohistochemistry.

3.7.2. Analysis of VGLUT1-positive populations

ImageJ 1.46 software (NIH, USA) was used to perform the analysis of the size of both VGLUT1-positive and VGLUT1-positive co-localizing with AAV-Ag22 populations.

Three independent images were selected for counting. For each image, channels were separated (Image > Colour > Split channels). Then, thresholds were adjusted for each channel manually (Image > Adjust > Threshold (using Yen and Over/Under functions)). Subsequently, binary maps were created (Process > Binary > Make binary) and VGLUT1 puncta were recognized automatically as particles greater than 0.02 pixel^2 in the VGLUT1 channel (Analyse > Analyse particles > 0.02-Infinity). The size of each ROI was measured and ROIs were superimposed to the binary map of AAV-Ag22 channel. ROIs were divided into two populations: ROIs with or without co-localizing with AAV-Ag22 particles.

3.8. Statistical analyses

GraphPad Prism 7.0a (GraphPad Software Incorporated, La Jolla, USA) was used to perform all statistical analyses and generate the graphs of the obtained results. The statistical methods used to analyse the current research results are as follows:

Data normality was assessed using three different statistical tests including, **Kolmogorov-Smirnov**, **Shapiro-Wilk** and **D'Agostino-Pearson tests**. Normally distributed data which were confirmed by at least two of the aforementioned tests were further analysed using parametric tests and statistical significance was accepted if $p < 0.05$ (confidence interval of 95 %). When data did not follow a Gaussian distribution, the nonparametric Kolmogorov-Smirnov test was used for statistical analysis.

A **standard two-way ANOVA** was used for assessing how a response is affected by two factors (genotype and time, genotype and treatment, etc.). This analysis was followed by multiple comparisons using *post hoc* **Holm-Sidak test**. The following data were analysed using a standard two-way ANOVA test: LTP data, spaced CFC, CFC, NOR and spine parameters.

A **repeated measures two-way ANOVA** was used for assessing how a response is affected by two factors (genotype and time), but when one of these factors was repeated (time). This statistical test was followed by multiple comparisons using *post hoc* **Holm-Sidak test**. A repeated measures two-way ANOVA test was used to analyse the discrimination ratio between contexts in spaced CFC at both recalls.

An **unpaired two-tailed t-test** was used to compare mean values of two independent groups with normal distribution. The following data were analysed using an unpaired two-tailed t-test: open field parameters, discrimination ratio in NOR and sociability test, spines head diameter after CRC in mushroom and thin spines, spine analysis after viral injections (using dendrites as independent values) and size of VGLUT1 populations. An **unpaired one-tailed t-test** was used to compare mean values of spine density after viral injections (using animals as independent values) as our comparison of $NT^{+/+}$ and $NT^{-/-}$ mice provided the experimental hypothesis regarding the expected direction of changes in rescue experiments. Data that were not normally distributed (filopodia density and spine head size after viral injections, using dendrites as independent values) were analysed using the **Kolmogorov-Smirnov test**.

The **Kolmogorov-Smirnov test** was used to compare the cumulative frequency distributions of two data sets. This test was used to analyse the cumulative frequency plots showing the distribution of the spine density and the spine head diameter.

4. RESULTS

4.1. Juvenile neurotrypsin-deficient mice show impairment in spaced LTP in CA3-CA1 synapses

It has been reported that the level of conventional theta-burst stimulation (TBS)-induced LTP is normal in hippocampal slices from neurotrypsin-deficient mice (Matsumoto-Miyai et al., 2009). However, the conventional protocol is not suited to detect enhancement of synaptic transmission due to formation of new spines, as nascent spines are mostly silent, i.e. lack AMPA receptors (Durand et al., 1996; Isaac et al., 1995; Liao et al., 1995; Petralia et al., 1999). Hence, we developed a new paradigm to verify the importance of neurotrypsin-dependent spinogenesis for functional synaptic plasticity.

Krámar and colleagues reported that a second theta-burst stimulation (TBS2) applied at least 60 minutes after first TBS (TBS1) doubled the level of potentiation (LTP) and induced actin polymerization in more synapses, as compared to TBS1, supporting the idea that a new population of synapses was potentiated by TBS2 (Kramár et al., 2012). It is plausible to assume that the new silent synapses, induced by agrin in the response to TBS of presynaptic axons, could become potentiated in the response to the second TBS applied 1 hour after the first TBS. This time interval is necessary for recruitment of postsynaptic density components to nascent synapses, which can be used as a scaffold for recruitment of AMPA receptors. This “spaced” form of LTP induced by two 1-hour spaced TBSs is accompanied by filopodia generation and their conversion into functional synapses (Kramár et al., 2012) and we expected that it could be reduced in neurotrypsin-deficient mice. As neurotrypsin is highly expressed in the hippocampus, we tested spaced LTP in CA3-CA1 synapses (**Fig. 4.1A**).

We recorded LTP induced by two 1 h-spaced TBS in $NT^{+/+}$ and $NT^{-/-}$ mice. Two-way ANOVA revealed significant effects of genotype ($F_{(1,36)} = 5.643$, $p = 0.023$) and “number of TBS” factor ($F_{(1,36)} = 8.018$, $p = 0.0075$), i.e. a difference between the levels of LTP induced by single and double/spaced stimulation. The Holm-Sidak *post hoc* test showed statistically significant differences in LTP levels 60 minutes after application of the second theta-burst train in all groups compared with the control wild-type group that received a second TBS (*$p < 0.05$, **$p < 0.01$) (**Fig. 4.1C**). Overall, these results indicate that, although $NT^{-/-}$ and $NT^{+/+}$ mice have a similar level of potentiation after TBS1, $NT^{-/-}$ mice show no additional potentiation after TBS2, unlike $NT^{+/+}$ mice (**Fig. 4.1C,D**). This suggests that a new population of synapses induced by agrin signalling could be potentiated by TBS2.

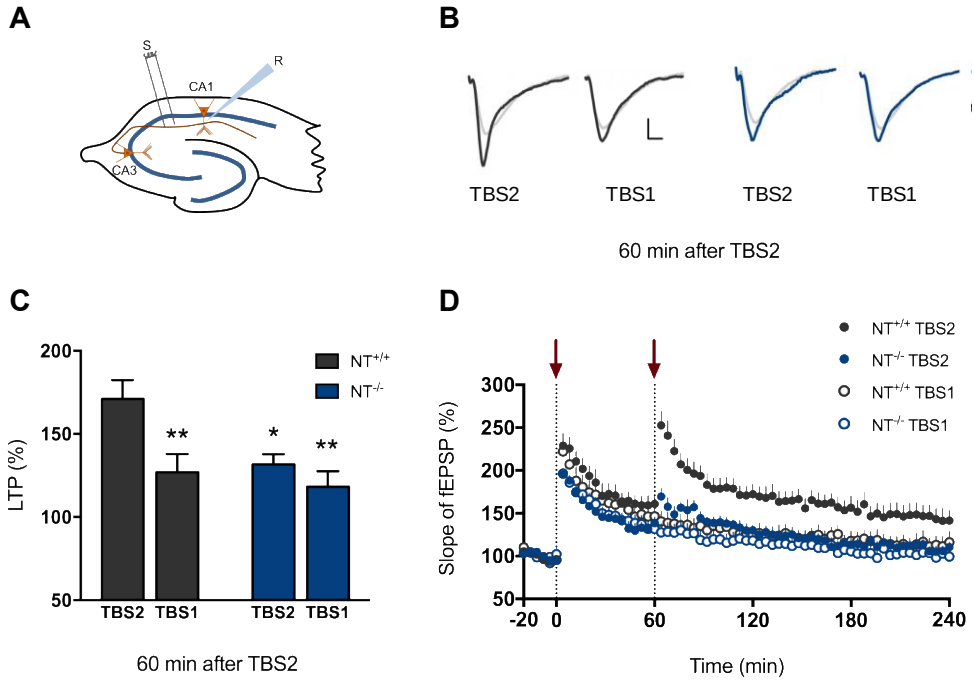

Fig. 4.1 | Spaced LTP in CA3-CA1 synapses in $NT^{-/-}$ and $NT^{+/+}$ hippocampal slices. A second theta-burst train (TBS2) does not produce additional potentiation in the $NT^{-/-}$ mice. **(A)** A schematic representation of hippocampal slice illustrating the position of both stimulating (positioned in the Schaffer collaterals) and recording (placed among apical dendrites of CA1 pyramidal cells) electrodes. **(B)** Representative traces of fEPSPs in $NT^{+/+}$ (dark grey) and $NT^{-/-}$ (blue) and their respectives baselines (light grey) 1h after TBS2 in hippocampal slices that received either 1xTBS (TBS1) or 2xTBS (TBS2). Scale bar, 0.5mV/2ms. **(C)** A bar graph summarizing mean LTP levels 60 min after TBS2. **(D)** Time courses of the slope of field excitatory postsynaptic potentials (fEPSPs) show impaired spaced LTP in neurotrypsin-deficient mice. Red arrows show time points when the first and second TBS were applied. All data are shown as mean ± SEM. The numbers of tested $NT^{+/+}$ and $NT^{-/-}$ slices/mice for each group are as follows: 12/7 ($NT^{+/+}$; 2xTBS), 10/6 ($NT^{+/+}$; 1xTBS), 9/6 ($NT^{-/-}$; 2xTBS) and 11/6 ($NT^{-/-}$; 1xTBS).

4.2. Behavioural characterization of juvenile neurotrypsin null mutant mice

In order to systematically investigate the behavioural alterations induced by the neurotrypsin null mutation and to eventually identify brain areas most prominently affected by the knockout of neurotrypsin, we focused on different behavioural paradigms and forms of memory formation. As previous experiments have implicated neurotrypsin in hippocampal plasticity, we used different hippocampus-dependent paradigms (“spaced” contextual fear conditioning, conventional fear conditioning) but also paradigms dependent on different cortical areas, such

as fear extinction, object recognition and sociability tests. These tests provided us with significant information about the relevance of neurotrypsin-mediated processes for different types of learning and behaviours.

4.2.1. Neurotrypsin-deficient mice exhibit normal anxiety-like behaviour and locomotor activity in the open field test

The open field test was used to assess anxiety levels, general locomotor activity and repetitive behaviours in $NT^{-/-}$ mice and their control littermates. Both groups of mice investigated the open field arena, spending similar time in the centre (~ 30 % of total time) ($t = 0.7217$, $df = 19$, $p = 0.4793$; **Fig. 4.2A**) and in the periphery of the arena (~ 70 % of total time) (*not shown*). Both genotypes showed similar defaecation habits during the open field test ($t = 1.635$, $df = 19$, $p = 0.1185$; **Fig. 4.2B**). We also did not find significant differences between $NT^{-/-}$ mice and their control littermates in the time spent for grooming activity ($t = 0.4353$, $df = 19$, $p = 0.6682$; **Fig. 4.2C**). Regarding general locomotor activity, both NT-deficient mice and their wild-type littermates exhibited similar distance travelled ($t = 0.6242$, $df = 19$, $p = 0.5399$; **Fig. 4.2D**), comparable average speed ($t = 0.6062$, $df = 19$, $p = 0.5516$; **Fig. 4.2E**) and equal immobility time duration ($t = 0.2809$, $df = 19$, $p = 0.7818$; **Fig 4.2F**).

Overall, these results show that neurotrypsin deficiency did not alter the general locomotor activity of these mice nor their anxiety levels, providing us with essential information to aid in the interpretation of the behavioural responses during the other behavioural tests.

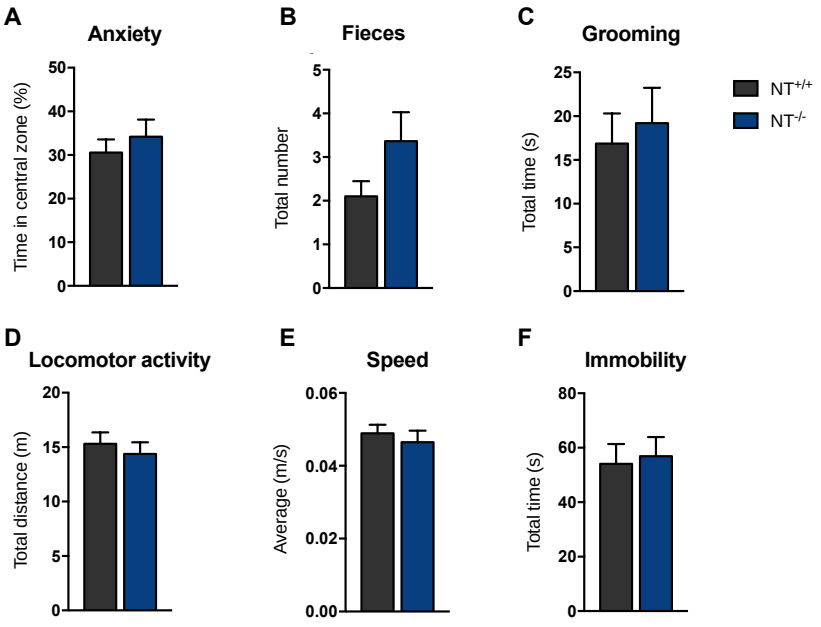

Fig. 4.2 | Behavioural parameters measured during the open field test performed by $NT^{-/-}$ and $NT^{+/+}$ mice. The following data is represented in each graph: **(A)** Time spent in the central zone of the arena. **(B)** The number of faecal boli produced during the open field test. **(C)** The time spent doing grooming. **(D)** The total distance travelled. **(E)** The average speed while travelling. **(F)** The total immobility time. The data are presented as mean ± SEM. $NT^{+/+}$, n = 10; $NT^{-/-}$, n = 11.

4.2.2 Neurotrypsin-deficient mice are less efficient in discrimination between contexts after spaced contextual fear conditioning

Learning of the context requires input from the hippocampus, particularly the dorsal part of hippocampus and CA3 region (Curzon et al., 2009), which are the same brain areas involved in the spaced LTP experiment. As neurotrypsin-deficient mice showed impairment in this previous experiment, we thought that spaced contextual fear conditioning could be a reasonable paradigm to test hippocampal neurotrypsin-dependent learning. Therefore, we designed a protocol of "spaced" contextual fear conditioning and extinction in which we applied 6x foot shocks (0.5 mA, 1 s) in the conditioned context (CC+), divided into two learning sessions (3x + 3x) with 1 hour-interval delay between both sessions (**Fig. 4.3A,C**). To evaluate fear memory, we measured freezing response (total freezing time) in the conditioned context (CC+) and in the neutral context (CC-) at day 2 (recall d2). To examine memory extinction, we analysed freezing levels at day 9 (recall d9), after 9 extinction sessions in CC+ to erase conditioned fear (**Fig. 4.3A,C**). Monitoring the freezing response in the CC- allowed us to measure the mice ability to differentiate between both contexts.

As it is shown in **Fig. 4.3D**, NT-deficiency did not affect the level of spontaneous freezing/immobility before CFC at day 0 (training) in both CC- and CC+. This level of freezing before CFC is the typical freezing level during exploration of novel environments in mice (5-10%).

Contrary to expectations, NT deficiency caused impairment neither in retrieval of contextual memory nor in memory extinction as both groups of mice were able to distinguish between the CC+ and the CC- contexts at memory recall d2 and reduced the fear response to similar levels in all genotypes and contexts at recall d9 (**Fig. 4.3E**). A two-way ANOVA revealed a significant effect of context ($F_{(1,42)} = 20.75$, $p < 0.0001$). The Holm-Sidak *post hoc* test showed significant differences in freezing levels between contexts during memory recall on d2 (*$p < 0.05$, ***$p < 0.001$).

However, $NT^{-/-}$ mice appeared to be less efficient in discrimination between contexts during the retrieval of fear memory (**Fig. 4.3B**). A two-way repeated measures ANOVA revealed a statistically significant effect of "recall day" factor ($F_{(1,21)} = 68.82$, $p < 0.0001$). The Holm-Sidak *post hoc* test showed a significant difference in context discrimination between both genotypes during memory recall on d2 (*$p < 0.05$).

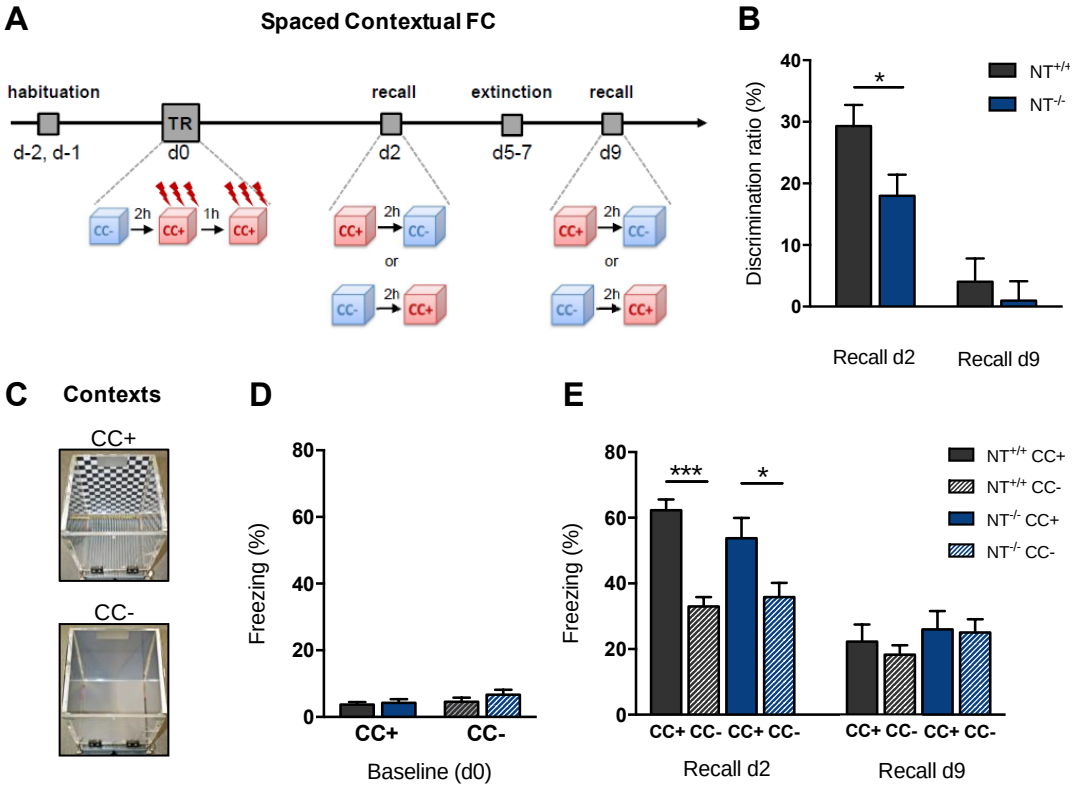

Fig. 4.3 | Spaced fear conditioning and extinction in $NT^{-/-}$ and $NT^{+/+}$ mice. $NT^{-/-}$ mice exhibit impairment neither in retrieving contextual fear memory nor in fear memory extinction. **(A)** The scheme and timeline of the experimental set-up. **(B)** Context discrimination on day 2 was significantly different between both groups of mice. **(C)** Conditioned context (CC+) and neutral context (CC-). **(D)** Freezing time in both contexts before fear conditioning (baseline). **(E)** Freezing time during retention of contextual fear memory revealed that both genotypes were able to distinguish between CC+ and CC- at recall on d2. Freezing time after extinction sessions showed extinction of fear memory in both genotypes at recall on d9. The data are shown as the mean ± SEM. $NT^{+/+}$, n = 10; $NT^{-/-}$, n = 13.

4.2.3. Neurotrypsin-deficient mice show significantly reduced fear memory in a milder protocol of contextual fear conditioning

Since there were genotype differences in the discrimination between contexts in the spaced contextual fear conditioning paradigm but they were very small, we thought that this could be due to a ceiling effect/saturation and generalization of the context. The generalization of fear conditioning is an important aspect of aversive learning. It is manifested as a loss of stimulus specificity and as the emotional sensitization of associative components of memory and leads to diminished signal discrimination and generalized anxiety (Ciocchi et al., 2010; Laxmi et al., 2003). For this reason, we thought that the spaced protocol with 6x foot shocks could have been too strong and have masked existing differences between genotypes. Therefore, we designed a milder fear conditioning protocol with 3x foot shocks and one single context (**Fig. 4.4A,B**). Despite this second CFC protocol was designed in a massed manner (without performing spaced learning sessions), several studies support that sleep plays an active role in replay of information and memory consolidation (Dudai et al., 2015; Graves et al., 2003; Rauchs et al., 2011). In this sense, acquisition plus consolidation can be viewed as a spaced stimulation (see Discussion for further details).

The results obtained indicate that neurotrypsin deficiency affected neither the level of freezing before fear conditioning (typical freezing level during fully unconstrained exploration of a novel environment is 5–10% in mice, **Fig. 4.4C**) nor the significant elevation of freezing between three unconditioned stimuli (UCS) (**Fig. 4.4D**). However, the freezing time in the conditioned context 24 h after conditioning was significantly smaller in the $NT^{-/-}$ mice (**Fig. 4.4E**), suggesting that neurotrypsin deficiency impairs formation or retrieval of contextual fear memory.

On the other hand, both genotypes similarly reduced their freezing levels after fear memory extinction, demonstrating that extinction of contextual fear memory was not altered by neurotrypsin deficiency (**Fig. 4.4E**).

A two-way ANOVA revealed significant effects of “recall day” factor ($F_{(1,19)} = 70.19$, $p < 0.0001$) and mouse genotype ($F_{(1,19)} = 4.541$, $p = 0.0464$), but no significant effect of “recall day” x “genotype” interaction ($F_{(1,19)} = 4.291$, $p = 0.0522$). The Holm-Sidak *post hoc* test showed a statistically significant difference in freezing levels after fear conditioning between genotypes (**$p < 0.01$).

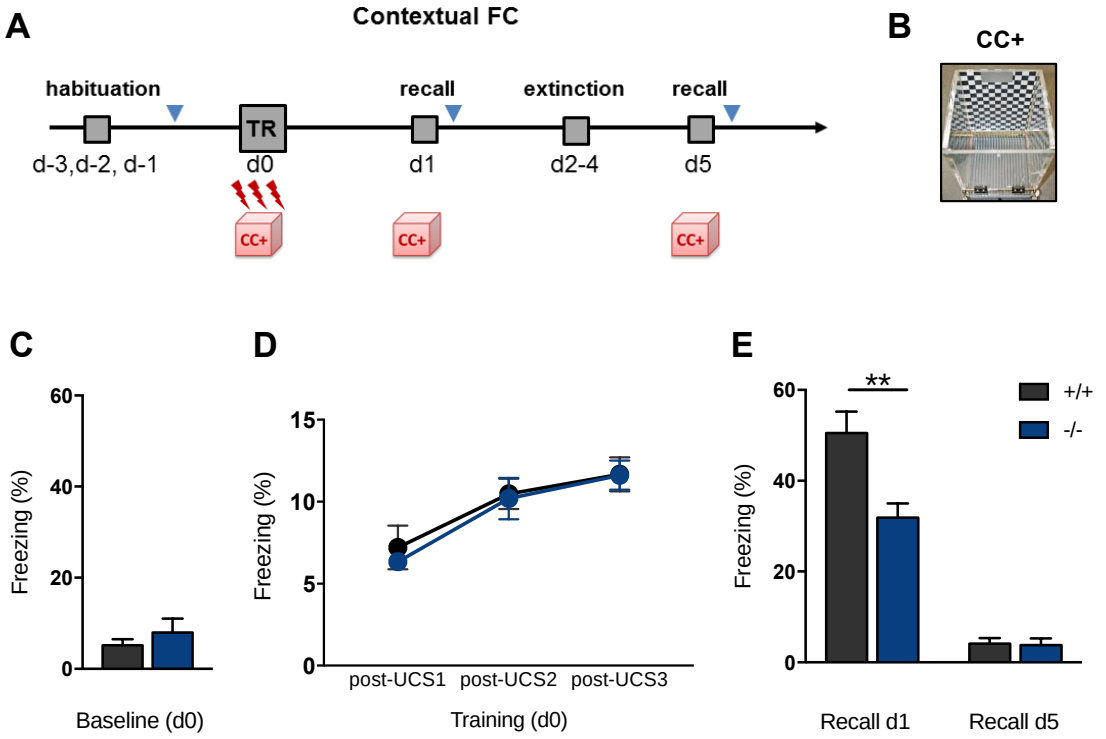

Fig. 4.4 | Contextual fear conditioning and extinction in $NT^{-/-}$ and $NT^{+/+}$ mice. Neurotrypsin deficiency impairs formation or retrieval of contextual fear memory **(A)** The scheme and timeline of the experimental set-up. Blue arrows indicate time points for sample collection for spine imaging (see 4.3.) **(B)** The conditioned context (CC+). **(C)** The freezing levels of both groups of mice in the CC+ context before they received the foot shocks were the standard values in mice exploring a novel environment. **(D)** The percentage of time the experimental subjects showed freezing behaviour in response to UCSs during the training session was not different between genotypes. **(E)** The freezing levels after fear conditioning are significantly reduced in the $NT^{-/-}$ mice. The data are shown as mean ± SEM. $NT^{+/+}$, n = 8; $NT^{-/-}$, n = 8.

4.2.4. Neurotrypsin-deficient mice show normal long-term memory in the novel object recognition test

Next, we were wondering whether neurotrypsin deficient mice would be impaired in the novel object recognition (NOR) test as it is one of the most popular methods for testing the neurobiology of non-spatial and non-aversive memory in rodents. However, despite its popularity and wide use, the underlying neural circuitry and mechanisms supporting NOR have not been clearly defined. Particularly, considerable debate has focused on which is the exact role of the hippocampus in the object memory that is encoded, consolidated and then retrieved during discrete stages of the NOR task. Nonetheless, there is a strong evidence that

the perirhinal cortex plays a crucial role in this memory task (Cohen and Stackman, 2015; see Discussion).

In order to study a form of long-term memory, we used the NOR test with a delay of 24 hours. Our data revealed that both genotypes spent a greater amount of time exploring the novel (N) than the familiar (F) objects during the second trial or retrieval session (**Fig. 4.5B,C**). A two-way ANOVA revealed a statistically significant effect of the "object" factor ($F_{(1,52)}$ = 29.04, p < 0.0001) but not of the "genotype" factor ($F_{(1,52)}$ = 0.3876, p = 0.5363), on the exploration duration during NOR test. The Holm-Sidak *post hoc* test showed a significant difference in total exploration time between the familiar and the novel objects (**p = 0.001, ***p = 0.0002) (**Fig. 4.5B**). Moreover, the discrimination ratio between the familiar and the novel objects was alike for both groups of mice (t = 0.7958, df = 15.62, p = 0.4381; **Fig. 4.5C**).

In summary, these results show that long-term novel object recognition memory is present in both genotypes in the novel object recognition task.

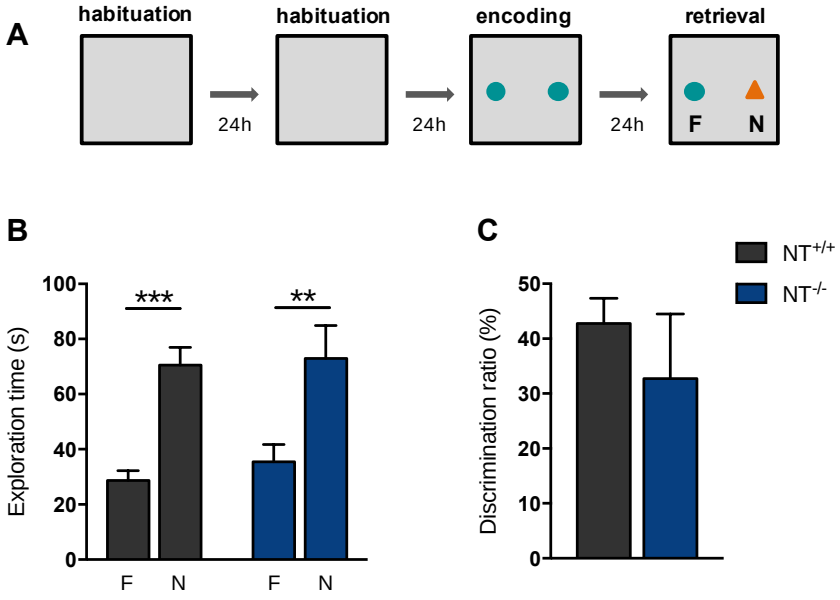

Fig. 4.5 | Novel object recognition test in $NT^{-/-}$ and $NT^{+/+}$ mice. Long-term novel object recognition memory is not different between genotypes. **(A)** The scheme and timeline of the experimental set-up. **(B)** The total exploration duration towards each object (familiar "F" and novel "N") during the retrieval (memory session) of the NOR test showed that both genotypes spent more time exploring the novel object. **(C)** The discrimination index between the familiar and the novel objects was not significantly different between both groups of mice. The data are presented as mean ± SEM. $NT^{+/+}$, n = 15; $NT^{-/-}$, n = 13.

4.2.5. Neurotrypsin-deficient mice reveal significantly lower sociability levels compared with NT WT mice in the three-chamber sociability test

Alterations in social behaviour are symptoms of several neuropsychiatric and neurological diseases. In particular, mental retardation is generally accompanied by a functional deficit in adaptive behaviour such as social skills and communication (Bieleck and Swender, 2004). Therefore, we investigated the social approach behaviour in the neurotrypsin-deficient mice.

To assess sociability levels, we performed the three-chamber sociability test. After 10 minutes of habituation in the three-chamber apparatus, we placed one stimulus mouse (S) inside a small cage in one end of the compartments and an empty cage (E) in the opposite compartment. The mouse performing the test was allowed to explore the whole apparatus for 10 minutes (**Fig. 4.6A**). The exploration time for both stimulus mouse and the empty cage were estimated. The time spent sniffing and directly touching the mouse and the empty cage was considered as exploration time.

We found that $NT^{-/-}$ mice have highly significantly lower sociability levels compared with their control wild-type littermates (**Fig. 4.6**). Two-way ANOVA showed a statistically significant effect of the “stimulus mouse” factor ($F_{(1,36)}$ = 26.88, $p < 0.0001$), a significant effect of “genotype” ($F_{(1,36)}$ = 6.193, $p = 0.0176$) and a significant interaction between the “stimulus mouse” and “genotype” factors ($F_{(1,36)}$ = 8.111, $p = 0.0072$). The Holm-Sidak *post hoc* test revealed a significant difference between the time spent exploring the stimulus mouse and the empty compartment for the wild-type group (****$p < 0.0001$) but not for the mutant ($p > 0.05$) (**Fig. 4.6B**). We observed similar results when we calculated a discrimination ratio in order to remove individual differences in the total exploration time ($t = 2.412$, $df = 18$, $p = 0.0267$; **Fig. 4.6C**).

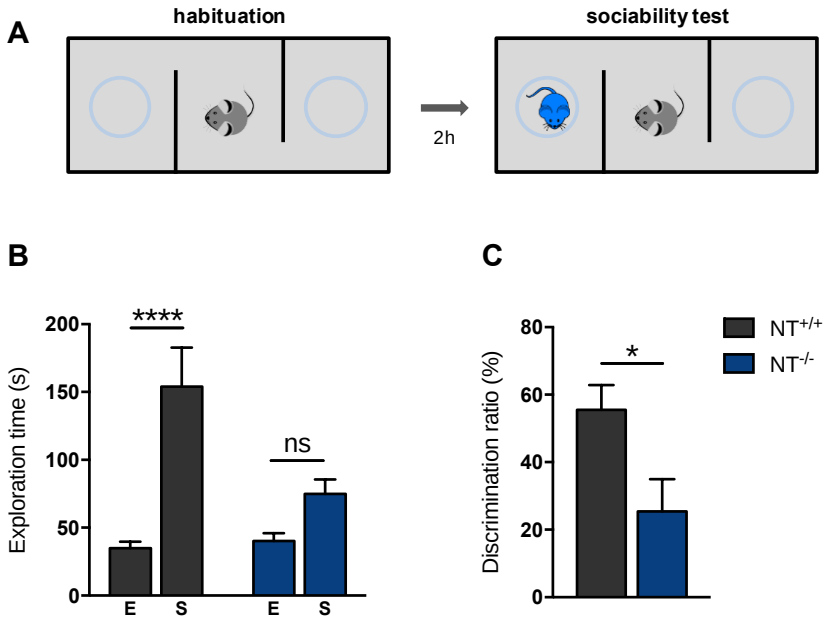

Fig. 4.6 | Three-chamber sociability test in $NT^{-/-}$ and $NT^{+/+}$ mice. NT-deficient mice showed highly significant deficits in sociability, compared with their control littermates. **(A)** The scheme and timeline of the experimental set-up. **(B)** The total exploration duration towards the "empty box" (E) and the "stimulus mouse" (S) during the sociability test showed that $NT^{-/-}$ mice have remarkable sociability deficit. **(C)** The discrimination index between the "empty" and the "stimulus mouse" compartment was significantly different between both groups of mice. The data are shown as mean ± SEM. $NT^{+/+}$, n = 9; $NT^{-/-}$, n = 11.

4.3. Spine analysis reveals striking differences between neurotrypsin-deficient mice and their control WT littermates

As LTP-dependent formation of filopodia is abolished in mice lacking neurotrypsin (Matsumoto-Miyai et al., 2009) and dendritic filopodia are thought to be direct precursors of new dendritic spines (Jontes and Smith, 2000; Yuste and Bonhoeffer, 2004; Ziv and Smith, 1996), we addressed the question how neurotrypsin affects spinogenesis and spine morphology in naïve conditions and upon learning.

In order to do that, we crossbred neurotrypsin with Thy1-EGFP mice, which have sparse labelling of a subset of principal cells (**Fig. 4.7**). Next, we analysed spine density and morphology in CA1 secondary apical dendrites (**Fig. 4.7C**) in naïve conditions, 24 h after contextual fear conditioning and 24 h after fear memory extinction (**Fig. 4.4A**).

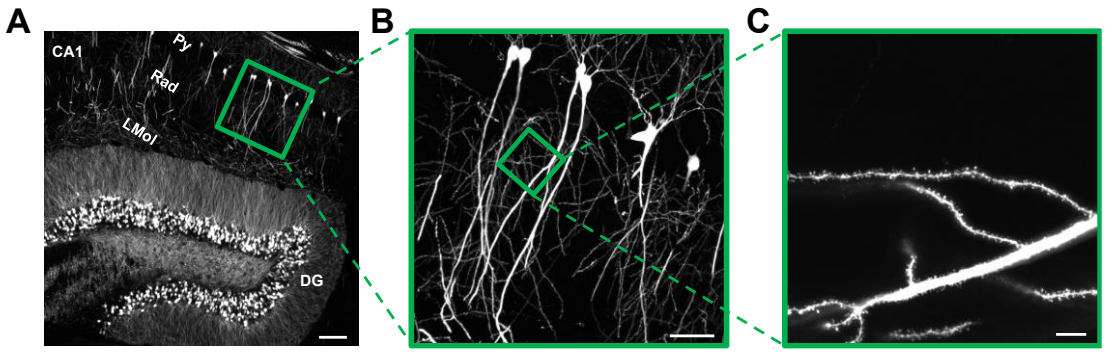

Fig. 4.7 | Hippocampal neurons from a NT/Thy1-EGFP mouse, imaged with a confocal laser scanning microscope. Maximal-intensity Z-projections are shown. **(A)** An overview image, showing the CA1 and DG hippocampal regions. Scale bar, 100 µm. **(B)** CA1 pyramidal neurons. Scale bar, 50 µm. **(C)** Representative image from a secondary apical dendrite. Scale bar, 10 µm. All images were acquired using a Zeiss LSM 700 confocal laser scanning microscope. CA1, *cornus ammonis 1*; Py, *stratum pyramidale*; Rad, *stratum radiatum*; LMol, *stratum lacunosum-moleculare*; DG, *dentate gyrus*.

First, we performed analysis considering spine measurements per dendrite as independent measures, as frequently done in the field (Burk et al., 2012; Giachero et al., 2015; Mendez et al., 2018; Petsophonsakul et al., 2017).The results revealed striking differences between the two genotypes. Neurotrypsin-deficient mice showed significantly reduced spine density in naïve conditions compared to their control wild-type littermates. Two-way ANOVA revealed a significant effect of the "genotype" factor ($F_{(1,243)}$ = 6.879, p = 0.0093), no effect of "condition" factor ($F_{(2,243)}$ = 0.4475, p = 0.6398), but a significant interaction between the "genotype" and the "condition" factors ($F_{(2,243)}$ = 4.378, p = 0.0136). The Holm-Sidak *post hoc* test showed a statistically significant difference in spine density between genotypes under naïve condition (**p < 0.0043) (**Fig. 4.8B**).

Cumulative frequency curves showed that the spine density distribution was shifted toward lower values in naïve NT-deficient mice (Kolmogorov-Smirnov test, p = 0.0168; **Fig. 4.8C**, left panel). There was no difference between genotypes after acquisition or extinction of fear conditioning (Kolmogorov-Smirnov test, p = 0.5748 and p = 0.2634, respectively; **Fig. 4.8C**, middle and right panels).

Interestingly, morphological analysis determined that percentage of thin/filopodia-like spines was significantly reduced in $NT^{-/-}$ mice (**Fig. 4.8G**), whereas the proportion of mushroom spines was higher in this genotype (**Fig. 4.8F**). In agreement with these observations, we found a statistically significant reduction of spine head size in wild-type mice. However, this reduction was not present after CFC (**Fig. 4.8D**). Regarding stubby spines, no significant differences were found between the two groups (**Fig. 4.8E**).

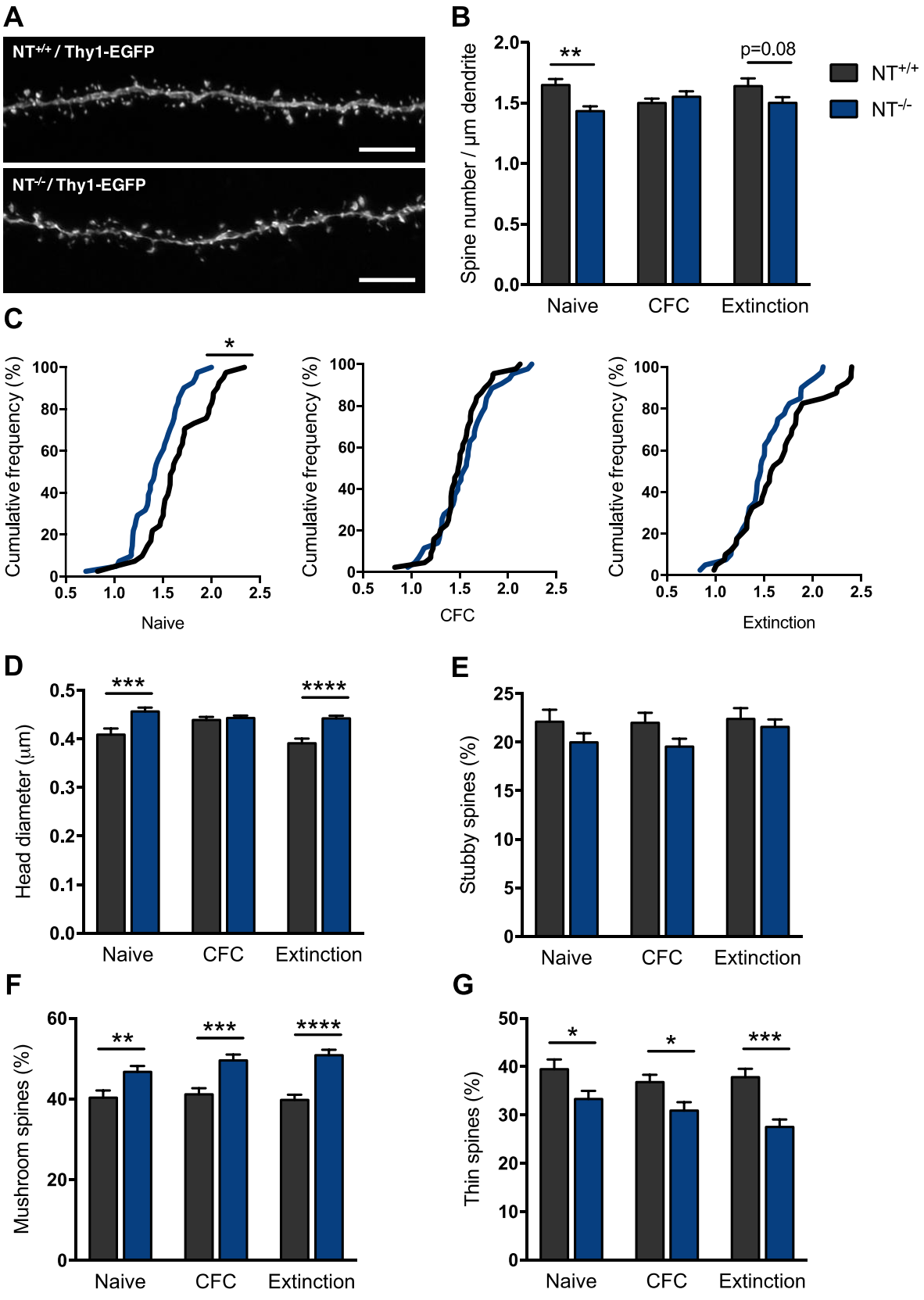
A
NT+/+ / Thy1-EGFP
NT-/- / Thy1-EGFP
B
Spine number / µm dendrite
**
p=0.08
NT+/+
NT-/-
Naive
CFC
Extinction
C
Cumulative frequency (%)
*
Naive
CFC
Extinction
D
Head diameter (µm)
***
****
E
Stubby spines (%)
F
Mushroom spines (%)
**
***
****
G
Thin spines (%)
*
*
***

Fig. 4.8 | Spine analysis in naïve and trained mice (measures per dendrite). Results from spine analysis showed striking differences between $NT^{+/+}$ and $NT^{-/-}$ mice. **(A)** Representative images of CA1 secondary apical dendrites from $NT^{+/+}$ mouse (upper panel) and their $NT^{-/-}$ littermate (lower panel). Scale bar, 5 µm. **(B)** Spine density was significantly decreased in $NT^{-/-}$ mice in naïve conditions. **(C)** Cumulative frequency plots showing the distribution of spine density at each condition. **(D)** Spine head size was significantly reduced in $NT^{+/+}$ compared with $NT^{-/-}$ mice in naïve and after extinction conditions. **(E)** The proportion of stubby spines was similar for both genotypes in all conditions. **(F)** The proportion of mushroom spines was increased in $NT^{-/-}$ mice in all conditions. **(G)** The proportion of thin spines was reduced in $NT^{-/-}$ mice in all conditions. The data are presented as mean ± SEM. The numbers of analysed $NT^{+/+}$ and $NT^{-/-}$ dendrites/mice for each group are the followings: 41/5 ($NT^{+/+}$; naïve), 44/5 ($NT^{+/+}$; CFC), 40/5 ($NT^{+/+}$; extinction), 41/5 ($NT^{-/-}$; naïve), 43/5 ($NT^{-/-}$; CFC) and 40/5 ($NT^{-/-}$; extinction).

Two-way ANOVA of the head size revealed a statistically significant effect of the “genotype” factor ($F_{(1,243)} = 26.92$, $p < 0.0001$), a significant effect of the “condition” factor ($F_{(2,243)} = 4.708$, $p = 0.0099$), and a significant interaction between the “genotype” and the “condition” factors ($F_{(2,243)} = 5.402$, $p = 0.0051$). The Holm-Sidak *post hoc* test showed a statistically significant difference in spine head diameter between genotypes under naïve and extinction conditions (***p = 0.0001, ****p < 0.0001) (**Fig. 4.8D**).

Two-way ANOVA of stubby spines indicated a statistically significant effect of the “genotype” factor ($F_{(1,243)} = 5$, $p = 0.0263$), but no significant effect of the “condition” factor ($F_{(2,243)} = 0.8074$, $p = 0.4472$), and no significant interaction between the “genotype” and the “condition” factors ($F_{(2,243)} = 0.3848$, $p = 0.6810$). The Holm-Sidak *post hoc* test revealed no significant differences in percentage of stubby spines between genotypes and conditions (**Fig. 4.8E**).

Two-way ANOVA of mushroom spines showed a statistically significant effect of the “genotype” factor ($F_{(1,243)} = 50.54$, $p < 0.0001$), but no significant effect of the “condition” factor ($F_{(2,243)} = 1.012$, $p = 0.3650$), and no significant interaction between the “genotype” and the “condition” factors ($F_{(2,243)} = 1.249$, $p = 0.2888$). The Holm-Sidak *post hoc* test revealed significant differences in percentage of mushroom spines between genotypes in all conditions (**p = 0.0028, ***p = 0.0001, ****p < 0.0001) (**Fig. 4.8F**).

Two-way ANOVA of thin spines revealed a significant effect of the “genotype” factor ($F_{(1,242)} = 28.6$, $p < 0.0001$), but no significant effect of the “condition” factor ($F_{(2,242)} = 2.42$, $p = 0.0911$), and no significant interaction between the “genotype” and the “condition” factors ($F_{(2,242)} = 1.025$, $p = 0.3604$). The Holm-Sidak *post hoc* test revealed significant differences in percentage of thin spines between genotypes in all conditions (*p = 0.0240, ***p = 0.0001) (**Fig. 4.8G**).

Considering all data together, we were wondering why the spine head diameter was not smaller in the control group after CFC, if in all conditions (also in CFC) the percentage of thin spines was higher in the control group and the percentage of mushroom spines was larger in the mutant group. We first thought that this could be due to the mushroom spines, that they could be bigger and more mature in the control group after CFC and therefore compensate for this difference. Thus, we evaluated the head diameter in the mushroom spines that were automatically detected by the software used for spine analysis. Surprisingly, we found that mushroom spine head size was very similar in both groups of mice ($t = 0.8187$, $df = 84$, $p = 0.4153$; **Fig. 4.9A**). Consequently, we decided to measure the head diameter in the thin spines after CFC. Interestingly, we observed that the thin spines were bigger and most likely more mature in the wild-type control group ($t = 3.745$, $df = 85$, $p = 0.0003$; **Fig. 4.9B**), suggesting that neurotrypsin-deficiency may specifically affect the maturation of thin/filopodia-like spines. In agreement with this, a cumulative frequency plot of spine head diameter of thin spines revealed that $NT^{-/-}$ mice had a leftward shift in the cumulative curve, indicating a reduction in the head diameter for this spine type in NT-deficient mice (Kolmogorov-Smirnov test, $p = 0.0001$; **Fig. 4.9D**).

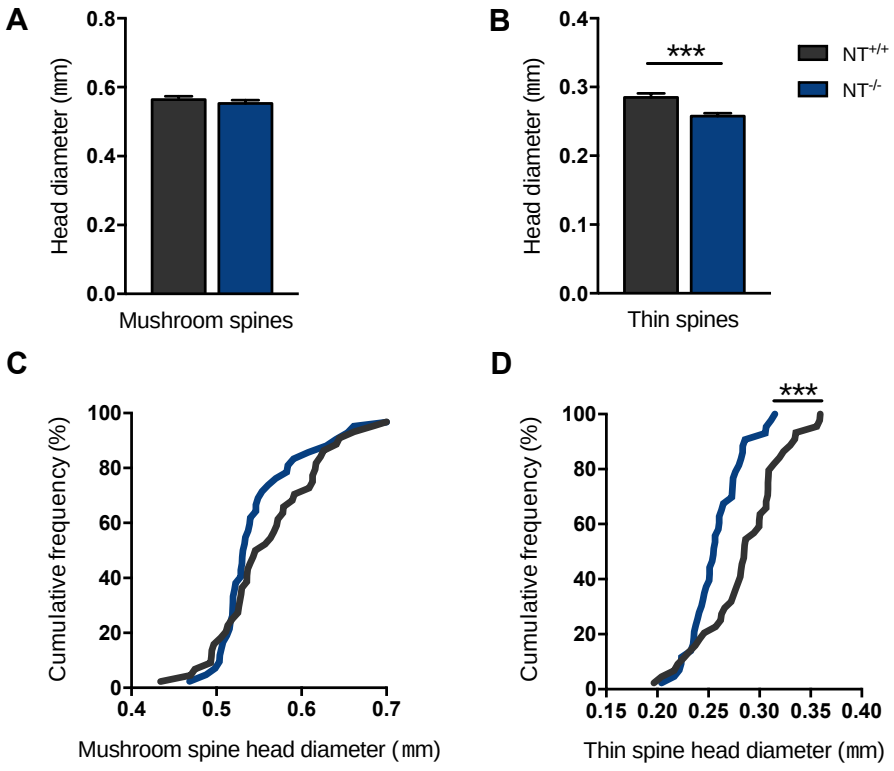

Fig. 4.9 | Spine head size in mushroom and thin spines after CFC (measures per dendrite). NT-deficient mice have smaller thin spines after CFC. **(A)** Head diameter of mushroom spines is alike in both genotypes. **(B)** Head diameter of thin spines is significantly reduced in $NT^{-/-}$ mice. **(C)** Cumulative frequency plot showing the distribution of spine head

diameter of mushroom spines population. **(D)** Cumulative frequency plot showing the distribution of spine head diameter of thin spines population. Note, that to show more clearly the difference between groups, the X-axes in C and D originates not at 0. The data are shown as mean ± SEM. The numbers of analysed $NT^{+/+}$ and $NT^{-/-}$ dendrites/mice are the followings: 44/5 ($NT^{+/+}$; CFC) and 43/5 ($NT^{-/-}$; CFC).

To analyse spine morphology more in depth, we decided to evaluate changes in absolute numbers of each spine type in all conditions (naïve, CFC and extinction), asking if the results would be similar to those obtained after analysing occurrence of difference spine types as percentage of total number of spines. Overall, the results for absolute frequencies showed a similar data pattern as the results for frequencies expressed in % (**Fig. 4.10**). However, surprisingly, we observed a statistically significant increase in mushroom spine density after CFC (#p = 0.032) compared to naïve conditions in the $NT^{-/-}$, but not in the $NT^{+/+}$ mice (**Fig. 4.10B**).

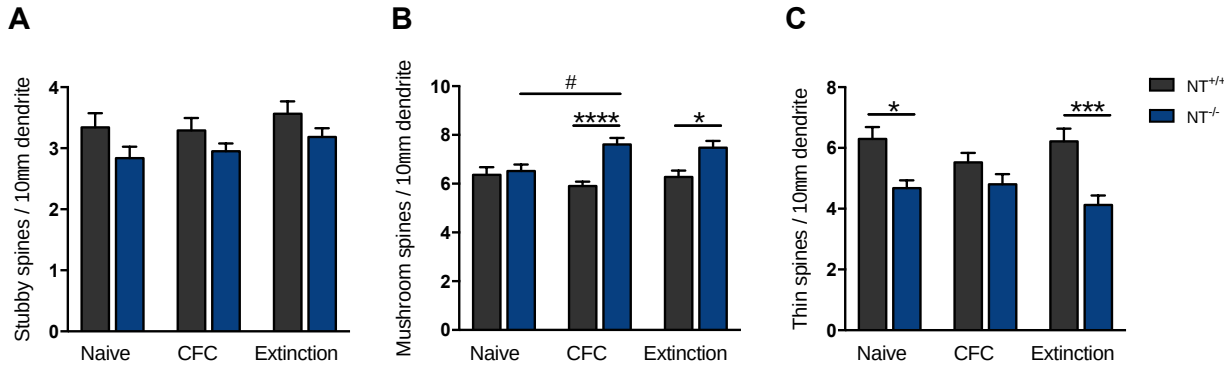

Fig. 4.10 | Spine morphology in naïve and trained mice (measures per dendrite). Results obtained by analysis of absolute numbers. **(A)** The number of stubby spines was similar for both genotypes in all conditions. **(B)** The number of mushroom spines was increased in $NT^{-/-}$ mice after CFC. **(C)** The number of thin spines was reduced in $NT^{-/-}$ mice in naïve and CFC groups. The data are shown as mean ± SEM. The numbers of analysed $NT^{+/+}$ and $NT^{-/-}$ dendrites/mice for each group are the followings: 41/5 ($NT^{+/+}$; naïve), 44/5 ($NT^{+/+}$; CFC), 40/5 ($NT^{+/+}$; extinction), 41/5 ($NT^{-/-}$; naïve), 43/5 ($NT^{-/-}$; CFC) and 40/5 ($NT^{-/-}$; extinction).

Finally, we also performed the same analysis done in **Fig. 4.8**, but calculating the average of measured dendrites (neurons) per animal. This is the most conservative way to perform spine analysis, as we do not need to assume independence of measurements obtained from the same animal. However, n = 5 may be not sufficient to have a statistical power to detect

significant differences. Therefore, our goal here was to asses whether we would see the same data pattern using another approach to analyse this data.

Neurotrypsin-deficient mice showed significantly reduced spine density in naïve conditions compared with their control wild-type littermates. Two-way ANOVA showed no significant effect of the "genotype" factor ($F_{(1,24)}$ = 3.723, p = 0.0656), no effect of the "condition" factor ($F_{(2,24)}$ = 0.3866, p = 0.6835), and no significant interaction between the "genotype" and the "condition" factors ($F_{(2,24)}$ = 2.122, p = 0.1418). The Holm-Sidak *post hoc* test revealed a statistically significant difference in spine density between genotypes under naïve condition (*p = 0.0389) (**Fig. 4.11B**).

Two-way ANOVA of the head size revealed a statistically significant effect of the "genotype" factor ($F_{(1,24)}$ = 5.516, p = 0.0274), but no significant effect of the "condition" factor ($F_{(2,24)}$ = 0.8789, p = 0.4282), and no significant interaction between the "genotype" and the "condition" factors ($F_{(2,24)}$ = 0.7547, p = 0.4810). The Holm-Sidak *post hoc* test showed no significant differences in spine head diameter between genotypes and conditions (**Fig. 4.11C**).

Two-way ANOVA of stubby spines indicated no significant effect of the "genotype" factor ($F_{(1,24)}$ = 1.063, p = 0.3128), no significant effect of the "condition" factor ($F_{(2,24)}$ = 0.3487, p = 0.7091), and no significant interaction between the "genotype" and the "condition" factors ($F_{(2,24)}$ = 0.187, p = 0.8307). The Holm-Sidak *post hoc* test revealed no significant differences in percentage of stubby spines between genotypes and conditions (**Fig. 4.11D**).

Two-way ANOVA of mushroom spines showed a statistically significant effect of the "genotype" factor ($F_{(1,24)}$ = 10.54, p = 0.0034), but no significant effect of the "condition" factor ($F_{(2,24)}$ = 0.1073, p = 0.8986), and no significant interaction between the "genotype" and the "condition" factors ($F_{(2,24)}$ = 0.1395, p = 0.8705). The Holm-Sidak *post hoc* test revealed no significant differences in percentage of mushroom spines between genotypes and conditions) (**Fig. 4.11E**).

Two-way ANOVA of thin spines revealed a significant effect of the "genotype" factor ($F_{(1,24)}$ = 4.899, p = 0.0366), but no significant effect of the "condition" factor ($F_{(2,24)}$ = 0.2295, p = 0.7967), and no significant interaction between the "genotype" and the "condition" factors ($F_{(2,24)}$ = 0.1133, p = 0.8934). The Holm-Sidak *post hoc* test revealed no significant differences in percentage of thin spines between genotypes and conditions) (**Fig. 4.11F**).

Overall, spine analysis after averaging values for all dendrites per animal provided very similar results than those obtained while analysing dendrites as independent values. Although *post hoc* analysis did not detect differences between genotypes and conditions (excluding the

significant difference in spine density between genotypes under naïve condition), two-way ANOVA showed a significant effect of the genotype in percentage of mushroom and thin spines, as well as in the head size diameter, supporting our previous results.

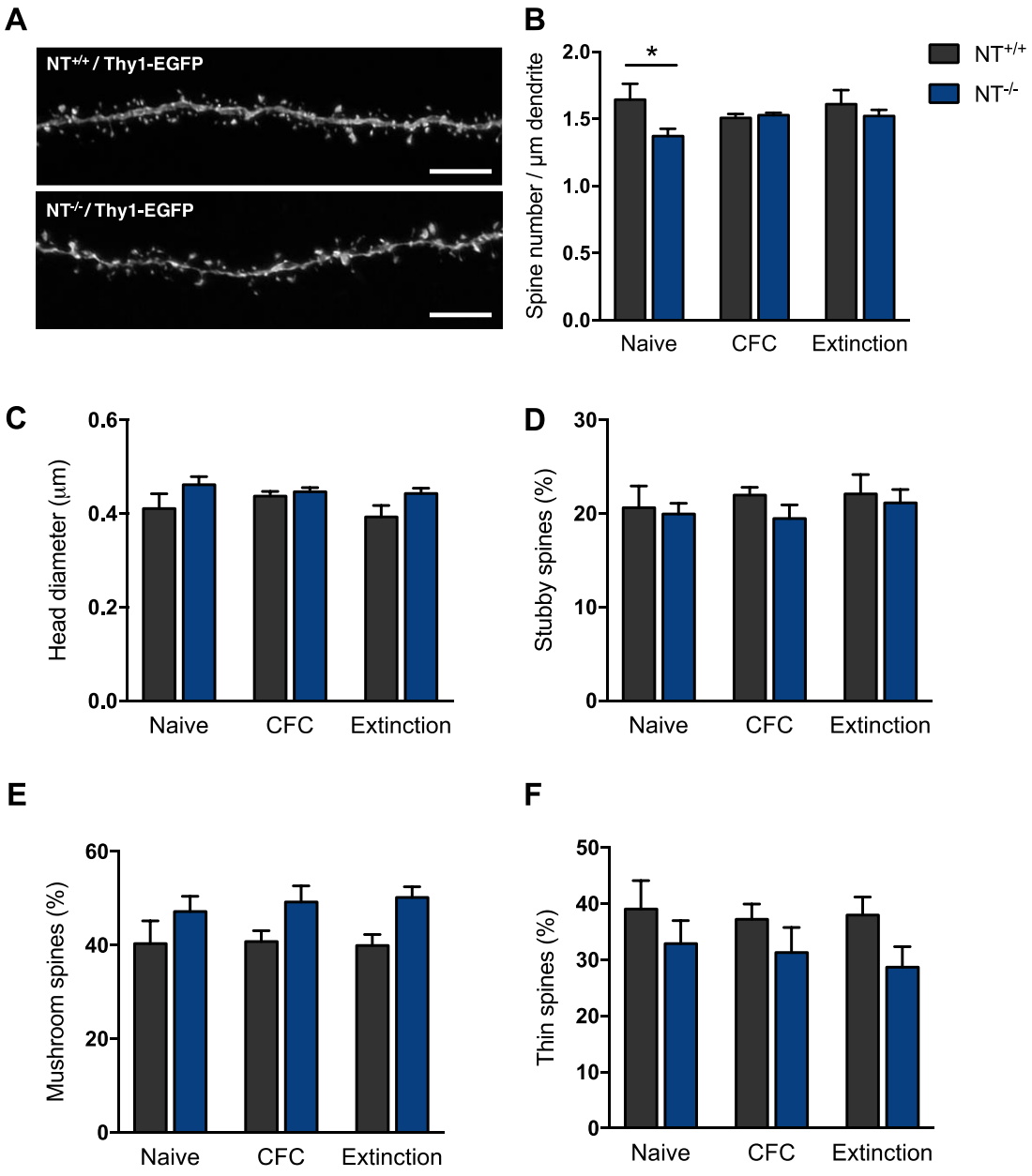

Fig. 4.11 | Spine analysis in naïve and trained mice (measures per animals). Results from spine analysis showed differences between $NT^{+/+}$ and $NT^{-/-}$ mice. **(A)** Representative images of CA1 secondary apical dendrites from $NT^{+/+}$ mouse (upper panel) and their $NT^{-/-}$ littermate (lower panel). Scale bar, 5 µm. **(B)** Spine density was significantly decreased in $NT^{-/-}$ mice in naïve conditions. **(C)** Spine head size was slightly reduced in $NT^{+/+}$ compared with $NT^{-/-}$ mice

in naïve and after extinction conditions. **(D)** The proportion of stubby spines was similar for both genotypes in all conditions. **(E)** The proportion of mushroom spines was increased in $NT^{-/-}$ mice in all conditions. **(F)** The proportion of thin spines was reduced in $NT^{-/-}$ mice in all conditions. The data are shown as mean ± SEM. $NT^{+/+}$, n = 5 / each condition; $NT^{-/-}$, n = 5 / each condition.

4.4. Analysing the involvement of agrin

As agrin is the only substrate of neurotrypsin identified so far and critically important for activity-dependent filopodia formation (Matsumoto-Miyai et al., 2009), we addressed the question whether agrin cleavage may be responsible for the putative effects of neurotrypsin deficiency. In first experiments, we asked whether we can rescue the spine loss present in neurotrypsin-deficient mice with an adeno-associated virus (AAV) expressing agrin-22. Therefore, we aimed to deliver agrin-22 in the hippocampus of neurotrypsin-deficient mice and evaluate its effect on dendritic spines. For that reason, we designed an AAV expressing agrin-22 specifically in neurons (under the synapsin promoter). The DNA construct included also a secretion signal sequence (Aricescu et al., 2006) and the reporter gene scarlet (**Fig. 4.12B**, upper scheme). As a control, we used a shorter version of agrin-22, agrin-15, which was shown to act as an agrin antagonist in hippocampal and cortical cultures (Hoover et al., 2003b) and in acute-slice preparations (Hilgenberg et al., 2006b) (**Fig. 4.12B**, lower scheme).

We injected $NT^{-/-}$ mice with either pAAV-Syn-Agrin22-Scarlet (AAV-Ag22) or pAAV-Syn-Agrin15-Scarlet (AAV-Ag15) at postnatal day 7 (P7). Subsequently, we collected samples for spine imaging at P24, after 3 consecutive days of habituation (**Fig. 4.12A**) in order to follow the same protocol than in previous spine imaging experiments (see 4.3. and **Fig. 4.4A**).

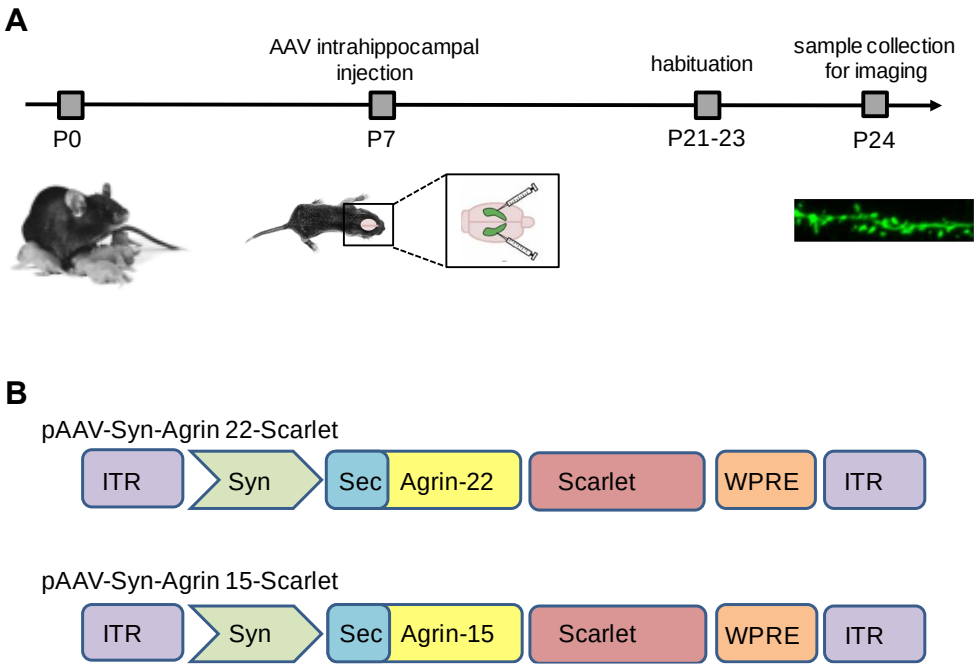

Fig. 4.12 | Experimental design of rescue experiments with AAV-Ag22. (A) Scheme of the time course of the experiment. **(B)** Scheme of the two AAV vectors used in this study: AAV-Ag22 and AAV-Ag15. The cassette contains agrin-22 or agrin-15 driven by the synapsin (Syn) promoter, a secretion signal sequence (Sec) and the reporter fluorescent protein scarlet.

4.4.1. *pAAV-Syn-Agrin 22-Scarlet* restores the spine loss present in the neurotrypsin-deficient mice

Results exhibited that AAV-Ag22 rescued the spine loss existent in the neurotrypsin-deficient mice. As shown in **Fig. 4.13C**, injection of AAV-Ag22 significantly increased the spine density in $NT^{-/-}$ mice ($t = 3.482$, $df = 48$, $p = 0.0011$) to similar levels than those previously observed in $NT^{+/+}$ mice. However, this was not detected when mice were injected with AAV-Ag15 (**Fig. 4.13C**).

Despite its effect on spine density, injection of AAV-Ag22 did not have any effects on spine morphology or on spine head size as shown in **Fig. 4.13D,E**. Nevertheless, filopodia density was slightly increased in mice injected with AAV-Ag22 compared with those injected with AAV-Ag15, but without reaching statistical significance (**Fig. 4.13E**, first graph from the right site).

To ensure proper injections, each hippocampal slice was imaged to detect Ag22-scarlet or Ag15-scarlet expression and only those animals with positive expression were selected for subsequent spine analysis. Both Ag22-scarlet and Ag15-scarlet labeling were diffusely distributed over neuronal somas from the *stratum pyramidale* and showed puncta distribution in the *stratum radiatum*. Distinctly, all mice injected with AAV-Ag15 exhibited a lower intensity of “agrin puncta” in the *stratum radiatum*, presumably because of less stability as agrin-15 is not found under physiological conditions in animals (**Fig. 4.13A,B**).

It should be also noted that signal from cell bodies in the *stratum pyramidale* was oversaturated to be able to see a suitable expression of agrin in the *stratum radiatum*, in where dendritic spines were analysed (**Fig. 4.13A,B**).

Finally, as it was done in 4.3., we performed the same analysis but calculating the average of measured dendrites (neurons) per animal. Similarly, we could also observe a statistically significant increase in spine density in $NT^{-/-}$ mice injected with AAV-Ag22 (one-tailed t-test, $t = 2.117$, $df = 5$, $p = 0.0439$) but no changes in spine morphology (**Fig. 4.14**).

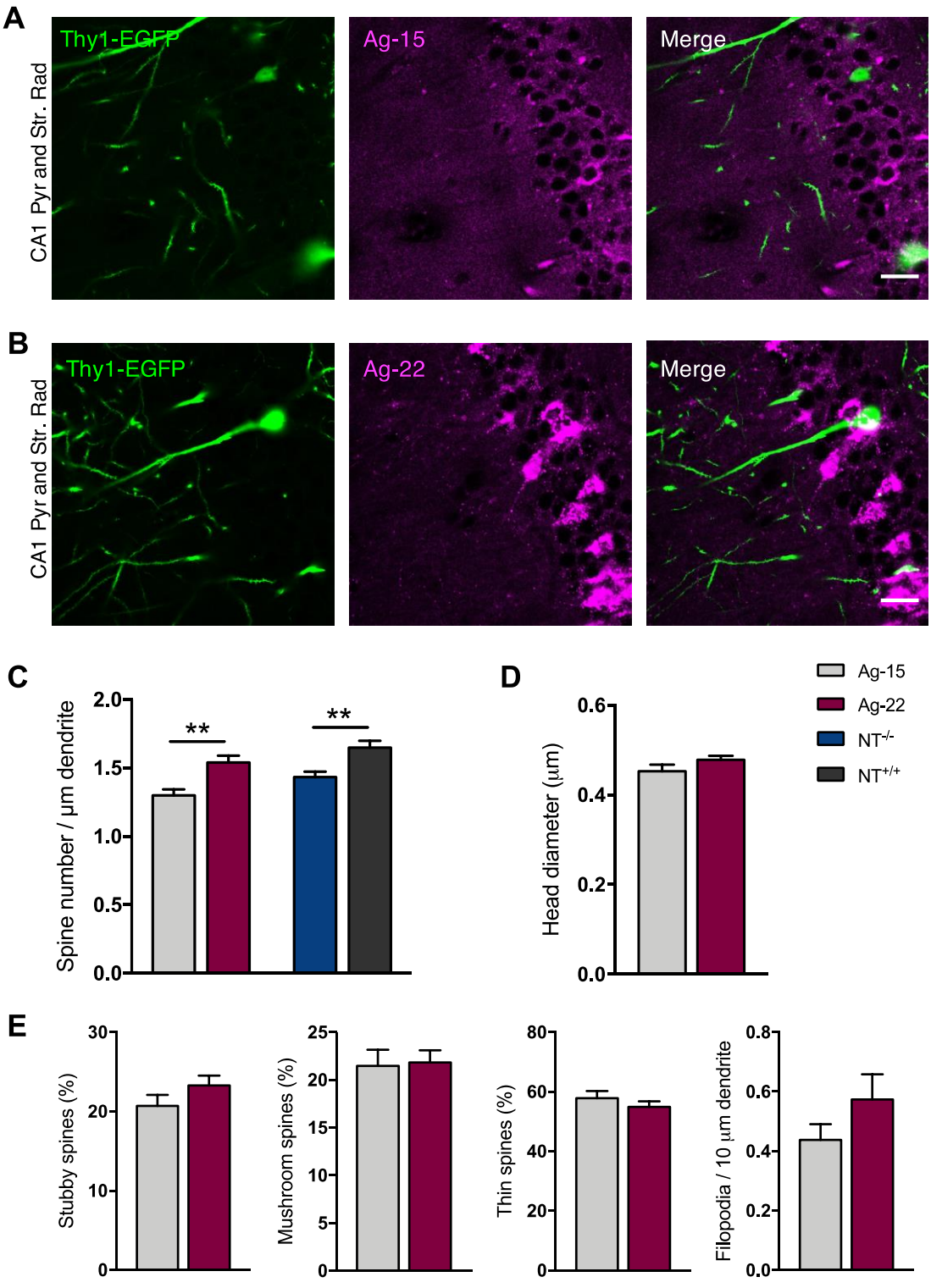

Fig. 4.13 | AAV-Ag22 restores the spine density in the NT$^{-/-}$ mice to the wild-type level. Results showed an increase in spine density in NT$^{-/-}$ mice after injection of AAV-Ag22. Data from graphs correspond to values obtained while analysing dendrites as independent measurements. **(A)** Representative hippocampal section showing Ag15-scarlet expression in CA1 *stratum pyramidale* and in *stratum radiatum*. Scale bar, 20 µm. **(B)** A representative hippocampal section showing Ag22-scarlet expression in the CA1 *stratum pyramidale* and in

stratum radiatum. Scale bar, 30 µm. **(C)** Spine density was significantly increased in $NT^{-/-}$ mice after injection of AAV-Ag22. Blue and dark grey bars show previous data from **Fig. 4.8B** to have reference values from $NT^{-/-}$ and $NT^{+/+}$ mice. **(D)** Spine head size was similar in both groups. **(E)** Spine morphology was alike in both groups. However, filopodia density was slightly increased in the AAV-Ag22 injected mice yet not statistically significant. The data are presented as mean ± SEM. The numbers of analysed dendrites/mice are the followings: 29/4 ($NT^{-/-}$ injected with AAV-Ag22) and 21/3 ($NT^{-/-}$ injected with AAV-Ag15).

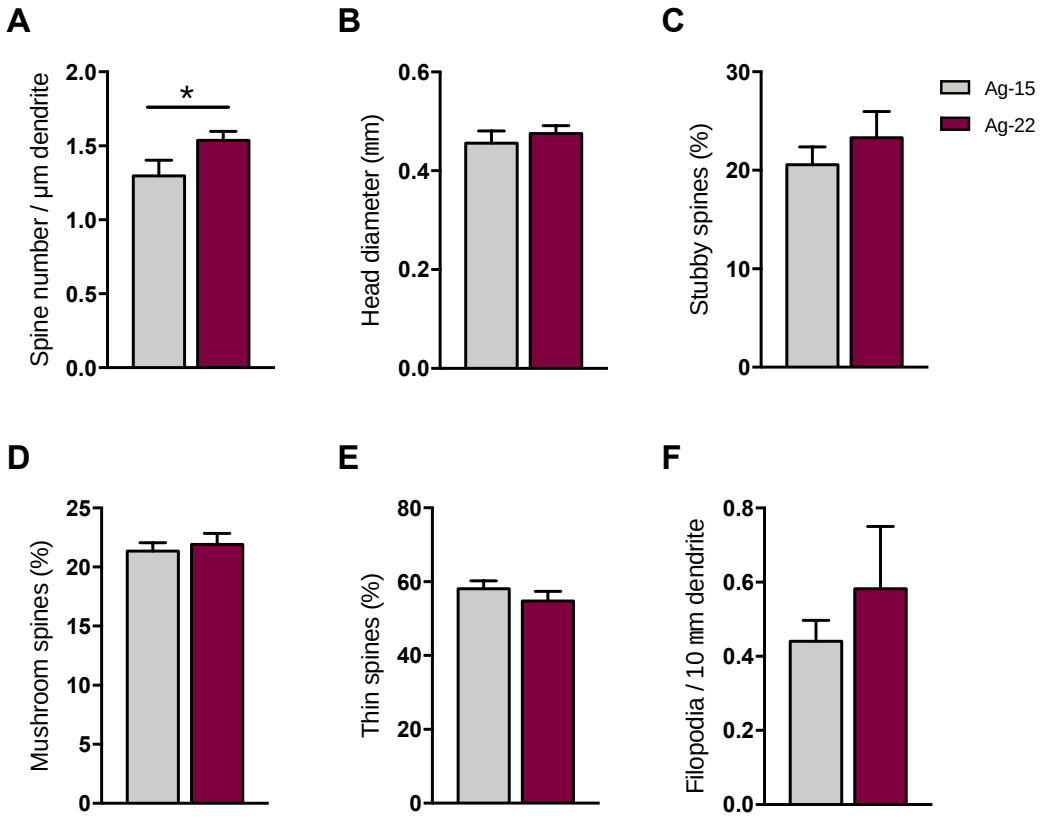

Fig. 4.14 | AAV-Ag22 restores the spine loss present in the $NT^{-/-}$ mice. Results showed an increase in spine density in $NT^{-/-}$ mice after injection of AAV-Ag22. Data from graphs correspond to values obtained while averaging values estimated for all dendrites per animal. **(A)** Spine density was significantly increased in $NT^{-/-}$ mice after injection of AAV-Ag22. **(B)** Spine head size was alike in both groups. **(C)** The proportion of stubby spines was similar in both groups. **(D)** The proportion of mushroom spines was similar in both groups. **(E)** The proportion of thin spines was alike in both groups. **(F)** The proportion of filopodia density was similar in both groups. The data are shown as mean ± SEM. $NT^{-/-}$ injected with AAV-Ag22, n = 4; $NT^{-/-}$ injected with AAV-Ag15, n = 3.

4.4.2. *pAAV-Syn-Agrin-22-Scarlet* co-localizes with the α3NKA agrin receptor and with the excitatory presynaptic marker VGLUT1

To determine whether Ag22-scarlet bound its already identified neuronal receptor α3NKA (Hilgenberg et al., 2006b), CA1 slices from brains injected with AAV-Ag22 were labelled with the α3NKA monoclonal antibody (XVIF9-G10; Novus Biologicals). Consistent with a previous *in vitro* study (Hilgenberg et al., 2006b), we observed an extensive overlap between the α3NKA and the "agrin puncta" expression in the *stratum radiatum* (**Fig. 4.15A**).

To confirm that AAV-Ag22 was properly delivered and expressed at synaptic sites, we stained CA1 slices from brains injected with AAV-Ag22 with the excitatory presynaptic marker VGLUT1 (vesicular glutamate transporter 1, 135304; Synaptic Systems). Co-localization of scarlet-tagged Ag22 and immunostained VGLUT1 showed agrin-22 to concentrate at synapses (**Fig. 4.15B**).

Taken together, these observations provide strong evidence that AAV-driven expression of agrin-22 is properly delivered to synaptic sites in the *stratum radiatum* and overlaps with its physiological neuronal receptor α3NKA.

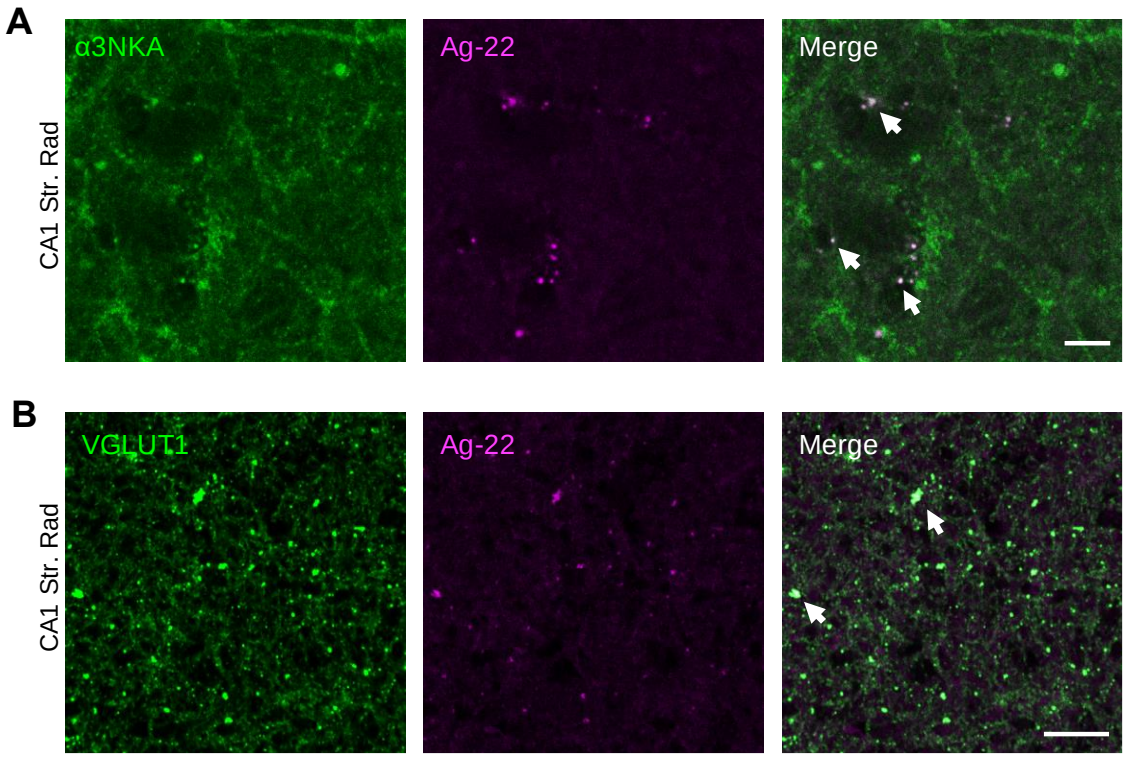

Fig. 4.15 | Ag22-scarlet co-localizes with the α3NKA agrin receptor and with the excitatory presynaptic marker VGLUT1. (A) Agrin-22 binding sites and α3NKA were co-localized, appearing as small puncta distributed over the CA1 *stratum radiatum*. Scale bar, 5

µm. **(B)** Double labelling with VGLUT1 revealed agrin-22 concentrated at excitatory synapses. Scale bar, 10 µm.

4.4.3. VGLUT1-positive presynaptic terminals co-localizing with AAV-Ag22 are bigger or forming clusters

Next, we decided to closer investigate the effect of Ag22-scarlet on VGLUT1 puncta. Interestingly, we found that VGLUT1-positive presynapses co-localizing with Ag22-scarlet were significantly bigger compared to those without Ag22-scarlet co-localization ($t = 11.72$, $df = 4$, $p = 0.0003$; **Fig. 4.16D**). In agreement with this, a cumulative frequency plot of VGLUT1-positive presynapses distribution revealed that the presynapses co-localizing with Ag22-scarlet had a rightward shift in the cumulative curve, indicating an enlargement of VLGUT1 presynapses co-localizing with Ag22-scarlet (Kolmogorov-Smirnov test, $p < 0.0001$; **Fig. 4.16E**). This striking observation suggests that Ag22-scarlet may induce synapse formation or aggregation of VGLUT1-positive synaptic vesicles at presynapses.

Finally, in order to examine whether these big structures are composed of pre- but also postsynaptic specializations, we stained CA1 slices from brains injected with AAV-Ag22 with the excitatory presynaptic marker VGLUT1 (vesicular glutamate transporter 1, 135304; Synaptic Systems) and the excitatory postsynaptic marker PSD95 (postsynaptic density protein 95, ab2723; Abcam). Interestingly, we observed complex synapses with multiple postsynaptic densities (see magnification on the upper-right corner of **Fig. 4.17**). However, super-resolution and/or electron microscopy is necessary to better understand organization of agrin-22-induced giant synapses.

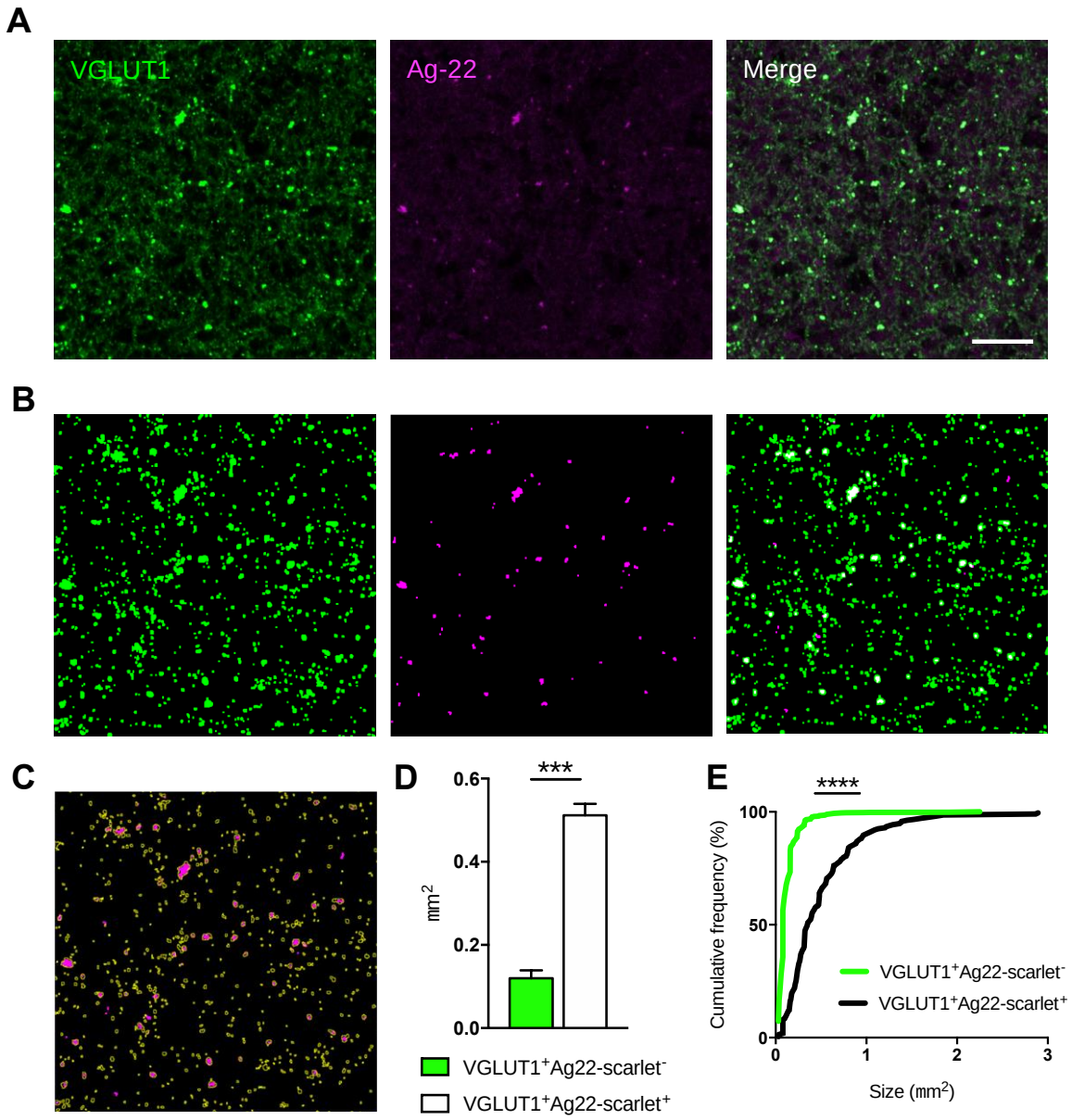

Fig. 4.16 | VGLUT1 puncta co-localizing with Ag22-scarlet are bigger in size or forming clusters. (A) Double labelling with VGLUT1 revealed agrin-22 concentrated at excitatory synapses. Scale bar, 10 µm. **(B)** Binary map of VGLUT1 (left), Ag22-scarlet (middle) and merged channels (right) with dilated pixels to visualize co-localized fluorescent signals. **(C)** ROIs corresponding to VGLUT1 binary map were superimposed on Ag22-scarlet binary map to analyse the size of both synapse populations. **(D)** VGLUT1 synapses co-localizing with Ag22-scarlet were significantly bigger. **(E)** Cumulative frequency plot showing the distribution by size of two populations of VGLUT1-positive presynapses associated or not with Ag22-scarlet. The data are shown as mean ± SEM. The numbers of analysed synapses/images are the followings: 1087/3 (VGLUT1$^+$Ag22-scarlet$^-$) and 214/3 (VGLUT1$^+$Ag22-scarlet$^+$).

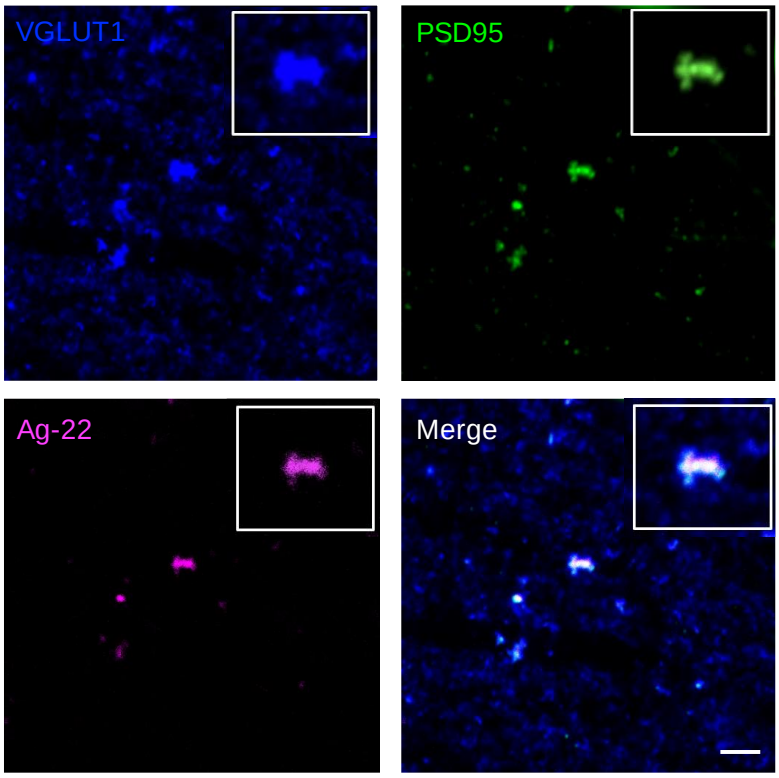

Fig. 4.17 | Ag22-scarlet co-localizes with the excitatory presynaptic marker VGLUT1 and the excitatory postsynaptic marker PSD95 in complex synapses with multiple postsynaptic densities. Triple labelling with VGLUT1 and PSD95 revealed agrin-22 concentrated at excitatory synapses. Scale bar, 4 µm.

5. DISCUSSION

Considering the knowledge gaps in the contemporary literature, the purpose of the current study was to elucidate the relevance of neurotrypsin-dependent mechanisms *in vivo*, emphasising on the importance of neurotrypsin for functional synaptic plasticity, its role in different types of learning and memory process, how neurotrypsin may modulate sociability and social interaction, and the impact of neurotrypsin-dependent cleavage of agrin in regulating dendritic spine formation and morphology.

Neurotrypsin mRNA is mainly expressed in neurons of the cerebral cortex, the hippocampus, and the lateral amygdala (Gschwend et al., 1997; Wolfer et al., 2001). We thought that it would be a good approach to start exploring neurotrypsin-dependent mechanisms in a brain area with high expression of neurotrypsin. Therefore, taking into account that we aimed to study the role of neurotrypsin *in vivo* from the cellular (functional synaptic plasticity) to the systemic (learning and memory) level, including its impact on the morphology and structure of dendritic spines, we focused our research on the hippocampus, as it is the most widely studied brain region that allows for applying several already standardized techniques that may help us to verify our hypotheses.

Previous studies determined the temporal expression pattern of neurotrypsin and the neurotrypsin-dependent agrin fragments in mouse brain samples from embryonic day 16 (E16) through the age of 2 years. In general, peak expression levels were detected between E16 and postnatal day 10 (P10) (Reif et al., 2007). The temporal course of agrin cleavage closely resembled the expression pattern of neurotrypsin, with peak levels also between E16 and P10. However, each brain area showed slightly different temporal expression pattern. For example, the highest expression of neurotrypsin in the hippocampus was detected between P4 and P24, particularly in CA1 (Wolfer et al., 2001). During later developmental stages, expression declined toward lower levels in early adulthood. Relatively low, but clearly detectable, expression of neurotrypsin was maintained throughout adult life (Reif et al., 2007).

In a prior major study on this topic, Matsumoto-Miyai and coauthors (2009) reported that the neurotrypsin-agrin system may serve as a coincidence detector for concomitant pre- and postsynaptic activation and it may be a potential player in LTP-associated synapse formation (Matsumoto-Miyai et al., 2009). They performed all experiments in slices from 4- to 6-week old neurotrypsin-deficient and wild-type mice. Considering that this study is one of the starting points of our research, and the neurotrypsin expression patterns detailed above, we conducted all the experiments detailed in this thesis in P24 to P35 old mice.

5.1. Contribution of neurotrypsin in functional synaptic plasticity

It was previously reported that the level of conventional theta-burst stimulation (TBS)-induced LTP is normal in acute hippocampal slices from neurotrypsin-deficient mice (Matsumoto-Miyai et al., 2009). However, the conventional LTP protocol is not suitable to distinguish an increase of synaptic transmission due to the formation of new spines, as nascent spines are mostly silent (i.e., lack AMPA receptors) (Durand et al., 1996; Isaac et al., 1995; Liao et al., 1995; Petralia et al., 1999). Hence, we developed a new paradigm to verify the importance of neurotrypsin-dependent mechanisms for functional synaptic plasticity.

Krámar and colleagues (2012) described that a second theta-burst stimulation (TBS2) applied after first TBS (TBS1) doubled the level of potentiation (LTP). They reported that the induction of additional LTP only occurred when the second train was delayed by about one hour. In addition, the second stimulation train doubled the population of densely F-actin positive spines above that caused by TBS1 alone, supporting the idea that a new population of synapses was potentiated by TBS2 (Kramár et al., 2012). This time interval (1 hour) is necessary for recruitment of postsynaptic density components to nascent synapses, which can be used as a scaffold for recruitment of NMDA and AMPA receptors. This spaced form of LTP induced by two 1-hour spaced TBSs is accompanied by filopodia generation and their conversion into functional synapses (Kramár et al., 2012) and we expected that it could be reduced in neurotrypsin-deficient mice.

Following the protocol from Krámar et al., 2012, we recorded LTP induced by two 1 h-spaced TBS in CA3-CA1 synapses from $NT^{+/+}$ and $NT^{-/-}$ mouse slices. Our extracellular recordings revealed that, although $NT^{-/-}$ and $NT^{+/+}$ mice have a similar level of potentiation after TBS1, $NT^{-/-}$ mice show no additional potentiation after TBS2, unlike $NT^{+/+}$ mice. This suggests that a new population of synapses induced by agrin signalling could be potentiated by TBS2.

5.2. Role of neurotrypsin in distinct forms of learning and memory

To systematically investigate the behavioural alterations induced by the neurotrypsin null mutation, to eventually identify brain regions most notably affected by the knockout of neurotrypsin, and to study the role of neurotrypsin in distinct forms of memory formation we used a battery of behavioural paradigms. As synaptic plasticity experiments have involved neurotrypsin in hippocampal plasticity, we accomplished different highly hippocampus-dependent tasks (spaced contextual fear conditioning and conventional fear conditioning), but also paradigms dependent on hippocampus, cortex and other brain regions, such as fear

extinction, novel object recognition and sociability tests. These tests provided us with significant knowledge about the relevance of neurotrypsin-dependent mechanisms for different learning processes and behaviours.

As the first step, we examined the general locomotor activity, presence of anxiety-related phenotypes and/or repetitive behaviours using the open field test, as such phenotypes could potentially interfere the perception of the animals' performance during memory tasks. Likewise, the open field test enabled the assessment of exploration of new environments, which is also dependent on the hippocampus (Daenen et al., 2001). Both neurotrypsin-deficient mice and their wild-type littermates investigated the open field arena, spending similar time in the centre (~ 30 % of total time) and in the periphery of the arena (~ 70 % of total time). Similarly, both genotypes showed equal defaecation habits during the task. We also did not find significant differences between the time they spent doing grooming activity. Concerning the general locomotor activity, both neurotrypsin knockout mice and their control littermates showed similar travelled distance, comparable average speed, and alike immobility time duration. Overall, these results indicated that neurotrypsin deficiency did not affect the anxiety levels, nor the general locomotor activity of these mice, providing us with crucial information to support the interpretation of the behavioural responses during other behavioural tasks.

To match the spaced LTP protocol at the behavioural level, we designed a protocol of spaced contextual fear conditioning. Pavlovian contextual fear conditioning (CFC) represents a form of associative learning that has been well used in many species (Kim and Jung, 2006). Learning of the context requires input from the hippocampus, especially the dorsal part of hippocampus and CA3 region. However, the amygdala, the frontal cortex, and the cingulate cortex are also involved in the acquisition of contextual fear memory (Curzon et al., 2009). Previously, selective impairment of LTP induced by strong stimuli at CA3-CA1 synapses has been associated with a deficit in CFC (Kochlamazashvili et al., 2010) or context discrimination (Jin et al., 2013). More recent studies have also described similar combinations of an impairment of context discrimination and altered LTP in the CA1 region (Darcy et al., 2014; Minge et al., 2017). Moreover, one study that links cognitive deficits during acute neuroinflammation supports also that the CA1 region is involved in context discrimination (Czerniawski and Guzowski, 2014).

Previous studies indicated that both hippocampal and amygdaloid NMDA receptors are involved in the acquisition of Pavlovian fear conditioning. This research implicates NMDA receptor-dependent LTP in these brain areas in the acquisition of conditional fear. Moreover, several studies have used a correlational approach to assess the role of hippocampal LTP in

contextual fear conditioning, suggesting that hippocampal LTP is required in encoding contextual representations (reviewed in Maren, 2001). Interestingly, although neurotrypsin knock out mice exhibited normal LTP, neurotrypsin activation is an NMDA receptor-dependent process (Matsumoto-Miyai et al., 2009). Therefore, this prompted the question whether neurotrypsin may play a role in the acquisition of contextual fear memory.

We designed a protocol of “spaced” contextual fear conditioning and extinction in which we applied 6x foot shocks (0.5 mA, 1 s) in the conditioned context (CC+), divided into two learning sessions (3x + 3x) with 1 hour-interval delay between both sessions. Contrary to expectations, NT deficiency did not cause impairment in the retrieval of contextual memory as both groups of mice were able to distinguish between the CC+ and the neutral context (CC-) at memory recall d2 (48h after the training session). However, $NT^{-/-}$ mice appeared to be less efficient in discrimination between contexts during the retrieval of fear memory.

The level of spontaneous freezing/immobility in both genotypes in the CC+ before they received the shock, but also in CC-, was not different. Mice showed no signs of anxiety or hyperactivity, and the episodes of freezing were not longer than 1-2 s and covering only 5-10% of the total session, which is the normal freezing level during exploration of novel environments (Tang et al., 2003).

Subsequent repeated presentation of the CS (the context) by itself without the UCS (the foot shocks) leads to a progressive reduction in the expression of conditioned fear response, as the CS no longer predicts the aversive outcome. This process is named extinction and it does not directly modify the original fear memory but yields the formation of a new association that competes with the original engram masking it. Thus, extinction implies new learning. The neural circuit for fear extinction involves amygdala, hippocampus, entorhinal cortex, and mPFC, specifically the infralimbic part (Baldi and Bucherelli, 2015; Curzon et al., 2009; Maren et al., 2013). NT deficiency did not impair extinction of the fear memory as both groups of mice reduced the fear response to similar levels at recall d9 (after nine extinction of fear memory sessions).

Combined results indicate that there may be significant redundancy in the neuroanatomical regions and compensatory mechanisms mediating fear conditioning (Curzon et al., 2009). This is not surprising as the ability to accurately and reliably store fear memories from frightening experiences is essential to survive in an ever-changing and potentially dangerous environment. This may partly justify why deficiency of neurotrypsin is not sufficient to result in an impairment of encoding and/or recalling of fear mnemonic process. Another possible explanation for the observed result could be due to a ceiling effect/saturation and

generalization of the context. Because natural stimuli rarely take place in the identical form from one encounter to the next, the ability to generalize learning across stimuli and across situations is crucial. It is equally as important to discriminate between different stimuli and situations, and thus limit generalization (specificity) to prevent inappropriate behavioural responses. Generalization and specificity, therefore, help to ensure survival in a constantly changing environment by applying learning only when appropriate: not too much or too little. This tight and delicate balance between generalization and specificity is an essential factor of any animal that has to learn from experience. One domain of learning and behaviour where this balance is particularly important is fear learning, wherein stimuli that anticipate an aversive event gain the ability to elicit defensive responses (Dunsmoor and Paz, 2015). The generalization of fear conditioning is manifested as a loss of stimulus specificity and as the emotional sensitization of associative components of memory and leads to diminished signal discrimination and generalized anxiety (Ciocchi et al., 2010; Laxmi et al., 2003). Therefore, the more generalization of the signal, the less discrimination. For this reason, we cannot conclude whether the observed difference in discrimination between contexts and genotypes is due to a worst fear memory of the neurotrypsin-deficient mice – this is unlikely as there is normal response to CC+ – or due to a generalization of the signal, which is more likely. Previous findings indicate that fear generalization is broadly tuned and sensitive to the amount of fear intensity in unconditioned stimuli (Dunsmoor et al., 2009). Indeed, it was shown that increasing foot shock intensities (Baldi et al., 2004; Dunsmoor et al., 2009) and number of foot shocks (Poulos et al., 2016) lead to generalization of context memory.

For this reason, we thought that the spaced protocol with 6x foot shocks could have been too strong and have masked existing differences between genotypes. Therefore, we designed a milder contextual fear conditioning protocol with 3x foot shocks and one single context (see more detailed discussion in 5.4). The results obtained indicate that the neurotrypsin-deficient mice freeze significantly less in the conditioned context 24 h after conditioning, suggesting that neurotrypsin null mutation impairs formation or retrieval of contextual fear memory. Importantly, neurotrypsin deficiency affected neither the level of freezing before fear conditioning (normal freezing level during fully unconstrained exploration of a novel environment is 5–10% in mice) nor the significant elevation of freezing between three unconditioned stimuli, indicating that differences between genotypes at the memory recall session are not due to distinct perception of the aversive stimulus or higher basal anxiety levels. On the other hand, both genotypes similarly reduced their freezing levels after fear memory extinction, demonstrating that extinction of contextual fear memory was not altered by the neurotrypsin deficiency.

Blaeser and colleagues (2006), presented a study in a mouse mutant of the CaM kinase kinase α isoform (CaMKKα), an upstream component of the Ca^{2+} /calmodulin kinase (CaMK) cascade that has been implicated in neuronal gene transcription, synaptic plasticity, and long-term memory consolidation. Interestingly, they showed that CaMKKα mutants exhibited normal long-term spatial memory formation and cued fear conditioning but showed deficits in contextual fear conditioning. In addition, they also exhibited impaired activation of the downstream kinase CaMKIV/Gr and its substrate, the transcription factor cyclic AMP-responsive element binding protein (CREB) upon fear conditioning. Like in our neurotrypsin knockout mice, these mutants exhibited normal LTP, normal levels of anxiety-like behaviour and no deficit at all in extinction of the freezing response (Blaeser et al., 2006). Interestingly, it was previously described that activation of the agrin receptor in neurons resulted in a tyrosine kinase-dependent increase in intracellular Ca^{2+} that engages both CaMKII and MAPK signal pathways (Hilgenberg and Smith, 2004). Moreover, CREB phosphorylation showed to be markedly decreased in neurotrypsin-deficient mice after a spatial learning task and social interaction compared to hippocampal neurons of their wild-type littermates (Mitsui et al., 2009), suggesting that the mechanisms downstream of the agrin receptor in neurons may be involved in this signalling pathway.

Despite this second CFC protocol was designed in a massed manner (without performing spaced learning sessions), several studies support that sleep plays an active role in memory consolidation (Dudai et al., 2015; Graves et al., 2003; Rauchs et al., 2011). During sleep, episodes and events experienced during active/awake time are replayed. In this sense, acquisition plus consolidation could be viewed as a spaced stimulation. Indeed, there are parallels between the sleep literature and the spacing effect studies (Bell et al., 2014; Smith and Scarf, 2017). In skill learning tasks, a period of sleep leads to better performance with no additional practice (Fischer and Born, 2009; Kuriyama et al., 2004; Walker and Stickgold, 2004). Interestingly, a previous study aimed to determine whether sleep is important for the consolidation of a single-trial fear conditioning task. They found that sleep deprivation after training impaired memory consolidation for contextual fear conditioning but had no effect on cued fear conditioning, suggesting that sleep may be particularly important for hippocampus-dependent tasks (Graves et al., 2003). Moreover, previous studies have described that memory consolidation for fear conditioning is impaired when protein kinase A (PKA) and protein synthesis inhibitors are administered at same time intervals as when sleep deprivation is effective, suggesting that sleep deprivation may act by changing these molecular pathways of memory storage (Bernabeu et al., 1997; Bourtchouladze et al., 1998; Schafe et al., 1999).

To study another form of long-term memory, we used the novel object recognition (NOR) test as it is one of the most popular methods for testing the neurobiology of non-spatial and non-aversive memory in rodents. However, despite its wide use and popularity, the underlying neural circuitry and mechanisms supporting NOR are still under discussion. There is a strong evidence that the perirhinal cortex is essential for this type of memory. However, the involvement of hippocampus in object memory remains under debate due to controversial findings across temporary and permanent hippocampal lesions studies. Nevertheless, as previously introduced (see 1.3.2c), several studies recently reviewed by Cohen and Stackman (2015) indicated that the hippocampus is essential for the retention of object recognition memory when the interval between sessions is longer than 10 min (Cohen and Stackman, 2015). Hence, the non-conditioned nature of the novel object recognition test presents a different instrument to test hippocampal-dependent memory if the delay between sessions is greater than 10 minutes.

Our data revealed that both neurotrypsin-deficient mice and their wild-type littermates spent a longer time exploring the novel than the familiar object during the second trial or retrieval session (24 h after presenting familiar objects). Moreover, the exploration duration towards the objects was similar between genotypes. Hence, these results show that long-term novel object recognition memory is intact in the novel object recognition task.

Thus, the neurotrypsin null mutation affects the behavioural performance in a different manner depending on the nature of the memory being studied (**Table 5.1**).

Type of memory tested	**Neurotrypsin-deficient mice**
Context discrimination in spaced CFC	↓
Fear extinction in spaced CFC	=
Conventional CFC	↓
Fear extinction in conventional CFC	=
Novel object recognition	=

↓ reduced or impaired; = not affected

Table 5.1 | Summary of the memory abilities showed by neurotrypsin-deficient mice.

5.3. Neurotrypsin modulates social interaction

Alterations in social behaviour are symptoms of several neuropsychiatric and neurological diseases. Particularly, mental retardation is generally accompanied by a functional deficit in adaptive behaviour such as social skills and communication (Bieleck and Swender, 2004).

Social interaction was tested on the experimental subjects, $NT^{-/-}$ and $NT^{+/+}$ mice, using the three-chamber sociability test, a widely used test paradigm to quantitatively measure this behaviour (Moy et al., 2004). We found that neurotrypsin-deficient mice have highly significantly lower sociability levels compared with their control wild-type littermates, as they spent much shorter amount of time exploring and sniffing the stimulus mouse. This outcome is opposite to a previous study in adult (14-20-week-old) neurotrypsin knockout mice in which they showed that both $NT^{-/-}$ and $NT^{+/+}$ mice sniffed the stimulus mouse for significantly longer than the empty cage. In addition, they performed a three-chamber social novelty test and described that both genotypes preferred the novel to the familiar mouse, suggesting normal social memory. However, neurotrypsin-deficient mice spent more time sniffing the familiar mouse than the wild-type did, indicating that the mutant mice had enhanced social interest even in a familiar mouse. Surprisingly, although normal sociability and social memory, adult neurotrypsin knockout mice showed markedly reduced CREB phosphorylation in hippocampal CA1 neurons after social interaction compared to their wild-type littermates (Mitsui et al., 2009). However, CREB analysis was not performed in the same animals that undergo the three-chamber sociability test. Mice that were tested for behavioural analysis were housed in single cages at least 1 week before starting the task. On the other hand, brain slices for CREB analysis came from group-housed animals at least 2 weeks before the test.

In addition, it is important to mention that Mitsui and colleagues (2009) used a different neurotrypsin knockout model for their experiments, in which the exon 1 of the PRSS12 gene (the gene encoding for neurotrypsin) was replaced (Mitsui et al., 2009), while we used the neurotrypsin knockout mouse model in which part of the exons 10 and 11 were replaced, resulting in a truncated neurotrypsin gene lacking the region encoding the proteolytic domain (Stephan et al., 2008). This latter model has been extensively used in the most relevant literature of the topic (Matsumoto-Miyai et al., 2009; Stephan et al., 2008). In addition, the difference in age may be essential as the level of neurotrypsin expression in hippocampus is declining after postnatal day 24 (Wolfer et al., 2001) and our study better fits to the age when neurotrypsin-dependent cleavage of agrin showed to be critical for the formation of filopodia.

The hippocampus is known to be crucial for social behaviour. A lesion of the hippocampus disrupted social memory. Furthermore, alterations of many genes expressed in the

hippocampus have been found to impair social behaviour (D'Adamo, 2002; Kwon et al., 2006; Morellini et al., 2007; Nishijima et al., 2006) and social recognition of familiar individuals (Lai, 2005). However, social interaction is a complex behaviour essential for many species and it has been shown that other brain areas, such as the ventral tegmental area, nucleus accumbens (Gunaydin et al., 2014), prefrontal cortex (Kumar et al., 2014), and the amygdala - particularly the basolateral complex (Felix-Ortiz and Tye, 2014) and the medial amygdala (Hong et al., 2014) -, are involved. Since expression of neurotrypsin mRNA showed to be high in neurons of the amygdala (Gschwend et al., 1997; Wolfer et al., 2001), it is plausible to speculate that some amygdala-dependent social paradigms may be impaired in the neurotrypsin-deficient mice.

5.4. Neurotrypsin-dependent cleavage of agrin plays a major role in regulating dendritic spine formation

As LTP-dependent formation of filopodia appeared to be abolished in mice lacking neurotrypsin (Matsumoto-Miyai et al., 2009) and dendritic filopodia are thought to be direct precursors of new dendritic spines (Jontes and Smith, 2000; Yuste and Bonhoeffer, 2004; Ziv and Smith, 1996), we hypothesised that neurotrypsin-dependent mechanisms may have an effect on spinogenesis and/or spine morphology. As neurotrypsin is released in an activity-dependent manner (Frischknecht et al., 2008), we investigated dendritic spines in both naïve mice and after learning. For assessing learning-induced spine formation we selected the contextual fear conditioning task because of two reasons. On one hand, we found that neurotrypsin-deficient mice are impaired in the formation or retrieval of CFC, as they have significantly lower freezing levels at the memory recall. On the other hand, we needed a protocol that strongly modulates spinogenesis and several studies provided evidence that FC lead to changes in spine density and/or morphology (Abate et al., 2018; Bender et al., 2018; Giachero et al., 2013, 2015; Lai et al., 2012; Petsophonsakul et al., 2017; Pignataro et al., 2013).

We found that neurotrypsin-deficient mice had significantly reduced spine density in CA1 secondary apical neurons in naïve conditions compared to their control wild-type littermates. This is in line with a previous study describing that a different knockout model of neurotrypsin had reduced spine density in neurons from CA1 region of hippocampus but not from cingulate cortex (Mitsui et al., 2009). However, it is not clear from their representative pictures if the analysis was performed in secondary or primary dendrites, and they do not provide this information in the manuscript.

Contrary to our expectations, no differences in spine density after acquisition or extinction of CFC (learning-dependent spinogenesis) were detected between genotypes. However, it seems that in wild-type mice, there is a tendency to reduce spine density after the acquisition of fear memory and to increase it again after extinction (going back to a similar scenario like that in naïve conditions). This is in line with a study that revealed that fear conditioning increased the rate of spine elimination, whereas fear extinction increased the rate of spine formation (Lai et al., 2012). Similarly, another study reported a significant decrease of total spine density after CFC, relative to home caged animals that did not undergo CFC (Sanders et al., 2012). This is consistent with a documented role of stress in decreasing spine density (Bloss et al., 2011; Chen et al., 2008). By contrast, some other studies have reported no changes in spine density after CFC (Giachero et al., 2013, 2015) or, alternatively, an increase of spines after CFC (Abate et al., 2018; Bender et al., 2018; Pignataro et al., 2013). The discrepancy between those studies might rely on the timing of sample collection for spine counting.

However, no spine dynamics were observed in neurotrypsin-deficient mice between conditions. Because fear memory is particularly important to elicit defensive responses to ensure the survival of species, it is not surprising that other mechanisms of structural plasticity may be involved and even compensate, partially or wholly, the neurotrypsin deficiency.

Interestingly, the morphological analysis determined that percentage of thin/filopodia-like spines was significantly reduced in $NT^{-/-}$ mice, whereas the proportion of mushroom spines was higher in this genotype. Regarding stubby spines, no significant differences were found between the two groups. Thin spines are highly dynamic protrusions that can grow, shrink or change into other spine subtypes (reviewed by Kasai et al., 2010). On the contrary, stubby and mushroom spines are less dynamic and are relatively stable (Holtmaat et al., 2005; De Roo et al., 2008). Thus, the higher percentage of thin spines in the wild-type mice likely reflects the morphological shift of spines that concurrently fulfil the needs for synaptic sites available for structural plasticity.

In agreement with the observed higher proportion of thin spines in the wild-type mice, we found a statistically significant reduction of the spine head size in this group of mice. However, this reduction was not present after CFC. We initially thought that this enlargement of the spine head size after CFC may be due to a difference in the mushroom spines, which might be larger and more mature in the control group after CFC and hence compensate for this difference. Accordingly, we measured the head diameter in the mushroom spines that were automatically detected by the software used for spine analysis. Surprisingly, we found that mushroom spine head size was alike in both groups of mice. Consequently, we evaluated the head diameter in

the thin spines after CFC. Strikingly, we observed that the thin spines were bigger and most likely more mature in the wild-type control group, suggesting that neurotrypsin-deficiency may specifically affect the maturation of thin/filopodia-like spines. Interestingly, enlargement of nascent spines revealed to be tightly coupled to formation and maturation of glutamatergic synapses (Zito et al., 2009).

As agrin is the only substrate of neurotrypsin identified so far and critically important for activity-dependent filopodia formation (Matsumoto-Miyai et al., 2009), we addressed the question whether agrin cleavage may be responsible for the observed spine loss in neurotrypsin-deficient mice. Interestingly, previous research described that the transmembrane isoform of agrin regulates dendritic filopodia (Mccroskery et al., 2009; McCroskery et al., 2006) and synapse formation (Mccroskery et al., 2009) in rat mature hippocampal neurons. Another study on agrin function in the CNS indicated that clustering of agrin using anti-agrin antibodies stimulated filopodia formation in mouse hippocampal neuronal culture (Annies et al., 2005). We wondered whether we can rescue the spine loss present in neurotrypsin-deficient mice with an adeno-associated virus (AAV) expressing agrin-22. As a control, we used a shorter version of agrin-22, agrin-15, which was shown to act as an agrin antagonist in hippocampal and cortical cultures (Hoover et al., 2003b) and in acute-slice preparations (Hilgenberg et al., 2006b; Tidow et al., 2010b). Results showed that AAV-Ag22 significantly increased the spine density in neurotrypsin-deficient mice to the levels observed in wild-type mice. This effect was not detected when mice were injected with AAV-Ag15, suggesting a specific effect of the product of neurotrypsin-dependent agrin cleavage in promoting spine formation. Despite its effect on spine density, injection of AAV-Ag22 did not have any impact on spine morphology or on spine head size. However, dendritic filopodia were slightly increased in mice injected with AAV-Ag22 compared with those injected with AAV-Ag15. Outstandingly, it was shown that the transmembrane form of agrin increased the number of dendritic spines in the external plexiform layer of the olfactory bulb. Moreover, expression of the antagonist agrin-15 interfered with the spine formation in the olfactory bulb (Burk et al., 2012).

Importantly, our data are in line with the hypothesis that AAV-Ag22 signals via its neuronal receptor α3NKA (Hilgenberg et al., 2006b), as we observed an extensive overlap between the α3NKA and the “agrin puncta” expression in the *stratum radiatum* of CA1. In addition, we confirmed that the AAV-Ag22 was properly delivered and expressed at synaptic sites as both VGLUT1 and PSD95 co-localized with Ag22-scarlet at synapses. Interestingly, we found that VGLUT1-positive puncta co-localizing with Ag22-scarlet were significantly bigger compared to those without Ag22-scarlet co-localization. This striking observation suggests that AAV-

Ag22 may induce synapse formation and/or clustering of VGLUT1-positive presynapses and PSD95-positive postsynapses. This is not surprising as it was previously described that spine growth precedes synapse formation in the adult neocortex *in vivo* (Knott et al., 2006). In addition, De Roo and colleagues (2008) reported that new spines, upon LTP, tend to be established in clusters, providing a potential mechanism for clustered plasticity specifically upon learning (De Roo et al., 2008). Interestingly, an increased clustering of potentiated synapses has also been observed in the previously discussed *in vitro* study from Krámar et al., (2012), which simulated spaced learning in the hippocampus (Kramár et al., 2012). More recently, several reviews on the topic suggest that clusters of functionally related synapses may serve as essential memory storage units in the brain (Kastellakis et al., 2015; Winnubst and Lohmann, 2012).

Overall, our results provide an *in vivo* evidence of the spinogenesis effects of agrin-22, the product of neurotrypsin-dependent agrin cleavage, and suggest that it might be an important mechanism for clustered plasticity and synapse formation.

5.5. Limitations of the model and outlook

Mental retardation results from deficiencies in an extensive number of higher brain functions, commonly summarized as cognitive functions (Ropers and Hamel, 2005). The presently available data on monogenic mutations resulting in mental retardation detail a relatively high percentage of genes that encode proteins implicated in both presynaptic vesicle release and dynamic functions of dendritic spines (Chelly and Mandel, 2001). These elements are important for the adaptive response of synapses to a change in functional needs summarized under the concept synaptic plasticity, which is evinced to play a crucial role in the implementation of cognitive functions (Ethell and Pasquale, 2005; Fiala et al., 2002).

In the last two decades, progress in genetic engineering has provided many transgenic mice that are used as genetic models for several neurodevelopmental and neurodegenerative diseases (Kreiner, 2015). Surprisingly, although in many cases these transgenic mice were developed precisely targeting the same causative mutations involved in the human disorders, they do not fully recapitulate the same symptoms as in the human disease (El-Brolosy and Stainier, 2017; Kreiner, 2015). Some transgenic mice fail to even show the phenotypic alterations associated with the modelled diseases (White et al., 2013), which suggests the possible existence of compensatory mechanisms.

One possibility to overcome the genetic compensatory mechanisms would be using conditional knockouts or knockdown approaches. Indeed, several recent studies have described phenotypic differences between knockouts and knockdowns with the same genetic target (Rossi et al., 2015). With the current experimental approach used in this thesis, we run the risk of some compensatory mechanisms that may be covering or attenuating the neurotrypsin-deficient phenotype. In fact, the phenotype of agrin-null mouse embryos and neurons suggests the possibility that other molecules, such as syndecan proteoglycans (Hsueh and Sheng, 1999) may compensate for the chronic absence of agrin in the brain. Therefore, it would be extremely interesting to address these questions using more sophisticated approaches for manipulation of neurotrypsin expression.

Another important point that should be better addressed in future studies is to closer investigate whether the impairment of neurotrypsin-deficient mice in spaced LTP are due to the spaced LTP-dependent filopodia and spine formation or due to other mechanisms. For that, it would be very interesting to use a synaptic probe that can label specifically recently activated spines (Hayashi-Takagi et al., 2015) and directly count the nascent synapses among all stimulated ones. Similarly, it would be also intriguing to evaluate the effects of AAV-Ag22 *in vivo* in terms of new dendritic spines generated after a cognitive behavioural task.

Recently, it was reported that the α3NKA may act as a neurotoxic receptor for the toxic amyloid beta oligomers (AβOs), which are known to accumulate in Alzheimer's disease (AD) and in animal models of AD. AβOs have been found to cause impaired synaptic plasticity, loss of memory function, tau hyperphosphorylation and tangle formation, synapse elimination, oxidative and endoplasmic reticulum stress, inflammatory microglial activation, and selective nerve cell death (di Chiara et al., 2017). They accumulate early in the disease process, in humans and in transgenic animal AD models (Lacor, 2004). Indeed, AβOs accumulate before the emergence of plaques. In addition, it was shown that amyloid plaques are not required for dementia but toxic AβOs are. AβOs, which have been examined in more than 3000 studies, are currently considered the major toxic form of Aβ (di Chiara et al., 2017). AβO-specific antibodies, developed to validate the existence of toxic AβOs in AD pathology, can prevent pathology and memory deficits in transgenic AD animals (Oddo et al., 2006). Other AβO-targeting antibodies have rescued behaviour in AD animal models (Dorostkar et al., 2014; Rasool et al., 2013). The essential question here is whether these achievements can be translated to humans. There have been multiple clinical trial failures of immunotherapy related to Aβ going back to 2000 (di Chiara et al., 2017).

There are several gaps in understanding the AβO-mediated mechanisms. Indeed, the better-understood steps occur downstream in the toxic pathway. These intracellular abnormalities

comprise excessive Ca^{2+} mobilization by hyperactive mGluR5 receptors; stimulation of Fyn protein tyrosine kinase; hyper-activation of NMDARs, which exacerbates Ca^{2+} build-up and generates reactive oxygen species (ROS) accumulation; pathological phosphorylation of tau; and bifurcating pathways leading to multiple pathological outcomes (Ferreira and Klein, 2011; Jarosz-Griffiths et al., 2016; Krafft and Klein, 2010; Viola and Klein, 2015). Studies investigating AβO binding have established saturation and high-affinity binding to cultured neurons and synaptosome preparations, specificity for particular neurons and brain regions, targeting of synapses and accumulation at dendritic spines among others (di Chiara et al., 2017). Several AβO binding proteins have been identified, and many have properties that make them promising candidates as toxin receptors. Initial evidence strongly suggested that binding to cellular prion protein was an essential step in the mechanism of AβO toxicity. Investigations of how externally oriented prion protein might bring about intracellular damage indicated coupling to the protein tyrosine kinase Fyn. Co-immuno-precipitation studies showed that AβO interact with complexes containing the GluR2 subunit of AMPARs. Moreover, single particle tracking of quantum dot-labeled AβO has shown the involvement of metabotropic glutamate receptors (mGluR5) in oligomer binding and clustering at synapses. The mGluR5 receptor appeared to act between AβO-affected prion protein and Fyn. NMDARs co-immunoprecipitated with AβO from detergent-extracted oligomer-treated rat synaptosomal membranes. In agreement with this finding, oligomer binding is abolished in dendrites of NMDAR knock-down neurons (reviewed in Ferreira and Klein, 2011; Viola and Klein, 2015). Intriguingly, it was recently described that the α3NKA (the agrin-22 targeting receptor) is a new candidate as it showed high affinity for AβOs derived from AD brain tissue. They found that binding led to an inhibition of ATPase activity, Ca^{2+} build-up, and apoptosis. In addition, they revealed that AβOs co-localized with the α3NKA in hippocampal neurons, particularly at dendritic spines (Ohnishi et al., 2015). Di Chiara et al., 2017 confirmed that AβOs bind to α3NKA *in vitro* and co-localize with α3NKA in mature hippocampal cultures. They showed that within minutes of exposure to AβOs, α3NKA became accumulated in dense clusters along dendrites. The clustering of α3NKA is in line with the previous observation that AβOs induce the clustering of mGluR5. mGluR5 is a Ca^{2+} mobilizing receptor, and it is regarded as a crucial mediator of AβO-elevated Ca^{2+} build-up and the ensued damage (di Chiara et al., 2017). Overall, the available data are in line with the hypothesis that AβO attachment to cell surfaces is transduced into a neurotoxic mechanism by an altered membrane protein topography seeded by AβO binding to α3NKA.

Interestingly, agrin-15, an agrin fragment that acts as an agrin antagonist, disrupted native agrin-22 - α3NKA interactions (Hilgenberg et al., 2006b) and inhibited spine formation in the olfactory bulb (Burk et al., 2012). It would be interesting to consider the hypothesis that AβO

may bind to the α3NKA with a similar mechanism than agrin-15. More importantly, it would be crucial to evaluate whether agrin-22 may compete with AβO for binding to the α3NKA and/or partially rescue the spine loss described in several AD mouse models.

6. CONCLUSIONS

- Young neurotrypsin-deficient and wild-type mice have a similar level of potentiation after the first TBS. However, after the second TBS which is expected to unmask LTP of newly formed synapses and is accompanied by filopodia generation, neurotrypsin-deficient mice showed no additional potentiation, unlike wild-type mice.

- Neurotrypsin knockout mice appeared to be less efficient in discrimination between neutral and conditioned context in the spaced fear conditioning paradigm.

- Neurotrypsin-deficient mice are impaired in contextual fear memory, as they showed significantly lower freezing levels in the conditioned context.

- In the novel object recognition task, both neurotrypsin-deficient mice and their wild-type littermates spent a longer amount of time exploring the novel than the familiar object during the memory recall session, suggesting that long-term novel object recognition memory is intact in the neurotrypsin-deficient mice.

- Neurotrypsin-deficient mice have significant deficits in sociability levels compared to their wild-type littermates.

- Spine analysis revealed significantly reduced spine density in neurotrypsin-deficient mice compared to their control wild-type littermates in naïve conditions.

- The morphological analysis determined that the percentage of thin/filopodia-like spines was significantly reduced in neurotrypsin-deficient mice, whereas the proportion of mushroom spines was higher in this genotype.

- AAV-Ag22 significantly increased the spine density in neurotrypsin-deficient mice to the levels observed in wild-type mice, suggesting that a deficit in proteolytic processing of agrin is the major mechanism responsible for spine abnormalities in neurotrypsin-deficient mice.

- VGLUT1-positive puncta co-localizing with Ag22-scarlet were significantly bigger compared to those not associated with Ag22-scarlet, suggesting that Ag22-scarlet may induce synapse formation or aggregation of VGLUT1-positive synaptic vesicles at presynapses.

7. REFERENCES

Abate, A.G., Colazingari, S., Conversi, D., and Bevilacqua, A. (2018). Dendritic spine density and EphrinB2 levels of hippocampal and anterior cingulate cortex neurons increase sequentially during formation of recent and remote fear memory in the mouse. Brain Res. Bull.

Annies, M., Bittcher, G., Ramseger, R., Rgen, J., Schinger, L., Wö, S., Porten, E., Abraham, C., Rü, M.A., and Krö Ger, S. (2005). Clustering transmembrane-agrin induces filopodia-like processes on axons and dendrites.

Apel, E.D., Roberds, S.L., Campbell, K.P., and Merlie, J.P. (1995). Rapsyn may function as a link between the acetylcholine receptor and the agrin-binding dystrophin-associated glycoprotein complex. Neuron *15*, 115–126.

Apel, E.D., Glass, D.J., Moscoso, L.M., Yancopoulos, G.D., and Sanes, J.R. (1997). Rapsyn is required for MuSK signaling and recruits synaptic components to a musk-containing scaffold. Neuron *18*, 623–635.

Arber, S., Barbayannis, F.A., Hanser, H., Schneider, C., Stanyon, C.A., Bernard, O., and Caroni, P. (1998). Regulation of actin dynamics through phosphorylation of cofilin by LIM-kinase. Nature *393*, 805–809.

Aricescu, A.R., Lu, W., and Jones, E.Y. (2006). A time- and cost-efficient system for high-level protein production in mammalian cells. Acta Crystallogr. Sect. D Biol. Crystallogr. *62*, 1243–1250.

Attwood, B.K., Bourgognon, J.M., Patel, S., Mucha, M., Schiavon, E., Skrzypiec, A.E., Young, K.W., Shiosaka, S., Korostynski, M., Piechota, M., et al. (2011). Neuropsin cleaves EphB2 in the amygdala to control anxiety. Nature *473*, 372–377.

Baldi, E., and Bucherelli, C. (2015). Brain Sites Involved In Fear Memory Reconsolidation And Extinction Of Rodents. Neurosci. Biobehav. Rev.

Baldi, E., Lorenzini, C.A., and Bucherelli, C. (2004). Footshock intensity and generalization in contextual and auditory-cued fear conditioning in the rat. Neurobiol. Learn. Mem. *81*, 162–166.

Bastrikova, N., Gardner, G.A., Reece, J.M., Jeromin, A., and Dudek, S.M. (2008). Synapse elimination accompanies functional plasticity in hippocampal neurons. Proc. Natl. Acad. Sci. U. S. A. *105*, 3123–3127.

Becker, N., Wierenga, C.J., Fonseca, R., Bonhoeffer, T., and Nägerl, U.V. (2008). LTD Induction Causes Morphological Changes of Presynaptic Boutons and Reduces Their Contacts with Spines. Neuron *60*, 590–597.

Bednarek, E., and Caroni, P. (2011). B-Adducin Is Required for Stable Assembly of New Synapses and Improved Memory Upon Environmental Enrichment. Neuron *69*, 1132–1146.

Bell, M.C., Kawadri, N., Simone, P.M., and Wiseheart, M. (2014). Long-term memory , sleep

, and the spacing effect. *22*, 276–283.

Bender, C., Giachero, M., Comas-Mutis, R., Molina, V., and Calfa, D. (2018). Stress influences the dynamics of hippocampal structural remodeling associated with fear memory extinction. Neurobiol. Learn. Mem.

Bennur, S., Shankaranarayana Rao, B.S., Pawlak, R., Strickland, S., McEwen, B.S., and Chattarji, S. (2007). Stress-induced spine loss in the medial amygdala is mediated by tissue-plasminogen activator. Neuroscience *144*, 8–16.

Bernabeu, R., Bevilaqua, L., Ardenghi, P., Bromberg, E., Schmitz, P., Bianchin, M., Izquierdo, I., and Medina, J.H. (1997). Involvement of hippocampal cAMP/cAMP-dependent protein kinase signaling pathways in a late memory consolidation phase of aversively motivated learning in rats. Proc. Natl. Acad. Sci. U. S. A. *94*, 7041–7046.

Bernardinelli, Y., Nikonenko, I., and Muller, D. (2014). Structural plasticity: mechanisms and contribution to developmental psychiatric disorders. Front. Neuroanat. *8*, 1–9.

Bieleck, J., and Swender, S. (2004). The Assessment of Social Functioning in Individuals With Mental Retardation. Behav. Modif. *28*, 694–708.

Bindels, D.S., Haarbosch, L., Van Weeren, L., Postma, M., Wiese, K.E., Mastop, M., Aumonier, S., Gotthard, G., Royant, A., Hink, M.A., et al. (2016). MScarlet: A bright monomeric red fluorescent protein for cellular imaging. Nat. Methods *14*, 53–56.

Blaeser, F., Sanders, M.J., Truong, N., Ko, S., Wu, L.J., Wozniak, D.F., Fanselow, M.S., Zhuo, M., and Chatila, T.A. (2006). Long-Term Memory Deficits in Pavlovian Fear Conditioning in Ca2+/Calmodulin Kinase Kinase -Deficient Mice. Mol. Cell. Biol. *26*, 9105–9115.

Bliss, T.V.P., and Lømo, T. (1973). Long-lasting potentiation of synaptic transmission in the dentate area of the anaesthetized rabbit following stimulation of the perforant path. J. Physiol. *232*, 331–356.

Bloss, E.B., Janssen, W.G., Ohm, D.T., Yuk, F.J., Wadsworth, S., Saardi, K.M., McEwen, B.S., and Morrison, J.H. (2011). Evidence for Reduced Experience-Dependent Dendritic Spine Plasticity in the Aging Prefrontal Cortex. J. Neurosci. *31*, 7831–7839.

Bock, J., and Braun, K. (1999). Blockade of N-methyl-D-aspartate receptor activation suppresses learning-induced synaptic elimination. Proc. Natl. Acad. Sci. U. S. A. *96*, 2485–2490.

Bolliger, M.F., Zurlinden, A., Luscher, D., Butikofer, L., Shakhova, O., Francolini, M., Kozlov, S. V., Cinelli, P., Stephan, A., Kistler, A.D., et al. (2010). Specific proteolytic cleavage of agrin regulates maturation of the neuromuscular junction. J. Cell Sci. *123*, 3944–3955.

Bosch, M., Castro, J., Saneyoshi, T., Matsuno, H., Sur, M., and Hayashi, Y. (2014). Structural and molecular remodeling of dendritic spine substructures during long-term potentiation. Neuron.

Bose, C.M., Qiu, D., Bergamaschi, a, Gravante, B., Bossi, M., Villa, a, Rupp, F., and

Malgaroli, a (2000). Agrin controls synaptic differentiation in hippocampal neurons. J. Neurosci. *20*, 9086–9095.

Bourne, J.N., and Harris, K.M. (2008). Balancing Structure and Funcion at Hippocampal Dendritic Spines. Annu Rev Neurosci *31*, 47–67.

Bouron, A., and Reuter, H. (1996). A role of intracellular Na+ in the regulation of synaptic transmission and turnover of the vesicular pool in cultured hippocampal cells. Neuron *17*, 969–978.

Bourtchouladze, R., Abel, T., Berman, N., Gordon, R., Lapidus, K., and Kandel, E.R. (1998). Different Training Procedures Recruit Either One or Two Critical Periods for Contextual Memory Consolidation, Each of Which Requires Protein Synthesis and PKA. Learn. Mem. *5*, 365–374.

Bramham, C.R. (2008). Local protein synthesis, actin dynamics, and LTP consolidation. Curr. Opin. Neurobiol. *18*, 524–531.

Burk, K., Desoeuvre, A., Boutin, C., Smith, M.A., Kröger, S., Bosio, A., Tiveron, M.-C., and Cremer, H. (2012). Agrin-Signaling Is Necessary for the Integration of Newly Generated Neurons in the Adult Olfactory Bulb. J. Neurosci. *32*, 3759–3764.

Burk, K., Ramachandran, B., Ahmed, S., Hurtado-Zavala, J.I., Awasthi, A., Benito, E., Faram, R., Ahmad, H., Swaminathan, A., McIlhinney, J., et al. (2017). Regulation of Dendritic Spine Morphology in Hippocampal Neurons by Copine-6. Cereb. Cortex 1–18.

Butz, M., Wörgötter, F., and van Ooyen, A. (2009). Activity-dependent structural plasticity. Brain Res. Rev. *60*, 287–305.

Calabresi, P., Napolitano, M., Centonze, D., Marfia, G.A., Gubellini, P., Teule, M.A., Berretta, N., Bernardi, G., Frati, L., Tolu, M., et al. (2000). Tissue plasminogen activator controls multiple forms of synaptic plasticity and memory. Eur J Neurosci *12*, 1002–1012.

Camp, L.A., Verkruyse, L.A., Afendis, S.J., Slaughter, C.A., and Hofmann, S.L. (1994). Molecular Cloning and Expression of Palmitoyl-protein Thioesterase. J. Biol. Chem. *269*, 23212–23219.

Caroni, P., Donato, F., and Muller, D. (2012). Structural plasticity upon learning: Regulation and functions. Nat. Rev. Neurosci. *13*, 478–490.

Chang, F.F., and Greenough, W.T. (1984). Transient and enduring morphological correlates of synaptic activity and efficacy in the rat hippocampal slice. Brain Res. *309*, 35–46.

Chelly, J., and Mandel, J.L. (2001). Monogenic causes of x-linked mental retardation. Nat. Rev. Genet. *2*, 669–680.

Chen, C.C., Bajnath, A., and Brumberg, J.C. (2015). The impact of development and sensory deprivation on dendritic protrusions in the mouse barrel cortex. Cereb. Cortex *25*, 1638–1653.

Chen, Y., Dube, C.M., Rice, C.J., and Baram, T.Z. (2008). Rapid Loss of Dendritic Spines

after Stress Involves Derangement of Spine Dynamics by Corticotropin-Releasing Hormone. J. Neurosci. *28*, 2903–2911.

Chen, Z.-L., Yoshida, S., Kato, K., Momota, Y., Suzuki, J., Tanaka, T., Ito, J., Nishino, H., Aimoto, S., Kiyama, H., et al. (1995). Expression and activity-dependent changes of a novel limbic-serine protease gene in the hippocampus. J. Neurosci. *15*, 5088.

Chevilley, A., Lesept, F., Lenoir, S., Ali, C., Parcq, J., and Vivien, D. (2015). Impacts of tissue-type plasminogen activator (tPA) on neuronal survival. Front. Cell. Neurosci. *9*.

di Chiara, T., DiNunno, N., Clark, J., Bu, R. Lo, Cline, E.N., Rollins, M.G., Gong, Y., Brody, D.L., Sligar, S.G., Velasco, P.T., et al. (2017). Alzheimer's toxic amyloid beta oligomers: Unwelcome visitors to the Na/K ATPase alpha3 docking station. Yale J. Biol. Med. *90*, 45–61.

Christmas, A.J., and Maxwell, D.R. (1970). A comparison of the effects of some benzodiazepines and other drugs on aggressive and exploratory behaviour in mice and rats. Neuropharmacology *9*, 17–29.

Cingolani, L.A., and Goda, Y. (2008). Actin in action: The interplay between the actin cytoskeleton and synaptic efficacy. Nat. Rev. Neurosci. *9*, 344–356.

Ciocchi, S., Herry, C., Grenier, F., Wolff, S.B.E., Letzkus, J.J., Vlachos, I., Ehrlich, I., Sprengel, R., Deisseroth, K., Stadler, M.B., et al. (2010). Encoding of conditioned fear in central amygdala inhibitory circuits. Nature *468*, 277–282.

Cohen, S.J., and Stackman, R.W. (2015). Assessing rodent hippocampal involvement in the novel object recognition task. A review. Behav. Brain Res. *285*, 105–117.

Conant, K., Lonskaya, I., Szklarczyk, A., Krall, C., Steiner, J., Maguire-Zeiss, K., and Lim, S.T. (2011). Methamphetamine-associated cleavage of the synaptic adhesion molecule intercellular adhesion molecule-5. J. Neurochem. *118*, 521–532.

Curzon, P., Rustay, N.R., and Browman, K.E. (2009). Cued and Contextual Fear Conditioning for Rodents. In Methods of Behavior Analysis in Neuroscience, (Taylor & Francis Group, LLC), pp. 19–37.

Czerniawski, J., and Guzowski, J.F. (2014). Acute Neuroinflammation Impairs Context Discrimination Memory and Disrupts Pattern Separation Processes in Hippocampus. J. Neurosci. *34*, 12470–12480.

D'Adamo, P. (2002). Deletion of the mental retardation gene Gdi1 impairs associative memory and alters social behavior in mice. Hum. Mol. Genet. *11*, 2567–2580.

Daenen, E.W.P.M., Van der Heyden, J.A., Kruse, C.G., Wolterink, G., and Van Ree, J.M. (2001). Adaptation and habituation to an open field and responses to various stressful events in animals with neonatal lesions in the amygdala or ventral hippocampus. Brain Res. *918*, 153–165.

Darcy, M.J., Jin, S.X., and Feig, L.A. (2014). R-Ras contributes to LTP and contextual discrimination. Neuroscience *277*, 334–342.

Davis, M. (1997). Neurobiology of fear responses: the role of the amygdala. J. Neuropsychiatry Clin. Neurosci. *9*, 382–402.

DeChiara, T.M., Bowen, D.C., Valenzuela, D.M., Simmons, M. V, Poueymirou, W.T., Thomas, S., Kinetz, E., Compton, D.L., Rojas, E., Park, J.S., et al. (1996). The receptor tyrosine kinase MuSK is required for neuromuscular junction formation in vivo. Cell *85*, 501–512.

Dityatev, A., Bukalo, O., and Schachner, M. (2008). Modulation of synaptic transmission and plasticity by cell adhesion and repulsion molecules. Neuron Glia Biol. *4*, 197–209.

Dityatev, A., Schachner, M., and Sonderegger, P. (2010). The dual role of the extracellular matrix in synaptic plasticity and homeostasis. Nat. Rev.

Dorostkar, M.M., Burgold, S., Filser, S., Barghorn, S., Schmidt, B., Anumala, U.R. a., Hillen, H., Klein, C., and Herms, J. (2014). Immunotherapy alleviates amyloid-associated synaptic pathology in an Alzheimer's disease mouse model. Brain *137*, 3319–3326.

Drakew, A., Müller, M., Gähwiler, B.H., Thompson, S.M., and Frotscher, M. (1996). Spine loss in experimental epilepsy: quantitative light and electron microscopic analysis of intracellularly stained CA3 pyramidal cells in hippocampal slice cultures. Neuroscience *70*, 31–45.

Dudai, Y., Karni, A., and Born, J. (2015). The Consolidation and Transformation of Memory. Neuron *88*, 20–32.

Dunsmoor, J.E., and Paz, R. (2015). Fear generalization and anxiety: behavioral and neural mechanisms. Biol. Psychiatry.

Dunsmoor, J.E., Mitroff, S.R., and Labar, K.S. (2009). Generalization of conditioned fear along a dimension of increasing fear intensity. 460–469.

Durand, G.M., Kovalchuk, Y., and Konnerth, A. (1996). Long-term potentiation and functional synapse induction in developing hippocampus. Nat. Lett. *381*.

Dziembowska, M., and Wlodarczyk, J. (2012). MMP9: A novel function in synaptic plasticity. Int. J. Biochem. Cell Biol. *44*, 709–713.

Echeverry, R., Wu, J., Haile, W.B., Guzman, J., and Yepes, M. (2010). Tissue-type plasminogen activator is a neuroprotectant in the mouse hippocampus. J.Clin.Invest *120*, 2194–2205.

Ehrlich, I., Klein, M., Rumpel, S., and Malinow, R. (2007). PSD-95 is required for activity-driven synapse stabilization. Proc. Natl. Acad. Sci. *104*, 4176–4181.

El-Brolosy, M.A., and Stainier, D.Y.R. (2017). Genetic compensation: A phenomenon in search of mechanisms. PLoS Genet. *13*, 1–17.

Engert, F., and Bonhoeffer, T. (1999). Dendritic spine changes associated with hippocampal long-term synaptic plasticity. Nature *399*, 66–70.

Ennaceur, A., and Delacour, J. (1988). A new one - trial test for neurobiological studies of

memory in rats . 1 " Behavioral data. Behav. Brain Res. *31*, 47–59.

Ethell, I.M., and Pasquale, E.B. (2005). Molecular mechanisms of dendritic spine development and remodeling. Prog. Neurobiol. *75*, 161–205.

Fauth, M., and Tetzlaff, C. (2016). Opposing Effects of Neuronal Activity on Structural Plasticity. Front. Neuroanat. *10*, 1–18.

Felix-Ortiz, A.C., and Tye, K.M. (2014). Amygdala Inputs to the Ventral Hippocampus Bidirectionally Modulate Social Behavior. J. Neurosci. *34*, 586–595.

Ferreira, S.T., and Klein, W.L. (2011). The Aβ oligomer hypothesis for synapse failure and memory loss in Alzheimer's disease. Neurobiol. Learn. Mem. *96*, 529–543.

Ferrer-Ferrer, M., and Dityatev, A. (2018). Shaping Synapses by the Neural Extracellular Matrix. Front. Neuroanat. *12*, 1–16.

Fiala, J.C., Spacek, J., and Harris, K.M. (2002). Cause or Consequence of Neurological Disorders? Dendritic Spinen Pathol. *39*, 1–34.

Fifková, E., and Van Harreveld, A. (1977). Long-lasting morphological changes in dendritic spines of dentate granular cells following stimulation of the entorhinal area. J. Neurocytol. *6*, 211–230.

Fischer, S., and Born, J. (2009). Anticipated Reward Enhances Offline Learning During Sleep. J. Exp. Psychol. Learn. Mem. Cogn. *35*, 1586–1593.

Forrest, M.P., Parnell, E., and Penzes, P. (2018). Dendritic structural plasticity and neuropsychiatric disease. Nat. Rev. Neurosci. *19*, 215–234.

Foster, M., and Sherrington, C. S. (1897). *A Text-Book of Physiology. Part III: The Central Nervous System.* London: Macmillan.

Frischknecht, R., and Happel, M.F.K. (2016). Impact of the extracellular matrix on plasticity in juvenile and adult brains. E-Neuroforum *7*, 1–6.

Frischknecht, R., Fejtova, A., Viesti, M., Stephan, A., and Sonderegger, P. (2008). Cellular/Molecular Activity-Induced Synaptic Capture and Exocytosis of the Neuronal Serine Protease Neurotrypsin. J. Neurosci. *28*, 1568–1579.

Gautam, M., Noakes, P.G., Moscoso, L., Rupp, F., Scheller, R.H., Merlie, J.P., and Sanes, J.R. (1996). Defective neuromuscular synaptogenesis in agrin-deficient mutant mice. Cell *85*, 525–535.

Giachero, M., Calfa, G.D., and Molina, V.A. (2013). Contextual fear memory following stress and fear conditioning Hippocampal structural plasticity accompanies the resulting contextual fear memory following stress and fear conditioning. 611–616.

Giachero, M., Calfa, G.D., and Molina, V.A. (2015). Hippocampal dendritic spines remodeling and fear memory are modulated by GABAergic signaling within the basolateral amygdala

complex. Hippocampus *25*, 545–555.

Giannone, G., Mondin, M., Grillo-Bosch, D., Tessier, B., Saint-Michel, E., Czöndör, K., Sainlos, M., Choquet, D., and Thoumine, O. (2013). Neurexin-1β Binding to Neuroligin-1 Triggers the Preferential Recruitment of PSD-95 versus Gephyrin through Tyrosine Phosphorylation of Neuroligin-1. Cell Rep. *3*, 1996–2007.

Gisler, C., Uscher, D., Atzle, P.S., Urr, S., Baici, A., Galliciotti, G., Reif, R., Bolliger, M.F., Kunz, B., and Sonderegger, P. (2013). Zymogen activation of neurotrypsin and neurotrypsin-dependent agrin cleavage on the cell surface are enhanced by glycosaminoglycans. Biochem. J *453*, 83–100.

Glass, D.J., Bowen, D.C., Stitt, T.N., Radziejewski, C., Bruno, J.A., Ryan, T.E., Gies, D.R., Shah, S., Mattsson, K., Burden, S.J., et al. (1996). Agrin acts via a MuSK receptor complex. Cell *85*, 513–523.

Gogolla, N., Caroni, P., Lüthi, A., and Herry, C. (2009). Perineuronal nets protect fear memories from erasure. Science (80-.). *325*, 1258–1261.

Graves, L., Heller, E., Pack, A., and Abel, T. (2003). Sleep deprivation selectively impairs memory consolidation for contextual fear conditioning. Learn. Mem. *10*, 168–176.

Gschwend, T.P., Krueger, S.R., Kozlov, S. V., Wolfer, D.P., and Sonderegger, P. (1997). Gschwend et al (1997). Neurotrypsin a novel multidomain serine protease expressed in the nervous system. Mol Cell Neurosci. Mol. Cell. Neurosci. *9*, 207–219.

Gunaydin, L.A., Grosenick, L., Finkelstein, J.C., Kauvar, I. V., Fenno, L.E., Adhikari, A., Lammel, S., Mirzabekov, J.J., Airan, R.D., Zalocusky, K.A., et al. (2014). Natural neural projection dynamics underlying social behavior. Cell *157*, 1535–1551.

Gundelfinger, E.D., Frischknecht, R., Choquet, D., and Heine, M. (2010). Converting juvenile into adult plasticity: A role for the brain's extracellular matrix. Eur. J. Neurosci. *31*, 2156–2165.

Hall, C.S. (1934). Emotional Behavior in the Rat. J. Comp. Psychol. *18*, 385–403.

Halpain, S., Hipolito, A., and Saffer, L. (1998). Regulation of F-actin stability in dendritic spines by glutamate receptors and calcineurin. J. Neurosci. *18*, 9835–9844.

Hartmann, J., Wagner, K. V., Dedic, N., Marinescu, D., Scharf, S.H., Wang, X.D., Deussing, J.M., Hausch, F., Rein, T., Schmidt, U., et al. (2012). Fkbp52 heterozygosity alters behavioral, endocrine and neurogenetic parameters under basal and chronic stress conditions in mice. Psychoneuroendocrinology *37*, 2009–2021.

Harvey, C.D., Yasuda, R., Zhong, H., and Svoboda, K. (2008). The Spread of Ras Activity. Science (80-.). *321*, 136–140.

Hayashi-Takagi, A., Takaki, M., Graziane, N., Seshadri, S., Murdoch, H., Dunlop, A.J., Makino, Y., Seshadri, A.J., Ishizuka, K., Srivastava, D.P., et al. (2010). Disrupted-in-Schizophrenia 1 (DISC1) regulates spines of the glutamate synapse via Rac1. Nat. Neurosci. *13*, 327–332.

Hayashi-Takagi, A., Yagishita, S., Nakamura, M., Shirai, F., Wu, Y.I., Loshbaugh, A.L., Kuhlman, B., Hahn, K.M., and Kasai, H. (2015). Labelling and optical erasure of synaptic memory traces in the motor cortex. Nature *525*, 333–338.

Hebb, D.O. (1949). The Organization of Behavior; A Neuropsychological Theory. Am. J. Psychol. *63*, 633.

Hilgenberg, L.G.W., and Smith, M.A. (2004). Agrin signaling in cortical neurons is mediated by a tyrosine kinase-dependent increase in intracellular Ca2+ that engages both CaMKII and MAPK signal pathways. J. Neurobiol. *61*, 289–300.

Hilgenberg, L.G.W., Hoover, C.L., and Smith, M.A. Evidence of an Agrin Receptor in Cortical Neurons.

Hilgenberg, L.G.W., Su, H., Gu, H., O'Dowd, D.K., and Smith, M.A. (2006). α3Na+/K+-ATPase Is a Neuronal Receptor for Agrin. Cell.

Hill, T.C., and Zito, K. (2013). LTP-Induced Long-Term Stabilization of Individual Nascent Dendritic Spines. J. Neurosci. *33*, 678–686.

Hirata, A., Yoshida, S., Inoue, N., Matsumoto-Miyai, K., Ninomiya, A., Taniguchi, M., Matsuyama, T., Kato, K., Iizasa, H., Kataoka, Y., et al. (2001). Abnormalities of synapses and neurons in the hippocampus of neuropsin-deficient mice. Mol. Cell. Neurosci. *17*, 600–610.

Hisanaga, A., Morishita, S., Suzuki, K., Sasaki, K., Koie, M., Kohno, T., and Hattori, M. (2012). A disintegrin and metalloproteinase with thrombospondin motifs 4 (ADAMTS-4) cleaves Reelin in an isoform-dependent manner. FEBS Lett. *586*, 3349–3353.

Hlushchenko, I., Koskinen, M., and Hotulainen, P. (2016). Dendritic spine actin dynamics in neuronal maturation and synaptic plasticity. Cytoskeleton *73*, 435–441.

Hofer, S.B., Mrsic-Flogel, T.D., Bonhoeffer, T., and Hübener, M. (2009). Experience leaves a lasting structural trace in cortical circuits. Nature *457*, 313–317.

Holtmaat, A.J.G.D., Trachtenberg, J.T., Wilbrecht, L., Shepherd, G.M., Zhang, X., Knott, G.W., and Svoboda, K. (2005). Transient and persistent dendritic spines in the neocortex in vivo. Neuron *45*, 279–291.

Hong, W., Kim, D.-W., and Anderson, D.J. (2014). Antagonistic Control of Social versus Repetitive Self-Grooming Behaviors by Separable Amygdala Neuronal Subsets. Cell *158*, 1348–1361.

Honkura, N., Matsuzaki, M., Noguchi, J., Ellis-Davies, G.C.R., and Kasai, H. (2008). The Subspine Organization of Actin Fibers Regulates the Structure and Plasticity of Dendritic Spines. Neuron *57*, 719–729.

Hoover, C.L., Hilgenberg, L.G.W., and Smith, M.A. (2003). The COOH-terminal domain of agrin signals via a synaptic receptor in central nervous system neurons. J. Cell Biol. *692310*, 21–9525.

Hotulainen, P., and Hoogenraad, C.C. (2010). Actin in dendritic spines: Connecting dynamics to function. J. Cell Biol. *189*, 619–629.

Hruska, M., Henderson, N.T., Xia, N.L., Le Marchand, S.J., and Dalva, M.B. (2015). Anchoring and synaptic stability of PSD-95 is driven by ephrin-B3. Nat. Neurosci. *18*, 1594–1605.

Hsueh, Y.P., and Sheng, M. (1999). Regulated expression and subcellular localization of syndecan heparan sulfate proteoglycans and the syndecan-binding protein CASK/LIN-2 during rat brain development. J. Neurosci. *19*, 7415–7425.

Huang, Y.Y., Bach, M.E., Lipp, H.P., Zhuo, M., Wolfer, D.P., Hawkins, R.D., Schoonjans, L., Kandel, E.R., Godfraind, J.M., Mulligan, R., et al. (1996). Mice lacking the gene encoding tissue-type plasminogen activator show a selective interference with late-phase long-term potentiation in both Schaffer collateral and mossy fiber pathways. Proc. Natl. Acad. Sci. *93*, 8699–8704.

Iijima, N., Tanaka, M., Mitsui, S., Yamamura, Y., Yamaguchi, N., and Ibata, Y. (1999). Expression of a serine protease (motopsin PRSS12) mRNA in the mouse brain: In situ hybridization histochemical study. Mol. Brain Res. *66*, 141–149.

Inoue, A., Setoguchi, K., Matsubara, Y., Okada, K., Sato, N., Iwakura, Y., Higuchi, O., and Yamanashi, Y. (2009). Dok-7 activates the muscle receptor kinase MuSK and shapes synapse formation. Sci. Signal. *2*, 1–9.

Isaac, J.T.R., Nicoll, R.A., and Malenka, R.C. (1995). Evidence for silent synapses: Implications for the expression of LTP. Neuron *15*, 427–434.

Ishikawa, Y., Horii, Y., Tamura, H., and Shiosaka, S. (2008). Neuropsin (KLK8)-Dependent and -Independent Synaptic Tagging in the Schaffer-Collateral Pathway of Mouse Hippocampus. J. Neurosci. *28*, 843–849.

Jarosz-Griffiths, H.H., Noble, E., Rushworth, J. V., and Hooper, N.M. (2016). Amyloid-β receptors: The good, the bad, and the prion protein. J. Biol. Chem. *291*, 3174–3183.

Ji, R.R., Bose, C.M., Lesuisse, C., Qiu, D., Huang, J.C., Zhang, Q., and Rupp, F. (1998). Specific agrin isoforms induce cAMP response element binding protein phosphorylation in hippocampal neurons. J Neurosci *18*, 9695–9702.

Jin, S.X., Arai, J., Tian, X., Kumar-Singh, R., and Feig, L.A. (2013). Acquisition of contextual discrimination involves the appearance of a RAS-GRF1/p38 mitogen-activated protein (MAP) kinase-mediated signaling pathway that promotes long term potentiation (LTP). J. Biol. Chem. *288*, 21703–21713.

Johansen, J.P., Cain, C.K., Ostroff, L.E., and Ledoux, J.E. (2011). Molecular mechanisms of fear learning and memory. Cell *147*, 509–524.

Jones, E.G. (1994). Santiago Ram??n y Cajal and the croonian lecture, March 1894. Trends Neurosci. *17*, 192–193.

Jontes, J.D., and Smith, S.J. (2000). Filopodia, spines, and the generation of synaptic

diversity. Neuron *27*, 11–14.

Kaczmarek, L. (1993). Molecular biology of vertebrate learning: Is c???fos a new beginning? J. Neurosci. Res. *34*, 377–381.

Kaczmarek, L. (2016). MMP-9 in Control of Synaptic Plasticity : a Subjective Account. Opera Medica Physiol. *2*, 103–111.

Kaidanovich-Beilin, O., Lipina, T., Vukobradovic, I., Roder, J., and Woodgett, J.R. (2011). Assessment of Social Interaction Behaviors. J. Vis. Exp. *0*, 1–6.

Kandel, E.R. (2001). The molecular biology of memory storage: A dialogue between gene and synapses. Science (80-.). *294*, 1030–1038.

Kandel, E.R., Dudai, Y., and Mayford, M.R. (2014). Review The Molecular and Systems Biology of Memory. Cell *157*, 163–186.

Kasai, H., Hayama, T., Ishikawa, M., Watanabe, S., Yagishita, S., and Noguchi, J. (2010a). Learning rules and persistence of dendritic spines. Eur. J. Neurosci. *32*, 241–249.

Kasai, H., Fukuda, M., Watanabe, S., Hayashi-Takagi, A., and Noguchi, J. (2010b). Structural dynamics of dendritic spines in memory and cognition. Trends Neurosci. *33*, 121–129.

Kastellakis, G., Cai, D.J., Mednick, S.C., Silva, A.J., and Poirazi, P. (2015). Synaptic clustering within dendrites: An emerging theory of memory formation. Prog. Neurobiol. *126*, 19–35.

Kim, J., and Jung, M. (2006). Neural circuits and mechanisms involved in Pavlovian fear conditioning: A critical review. Neurosci Biobehav Rev. *30*, 188–202.

Kim, J.J., and Fanselow, M.S. (1992). Modalilty-specific retrograde amnesia of fear. Science (80-.). *256*, 675–677.

Kim, N., Stiegler, A.L., Cameron, T.O., Hallock, P.T., Gomez, A.M., Huang, J.H., Hubbard, S.R., Dustin, M.L., and Burden, S.J. (2008). Lrp4 Is a Receptor for Agrin and Forms a Complex with MuSK. Cell *135*, 334–342.

Kirov, S.A., and Harris, K.M. (1999). Dendrites are more spiny on mature hippocampal neurons when synapses are inactivated. Nat. Neurosci. *2*, 878–883.

Kirov, S.A., Goddard, C.A., and Harris, K.M. (2004). Age-dependence in the homeostatic upregulation of hippocampal dendritic spine number during blocked synaptic transmission. Neuropharmacology *47*, 640–648.

Kleindienst, T., Winnubst, J., Roth-Alpermann, C., Bonhoeffer, T., and Lohmann, C. (2011). Activity-dependent clustering of functional synaptic inputs on developing hippocampal dendrites. Neuron *72*, 1012–1024.

Knott, G.W., Holtmaat, A., Wilbrecht, L., Welker, E., and Svoboda, K. (2006). Spine growth precedes synapse formation in the adult neocortex in vivo. Nat. Neurosci. *9*, 1117–1124.

Kochlamazashvili, G., Henneberger, C., Bukalo, O., Dvoretskova, E., Senkov, O., Lievens, P.M., Westenbroek, R., Engel, A.K., Catterall, W.A., Rusakov, D.A., et al. (2010). The Extracellular Matrix Molecule Hyaluronic Acid Regulates Hippocampal Synaptic Plasticity by Modulating Postsynaptic L-Type Ca 2 + Channels. Neuron *67*, 116–128.

Kondratiuk, I., Łęski, S., Urbańska, M., Biecek, P., Devijver, H., Lechat, B., Van Leuven, F., Kaczmarek, L., and Jaworski, T. (2017). GSK-3β and MMP-9 Cooperate in the Control of Dendritic Spine Morphology. Mol Neurobiol *54*, 200–211.

Kornau, H.C., Schenker, L.T., Kennedy, M.B., and Seeburg, P.H. (1995). Domain interaction between NMDA receptor subunits and the postsynaptic density protein PDS-95. Science (80-.). *269*, 1737–1740.

Krafft, G.A., and Klein, W.L. (2010). ADDLs and the signaling web that leads to Alzheimer's disease. Neuropharmacology *59*, 230–242.

Kramár, E.A., Babayan, A.H., Gavin, C.F., Cox, C.D., Jafari, M., Gall, C.M., Rumbaugh, G., Lynch, G., and Richard Thompson, by F. (2012). Synaptic evidence for the efficacy of spaced learning. PNAS *109*, 5121–5126.

Kreiner, G. (2015). Compensatory mechanisms in genetic models of neurodegeneration: are the mice better than humans? Front. Cell. Neurosci. *9*, 1–6.

Krstic, D., Rodriguez, M., and Knuesel, I. (2012). Regulated Proteolytic Processing of Reelin through Interplay of Tissue Plasminogen Activator (tPA), ADAMTS-4, ADAMTS-5, and Their Modulators. PLoS One *7*, 1–11.

Kumar, S., Hultman, R., Hughes, D., Michel, N., Katz, B.M., and Dzirasa, K. (2014). Prefrontal cortex reactivity underlies trait vulnerability to chronic social defeat stress. Nat. Commun. *5*, 1–9.

Kummer, T.T., Misgeld, T., and Sanes, J.R. (2006). Assembly of the postsynaptic membrane at the neuromuscular junction: Paradigm lost. Curr. Opin. Neurobiol. *16*, 74–82.

Kuriyama, K., Stickgold, R., and Walker, M.P. (2004). Sleep-dependent learning and motor-skill complexity. Learn. Mem. *11*, 705–713.

Kwon, C.H., Luikart, B.W., Powell, C.M., Zhou, J., Matheny, S.A., Zhang, W., Li, Y., Baker, S.J., and Parada, L.F. (2006). Pten Regulates Neuronal Arborization and Social Interaction in Mice. Neuron *50*, 377–388.

Lacor, P.N. (2004). Synaptic Targeting by Alzheimer's-Related Amyloid Oligomers. J. Neurosci. *24*, 10191–10200.

Lai, W.-S. (2005). Recognition of Familiar Individuals in Golden Hamsters: A New Method and Functional Neuroanatomy. J. Neurosci. *25*, 11239–11247.

Lai, C.S.W., Franke, T.F., and Gan, W.-B. (2012). Opposite effects of fear conditioning and extinction on dendritic spine remodelling. Nature *482*.

Lavond, D.G., Kim, J.J., and Thompson, R.F. (1993). Mammalian brain substrates of aversive classical conditioning. Annu. Rev. Psychol *44*, 317–342.

Laxmi, T.R., Stork, O., and Pape, H.C. (2003). Generalisation of conditioned fear and its behavioural expression in mice. Behav. Brain Res. *145*, 89–98.

Leger, M., Quiedeville, A., Bouet, V., Haelewyn, B., Boulouard, M., Schumann-Bard, P., and Freret, T. (2013). Object recognition test in mice. Nat. Protoc. *8*, 2531–2537.

Liao, D., Hessler, N.A., and Malinow, R. (1995). Activation of postsynaptically silent synapses during pairing-induced LTP in CA1 region of hippocampal slice. Nat. Lett. *375*.

Lisman, J., Yasuda, R., and Raghavachari, S. (2012). Mechanisms of CaMKII action in long-term potentiation. Nat. Rev. Neurosci. *13*, 169–182.

Llinás, R.R. (2003). The contribution of Sntiago Ramon y Cajal to functional neuroscience.pdf. *4*, 2001–2004.

Lonskaya, I., Partridge, J., Lalchandani, R.R., Chung, A., Lee, T., Vicini, S., Hoe, H.S., Lim, S.T., and Conant, K. (2013). Soluble ICAM-5, a Product of Activity Dependent Proteolysis, Increases mEPSC Frequency and Dendritic Expression of GluA1. PLoS One *8*, 1–12.

Malenka, R.C., and Bear, M.F. (2004). LTP and LTD: An embarrassment of riches. Neuron *44*, 5–21.

Malenka, R.C., and Nicoll, R.A. (1999). Long-term potentiation - A decade of progress? Science (80-.). *285*, 1870–1874.

Maletic-Savatic, M., Malinow, R., and Svoboda, K. (1999). Rapid dendritic morphogenesis in CA1 hippocampal dendrites induced by synaptic activity. Science (80-.). *283*, 1923–1927.

Malinow, R., and Malenka, R.C. (2002). AMPA Receptor Trafficking and Synaptic Plasticity. Annu. Rev. Neurosci. *25*, 103–126.

Maren, S. (2001). Neurobiology of Pavlovian Fear Conditioning. Annu Rev Neurosci *24*, 897–931.

Maren, S., Phan, K.L., Liberzon, I., Health, M., Line, S., and Arbor, A. (2013). The contextual brain: implications for fear conditioning, extinction and psychopathology. Nat. Rev. Neurosci. *14*, 417–428.

Masana, M., Su, Y.A., Liebl, C., Wang, X.D., Jansen, L., Westerholz, S., Wagner, K. V., Labermaier, C., Scharf, S.H., Santarelli, S., et al. (2014). The stress-inducible actin-interacting protein DRR1 shapes social behavior. Psychoneuroendocrinology *48*, 98–110.

Mataga, N., Nagai, N., and Hensch, T.K. (2002). Permissive proteolytic activity for visual cortical plasticity. Proc. Natl. Acad. Sci. U. S. A. *99*, 7717–7721.

Matsumoto-Miyai, K., Ninomiya, A., Yamasaki, H., Tamura, H., Nakamura, Y., and Shiosaka, S. (2003). NMDA-dependent proteolysis of presynaptic adhesion molecule L1 in the

hippocampus by neuropsin. J. Neurosci. *23*, 7727–7736.

Matsumoto-Miyai, K., Sokolowska, E., Zurlinden, A., Gee, C.E., Lüscher, D., Hettwer, S., Wölfel, J., Ladner, A.P., Ster, J., Gerber, U., et al. (2009). Coincident Pre- and Postsynaptic Activation Induces Dendritic Filopodia via Neurotrypsin-Dependent Agrin Cleavage. Cell.

Matsuzaki, M., Ellis-davies, G.C.R., Nemoto, T., Miyashita, Y., Iino, M., and Kasai, H. (2001). Dendritic spine geometry is critical for AMPA receptor expression in hippocampal CA1 pyramidal neurons. Nat. Neurosci. *4*.

Matsuzaki, M., Honkura, N., Ellis-Davies, G.C.R., and Kasai, H. (2004). Structural basis of long-term potentiation in single dendritic spines. Nat. Lett. *429*.

McClure, C., Cole, K.L.H., Wulff, P., Klugmann, M., and Murray, A.J. (2011). Production and Titering of Recombinant Adeno-associated Viral Vectors. J. Vis. Exp. 5–10.

Mccroskery, S., Bailey, A., Lin, L., and Daniels, M.P. (2009). Transmembrane Agrin Regulates Dendritic Filopodia and Synapse Formation in Mature Hippocampal Neuron Cultures. Neuroscience *163*, 168–179.

McCroskery, S., Chaudhry, A., Lin, L., and Daniels, M.P. (2006). Transmembrane agrin regulates filopodia in rat hippocampal neurons in culture. Mol. Cell. Neurosci. *33*, 15–28.

Mendez, P., De Roo, M., Poglia, L., Klauser, P., and Muller, D. (2010). N-cadherin mediates plasticity-induced long-term spine stabilization. J. Cell Biol. *189*, 589–600.

Mendez, P., Stefanelli, T., Flores, C.E., Muller, D., and Lüscher, C. (2018). Homeostatic Plasticity in the Hippocampus Facilitates Memory Extinction. Cell Rep. *22*, 1451–1461.

Michaluk, P., Mikasova, L., Groc, L., Frischknecht, R., Choquet, D., and Kaczmarek, L. (2009). Matrix Metalloproteinase-9 Controls NMDA Receptor Surface Diffusion through Integrin 1 Signaling. J. Neurosci. *29*, 6007–6012.

Michaluk, P., Wawrzyniak, M., Alot, P., Szczot, M., Wyrembek, P., Mercik, K., Medvedev, N., Wilczek, E., De Roo, M., Zuschratter, W., et al. (2011). Influence of matrix metalloproteinase MMP-9 on dendritic spine morphology. J. Cell Sci. *124*, 3369–3380.

Minge, D., Senkov, O., Kaushik, R., Herde, M.K., Tikhobrazova, O., Wulff, A.B., Mironov, A., Van Kuppevelt, T.H., Oosterhof, A., Kochlamazashvili, G., et al. (2017). Heparan Sulfates Support Pyramidal Cell Excitability, Synaptic Plasticity, and Context Discrimination. Cereb. Cortex *27*, 903–918.

Misgeld, T., Kummer, T.T., Lichtman, J.W., and Sanes, J.R. (2005). Agrin promotes synaptic differentiation by counteracting an inhibitory effect of neurotransmitter. Proc. Natl. Acad. Sci. *102*, 11088–11093.

Mitsui, S., Osako, Y., Yokoi, F., Dang, M.T., Yuri, K., Li, Y., and Yamaguchi, N. (2009). A mental retardation gene, motopsin/neurotrypsin/prss12, modulates hippocampal function and social interaction. Eur. J. Neurosci.

Molinari, F., Rio, M., Virginia, M., Férechté, E.-R., Augé, J., Bacq, D., Briault, S., Vekemans, M., Munnich, A., Attié-Bitach, T., et al. (2002). Truncating Neurotrypsin Mutation in Autosomal Recessive Nonsyndromic Mental Retardation. Science (80-.). *298*.

Morellini, F., Lepsveridze, E., Kähler, B., Dityatev, A., and Schachner, M. (2007). Reduced reactivity to novelty, impaired social behavior, and enhanced basal synaptic excitatory activity in perforant path projections to the dentate gyrus in young adult mice deficient in the neural cell adhesion molecule CHL1. Mol. Cell. Neurosci. *34*, 121–136.

Morellini, F., Malyshev, A., Volgushev, M., Chistiakova, M., Papashvili, G., Fellini, L., Kleene, R., Schachner, M., and Dityatev, A. (2017). Impaired Fear Extinction Due to a Deficit in Ca2+ Influx Through L-Type Voltage-Gated Ca2+ Channels in Mice Deficient for Tenascin-C. Front. Integr. Neurosci. *11*, 1–10.

Moser, M.B., Trommald, M., and Andersen, P. (1994). An increase in dendritic spine density on hippocampal CA1 pyramidal cells following spatial learning in adult rats suggests the formation of new synapses. Proc. Natl. Acad. Sci. U. S. A. *91*, 12673–12675.

Moy, S.S., Nadler, J.J., Perez, A., Barbaro, R.P., Johns, J.M., Magnuson, T.R., Piven, J., and Crawley, J.N. (2004). Sociability and preference for social novelty in five inbred strains: An approach to assess autistic-like behavior in mice. Genes, Brain Behav. *3*, 287–302.

Muller, M., Gahwiler, B.H., Rietschin, L., and Thompson, S.M. (1993). Reversible loss of dendritic spines and altered excitability after chronic epilepsy in hippocampal slice cultures. Proc. Natl. Acad. Sci. *90*, 257–261.

Nägerl, U.V., Eberhorn, N., Cambridge, S.B., and Bonhoeffer, T. (2004). Bidirectional activity-dependent morphological plasticity in hippocampal neurons. Neuron *44*, 759–767.

Nägerl, U.V., Willig, K.I., Hein, B., Hell, S.W., and Bonhoeffer, T. (2008). Live-cell imaging of dendritic spines by STED microscopy. PNAS *105*, 18982–18987.

Nakahata, Y., and Yasuda, R. (2018). Plasticity of Spine Structure: Local Signaling, Translation and Cytoskeletal Reorganization. Front. Synaptic Neurosci. *10*, 1–13.

Nakayama, K. (2005). Diminished Neuronal Activity Increases Neuron-Neuron Connectivity Underlying Silent Synapse Formation and the Rapid Conversion of Silent to Functional Synapses. J. Neurosci. *25*, 4040–4051.

Nikonenko, I., Jourdain, P., and Muller, D. (2003). Presynaptic remodeling contributes to activity-dependent synaptogenesis. J. Neurosci. *23*, 8498–8505.

Nishijima, I., Yamagata, T., Spencer, C.M., Weeber, E.J., Alekseyenko, O., Sweatt, J.D., Momoi, M.Y., Ito, M., Armstrong, D.L., Nelson, D.L., et al. (2006). Secretin receptor-deficient mice exhibit impaired synaptic plasticity and social behavior. Hum. Mol. Genet. *15*, 3241–3250.

Nishimune, H. (2018). Practical Anatomy of the Neuromuscular junction in health and disease. *36*, 231–240.

Norris, E.H., and Strickland, S. (2007). Modulation of NR2B-regulated contextual fear in the hippocampus by the tissue plasminogen activator system. Proc. Natl. Acad. Sci. *104*, 13473–13478.

OConnor, L.T., Lauterborn, J.C., Smith, M.A., and Gall, C.M. (1995). Expression of Agrin Messenger-Rna Is Altered Following Seizures in Adult-Rat Brain. Mol. Brain Res. *33*, 277–287.

Oddo, S., Caccamo, A., Tran, L., Lambert, M.P., Glabe, C.G., Klein, W.L., and LaFerla, F.M. (2006). Temporal profile of amyloid-beta (Abeta) oligomerization in an in vivo model of Alzheimer disease: A link between Abeta and tau pathology. J. Biol. Chem. *281*, 1599–1604.

Oh, W.C., Hill, T.C., and Zito, K. (2012). Synapse-speci fi c and size-dependent mechanisms of spine structural plasticity accompanying synaptic weakening. PNAS *110*.

Ohnishi, T., Yanazawa, M., Sasahara, T., Kitamura, Y., Hiroaki, H., Fukazawa, Y., Kii, I., Nishiyama, T., Kakita, A., Takeda, H., et al. (2015). Na, K-ATPase α3 is a death target of Alzheimer patient amyloid-β assembly. Proc. Natl. Acad. Sci. *112*, E4465–E4474.

Okada, K., Inoue, A., Okada, M., Murata, Y., Kakuta, S., Jigami, T., Kubo, S., Shiraishi, H., Eguchi, K., Motomura, M., et al. (2006). The muscle protein Dok-7 is essential for neuromuscular synaptogenesis. Science (80-.). *312*, 1802–1805.

Okamoto, K., Nagai, T., Miyawaki, A., and Hayashi, Y. (2004). Rapid and persistent modulation of actin dynamics regulates postsynaptic reorganization underlying bidirectional plasticity. Nat. Neurosci. *7*, 1104–1112.

Oray, S., Majewska, A., and Sur, M. (2004). Dendritic spine dynamics are regulated by monocular deprivation and extracellular matrix degradation. Neuron *44*, 1021–1030.

Ostroff, L.E., Fiala, J.C., Allwardt, B., and Harris, K.M. (2002). Polyribosomes redistribute from dendritic shafts into spines with enlarged synapses during LTP in developing rat hippocampal slices. Neuron *35*, 535–545.

De Paola, V., Holtmaat, A., Knott, G., Song, S., Wilbrecht, L., Caroni, P., and Svoboda, K. (2006). Cell type-specific structural plasticity of axonal branches and boutons in the adult neocortex. Neuron *49*, 861–875.

Pavlov, I.P. (1927). Conditioned reflexes: an investigation of the physiological activity of the cerebral cortex. Oxford Univ. Press xv-430.

Pawlak, R., Nagai, N., Urano, T., Napiorkowska-Pawlak, D., Ihara, H., Takada, Y., Collen, D., and Takada, A. (2002). Rapid, specific and active site-catalyzed effect of tissue-plasminogen activator on hippocampus-dependent learning in mice. Neuroscience *113*, 995–1001.

Pawlak, R., Rao, B.S.S., Melchor, J.P., Chattarji, S., McEwen, B., and Strickland, S. (2005). Tissue plasminogen activator and plasminogen mediate stress-induced decline of neuronal and cognitive functions in the mouse hippocampus. Proc. Natl. Acad. Sci. *102*, 18201–18206.

Peng, S., Xu, J., Pelkey, K.A., Chandra, G., Zhang, Z., Bagh, M.B., Yuan, X., Wu, L.-G.,

Mcbain, C.J., and Mukherjee, A.B. (2015). Suppression of agrin-22 production and synaptic dysfunction in Cln1 À/À mice. Ann. Clin. Transl. Neurol. *2*, 1085–1104.

Petralia, R.S., Esteban, J.A., Wang, Y.X., Partridge, J.G., Zhao, H.M., Wenthold, R.J., and Malinow, R. (1999). Selective acquisition of AMPA receptors over postnatal development suggests a molecular basis for silent synapses. Nat. Neurosci. *2*, 31–36.

Petsophonsakul, P., Richetin, K., Andraini, T., Roybon, L., and Rampon, C. (2017). Memory formation orchestrates the wiring of adult-born hippocampal neurons into brain circuits. Brain Struct. Funct. *222*, 2585–2601.

Pignataro, A., Middei, S., Borreca, A., and Ammassari-Teule, M. (2013). Indistinguishable pattern of amygdala and hippocampus rewiring following tone or contextual fear conditioning in C57BL/6 mice. Front. Behav. Neurosci. *7*, 1–7.

Poulos, A.M., Mehta, N., Lu, B., Amir, D., Livingston, B., Santarelli, A., Zhuravka, I., and Fanselow, M.S. (2016). Conditioning- and time-dependent increases in context fear and generalization. Learn. Mem. *23*, 379–385.

Prut, L., and Belzung, C. (2003). The open field as a paradigm to measure the effects of drugs on anxiety-like behaviors: A review. Eur. J. Pharmacol. *463*, 3–33.

Qian, X., Riccio, A., Zhang, Y., and Ginty, D.D. (1998). Identification and characterization of novel substrates of Trk receptors in developing neurons. Neuron *21*, 1017–1029.

Rasool, S., Martinez-Coria, H., Wu, J.W., Laferla, F., and Glabe, C.G. (2013). Systemic vaccination with anti-oligomeric monoclonal antibodies improves cognitive function by reducing Aβ deposition and tau pathology in 3xTg-AD mice. J. Neurochem. *126*, 473–482.

Rauchs, G., Feyers, D., Landeau, B., Bastin, C., Luxen, A., Maquet, P., and Collette, F. (2011). Sleep Contributes to the Strengthening of Some Memories Over Others, Depending on Hippocampal Activity at Learning. J. Neurosci. *31*, 2563–2568.

Reif, R., Sales, S., Hettwer, S., Dreier, B., Gisler, C., Wölfel, J., Lüscher, D., Zurlinden, A., Stephan, A., Ahmed, S., et al. (2007). Specific cleavage of agrin by neurotrypsin, a synaptic protease linked to mental retardation. FASEB J. *21*, 3468–3478.

Reif, R., Sales, S., Dreier, B., Lüscher, D., Wölfel, J., Gisler, C., Baici, A., Kunz, B., and Sonderegger, P. (2008). Purification and enzymological characterization of murine neurotrypsin. Protein Expr. Purif.

Reinhard, N.R., Van Helden, S.F., Anthony, E.C., Yin, T., Wu, Y.I., Goedhart, J., Gadella, T.W.J., and Hordijk, P.L. (2016). Spatiotemporal analysis of RhoA/B/C activation in primary human endothelial cells. Sci. Rep. *6*, 1–16.

Ripley, B., Otto, S., Tiglio, K., Williams, M.E., and Ghosh, A. (2011). Regulation of synaptic stability by AMPA receptor reverse signaling. Proc. Natl. Acad. Sci. *108*, 367–372.

Roberts, T.F., Tschida, K. a, Klein, M.E., and Mooney, R. (2010). Rapid spine stabilization and synaptic enhancement at the onset of behavioural learning. Nature *463*, 948–952.

Rodriguez, A., Ehlenberger, D.B., Dickstein, D.L., Hof, P.R., and Wearne, S.L. (2008). Automated three-dimensional detection and shape classification of dendritic spines from fluorescence microscopy images. PLoS One *3*.

Roeleveld, N., and Zielhuis, G.A. (1997). The prevalence of mental retardation: a critical review of recent literature. Dev. Med. & Child Neurol. *39*, 125–132.

De Roo, M., Klauser, P., and Muller, D. (2008). LTP promotes a selective long-term stabilization and clustering of dendritic spines. PLoS Biol. *6*, 1850–1860.

Ropers, H.-H., and Hamel, B.C.J. (2005). X-linked mental retardation. Nat. Rev. Genet. *6*, 46–57.

Rossi, A., Kontarakis, Z., Gerri, C., Nolte, H., Hölper, S., Krüger, M., and Stainier, D.Y.R. (2015). Genetic compensation induced by deleterious mutations but not gene knockdowns. Nature *524*, 230–233.

Sabatini, B.L., Oertner, T.G., and Svoboda, K. (2002). The Life Cycle of Ca2+ Ions in Dendritic Spines. Neuron *33*, 439–452.

Sacktor, T.C. (2011). How does PKM zeta maintain long-term memory? Nat. Rev. Neurosci. *12*, 9–15.

Samson, A.L., and Medcalf, R.L. (2006). Tissue-Type Plasminogen Activator: A Multifaceted Modulator of Neurotransmission and Synaptic Plasticity. Neuron *50*, 673–678.

Sanders, J., Cowansage, K., Baumgartel, K., and Mayford, M. (2012). Elimination of Dendritic Spines with Long-Term Memory Is Specific to Active Circuits. J. Neurosci. *32*, 12570–12578.

Schafe, G.E., Nadel, N. V., Sullivan, G.M., Harris, A., and LeDoux, J.E. (1999). Memory Consolidation for Contextual and Auditory Fear Conditioning Is Dependent on Protein Synthesis, PKA, and MAP Kinase. Learn. Mem. *6*, 97–110.

Senkov, O., Sun, M., Weinhold, B., Gerardy-Schahn, R., Schachner, M., and Dityatev, A. (2006). Polysialylated Neural Cell Adhesion Molecule Is Involved in Induction of Long-Term Potentiation and Memory Acquisition and Consolidation in a Fear-Conditioning Paradigm. J. Neurosci. *26*, 10888–109898.

Shimizu, C., Yoshida, S., Kato, K., Momota, Y., Matsumoto, K., Shiosaka, T., Midorikawa, R., Kamachi, T., Kawabe, A., Shiosaka, S., et al. (1998). Characterization of Recombinant and Brain Neuropsin , a Plasticity-related Serine Characterization of Recombinant and Brain Neuropsin , a Plasticity-related Serine Protease *. *273*, 11189–11196.

Sigler, A., Oh, W.C., Imig, C., Altas, B., Kawabe, H., Cooper, B.H., Kwon, H.B., Rhee, J.S., and Brose, N. (2017). Formation and Maintenance of Functional Spines in the Absence of Presynaptic Glutamate Release. Neuron *94*, 304–311.e4.

Smith, C.D., and Scarf, D. (2017). Spacing repetitions over long timescales: A review and a reconsolidation explanation. Front. Psychol. *8*, 1–17.

Stawarski, M., Stefaniuk, M., Wlodarczyk, J., Heck, N., Huntley, G.W., and Arbuthnott, G.W. (2014). Matrix metalloproteinase-9 involvement in the structural plasticity of dendritic spines.

Stephan, A., Mateos, J.M., Kozlov, S. V, Cinelli, P., Kistler, A.D., Hettwer, S., Rülicke, T., Streit, P., Kunz, B., and Sonderegger, P. (2008). Neurotrypsin cleaves agrin locally at the synapse. FASEB J.

Stettler, D.D., Yamahachi, H., Li, W., Denk, W., and Gilbert, C.D. (2006). Axons and synaptic boutons are highly dynamic in adult visual cortex. Neuron *49*, 877–887.

Stromme, P. (2000). Aetiology in severe and mild mental retardation: a population-based study of Norwegian children. Dev. Med. Child Neurol. *42*, 76–86.

Szepesi, Z., Hosy, E., Ruszczycki, B., Bijata, M., Pyskaty, M., Bikbaev, A., Heine, M., Choquet, D., Kaczmarek, L., and Wlodarczyk, J. (2014). Synaptically released matrix metalloproteinase activity in control of structural plasticity and the cell surface distribution of GluA1-AMPA receptors. PLoS One *9*.

Takeuchi, T., Duszkiewicz, A.J., and Morris, R.G.M. (2013). The synaptic plasticity and memory hypothesis: encoding, storage and persistence. Philos. Trans. R. Soc. B Biol. Sci. *369*, 20130288–20130288.

Tamura, H., Ishikawa, Y., Hino, N., Maeda, M., Yoshida, S., Kaku, S., and Shiosaka, S. (2006). Neuropsin is essential for early processes of memory acquisition and Schaffer collateral long-term potentiation in adult mouse hippocampus in vivo. J. Physiol. *570*, 541–551.

Tamura, H., Kawata, M., Hamaguchi, S., Ishikawa, Y., and Shiosaka, S. (2012). Processing of Neuregulin-1 by Neuropsin Regulates GABAergic Neuron to Control Neural Plasticity of the Mouse Hippocampus. J. Neurosci. *32*, 12657–12672.

Tang, J., Wagner, S., Schachner, M., Dityatev, A., and Wotjak, C.T. (2003). Potentiation of amygdaloid and hippocampal auditory-evoked potentials in a discriminatory fear-conditioning task in mice as a function of tone pattern and context. Eur. J. Neurosci. *18*, 639–650.

Tauchi, R., Imagama, S., Natori, T., Ohgomori, T., Muramoto, A., Shinjo, R., Matsuyama, Y., Ishiguro, N., and Kadomatsu, K. (2012). The endogenous proteoglycan-degrading enzyme ADAMTS-4 promotes functional recovery after spinal cord injury. J. Neuroinflammation *9*, 53.

Tian, X., Kai, L., Hockberger, P.E., Wokosin, D.L., and Surmeier, D.J. (2010). MEF-2 regulates activity-dependent spine loss in striatopallidal medium spiny neurons. Mol. Cell. Neurosci. *44*, 94–108.

Tidow, H., Aperia, A., Nissen, P., Skou, J.C., Kaplan, J.H., Aizman, O., al., et, Miyakawa-Naito, A., al., et, Yuan, Z., et al. (2010a). How are ion pumps and agrin signaling integrated? Trends Biochem. Sci. *35*, 653–659.

Tokuoka, H., and Goda, Y. (2008). Activity-dependent coordination of presynaptic release probability and postsynaptic GluR2 abundance at single synapses. Proc. Natl. Acad. Sci. U. S. A. *105*, 14656–14661.

Toni, N., Buchs, P.A., Nikonenko, I., Bron, C.R., and Muller, D. (1999). LTP promotes formation of multiple spine synapses between a single axon terminal and a dendrite. Nature *402*, 421–425.

Tønnesen, J., Nadrigny, F., Willig, K.I., Wedlich-Söldner, R., and Nägerl, V. (2011). Two-Color STED Microscopy of Living Synapses Using A Single Laser-Beam Pair. Biophys. J. *101*, 2545–2552.

Tønnesen, J., Katona, G., Rózsa, B., and Nägerl, U.V. (2014). Spine neck plasticity regulates compartmentalization of synapses. Nat. Publ. Gr. *17*, 678–685.

Trommald, M., Hulleberg, G., and Andersen, P. (1996). Long term potentiation is associated with new excitatory spine synapses on rat dentate granule cells. Learn. Mem. *3218±228*, 736±749.

Tsilibary, E., Tzinia, A., Radenovic, L., Stamenkovic, V., Lebitko, T., Mucha, M., Pawlak, R., Frischknecht, R., and Kaczmarek, L. (2014). Chapter 6 – Neural ECM proteases in learning and synaptic plasticity. In Progress in Brain Research, pp. 135–157.

Vaillend, C. (2002). Mechanisms of Neuronal Hyperexcitability Caused by Partial Inhibition of Na+-K+-ATPases in the Rat CA1 Hippocampal Region. J. Neurophysiol. *88*, 2963–2978.

Vesa, J Hellsten , E Verkruyse, L. (1995). Mutations in the palmitoyl protein thiosterase gene causing infantile neuronal ceroid lipofuscinosis. Nat. Lett. *376*, 584–587.

Viola, K.L., and Klein, W.L. (2015). Amyloid β oligomers in Alzheimer's disease pathogenesis, treatment, and diagnosis. Acta Neuropathol. *129*, 183–206.

Vlachos, A., Helias, M., Becker, D., Diesmann, M., and Deller, T. (2013). NMDA-receptor inhibition increases spine stability of denervated mouse dentate granule cells and accelerates spine density recovery following entorhinal denervation in vitro. Neurobiol. Dis. *59*, 267–276.

Vogel-Ciernia, A., and Wood, M. (2015). Examining object location and object recognition memory in mice. Curr. Protoc. Neurosci. *69*, 1–22.

Volk, L.J., Bachman, J.L., Johnson, R., Yu, Y., and Huganir, R.L. (2013). PKM-ζ is not required for hippocampal synaptic plasticity, learning and memory. Nature *493*, 420–423.

Walker, M.P., and Stickgold, R. (2004). Sleep-dependent learning and memory consolidation. Neuron *44*, 121–133.

Walsh, R.N., and Cummins, R.A. (1976). The Open-Field. Psychol. Bull. *83*, 482–504.

Wang, X., Bozdagi, O., Nikitczuk, J.S., Zhai, Z.W., Zhou, Q., and Huntley, G.W. (2008a). Extracellular proteolysis by matrix metalloproteinase-9 drives dendritic spine enlargement and long-term potentiation coordinately. Proc. Natl. Acad. Sci. U. S. A. *105*, 19520–19525.

Wang, Y., Luo, W., and Reiser, G. (2008b). Trypsin and trypsin-like proteases in the brain: Proteolysis and cellular functions. Cell. Mol. Life Sci. *65*, 237–252.

Washbourne, P., Bennett, J.E., and McAllister, A.K. (2002). Rapid recruitment of NMDA receptor transport packets to nascent synapses. Nat. Neurosci. *5*, 751–759.

White, J.K., Gerdin, A.K., Karp, N.A., Ryder, E., Buljan, M., Bussell, J.N., Salisbury, J., Clare, S., Ingham, N.J., Podrini, C., et al. (2013). XGenome-wide generation and systematic phenotyping of knockout mice reveals new roles for many genes. Cell *154*.

Wiegert, J.S., and Oertner, T.G. (2013). Long-term depression triggers the selective elimination of weakly integrated synapses. Proc. Natl. Acad. Sci. *110*, E4510–E4519.

Winnubst, J., and Lohmann, C. (2012). Synaptic clustering during development and learning: the why, when, and how. Front. Mol. Neurosci. *5*, 1–9.

Wittenmayer, N., Korber, C., Liu, H., Kremer, T., Varoqueaux, F., Chapman, E.R., Brose, N., Kuner, T., and Dresbach, T. (2009). Postsynaptic Neuroligin1 regulates presynaptic maturation. Proc. Natl. Acad. Sci. *106*, 13564–13569.

Wlodarczyk, J., Mukhina, I., Kaczmarek, L., and Dityatev, A. (2011). Extracellular matrix molecules, their receptors, and secreted proteases in synaptic plasticity. Dev. Neurobiol. *71*, 1040–1053.

Wolfer, D.P., Lang, R., Cinelli, P., Madani, R., and Sonderegger, P. (2001). Wolfer et al (2001). Multiple roles of neurotrypsin in tissue morphogenesis and nervous system development suggested by the mRNA expression pattern. Mol Cell Neurosci. Mol. Cell. Neurosci. *18*, 407–433.

Xie, Z., Srivastava, D.P., Photowala, H., Kai, L., Cahill, M.E., Woolfrey, K.M., Shum, C.Y., Surmeier, D.J., and Penzes, P. (2007). Kalirin-7 Controls Activity-Dependent Structural and Functional Plasticity of Dendritic Spines. Neuron *56*, 640–656.

Xiong, B., Li, A., Lou, Y., Chen, S., Long, B., Peng, J., Yang, Z., Xu, T., Yang, X., Li, X., et al. (2017). Precise Cerebral Vascular Atlas in Stereotaxic Coordinates of Whole Mouse Brain. Front. Neuroanat. *11*, 1–17.

Xu, T., Yu, X., Perlik, A.J., Tobin, W.F., Zweig, J.A., Tennant, K., Jones, T., and Zuo, Y. (2009). Rapid formation and selective stabilization of synapses for enduring motor memories. Nature *462*, 915–919.

Yamagata, Y., Kobayashi, S., Umeda, T., Inoue, A., Sakagami, H., Fukaya, M., Watanabe, M., Hatanaka, N., Totsuka, M., Yagi, T., et al. (2009). Kinase-Dead Knock-In Mouse Reveals an Essential Role of Kinase Activity of Ca2+/Calmodulin-Dependent Protein Kinase II in Dendritic Spine Enlargement, Long-Term Potentiation, and Learning. J. Neurosci. *29*, 7607–7618.

Yang, G., Feng, P., and Wen-Biao, G. (2009). Stably maintained dendritic spines are associated with lifelong memories. Nature *45*, 1031–1041.

Yu, X., Wang, G., Gilmore, A., Yee, A.X., Li, X., Xu, T., Smith, S.J., Chen, L., and Zuo, Y. (2013). Accelerated Experience-Dependent Pruning of Cortical Synapses in Ephrin-A2 Knockout Mice. Neuron *80*, 64–71.

Yuste, R., and Bonhoeffer, T. (2001). Morphological changes in dendritic spines associated with long-term synaptic plasticity. Annu. Rev. Neurosci *24*, 1071–1089.

Yuste, R., and Bonhoeffer, T. (2004). Genesis of dendritic spines: insights from ultrastructural and imaging studies. Nat. Rev. Neurosci. *5*, 24–34.

Zhou, Q., Homma, K.J., and Poo, M. (2004). Shrinkage of Dendritic Spines Associated with Long-Term Depression of Hippocampal Synapses. Neuron *44*, 749–757.

Zielinski, K. (2006). Jerzy Konorski on brainassociations. 1–16.

Zimprich, A., Niessing, J., Cohen, L., Garrett, L., Einicke, J., Sperling, B., Schmidt, M. V., and Hölter, S.M. (2017). Assessing Sociability, Social Memory, and Pup Retrieval in Mice. Curr. Protoc. Mouse Biol. *7*, 287–305.

Zito, K., Scheuss, V., Knott, G., Hill, T., and Svoboda, K. (2009). Rapid Functional Maturation of Nascent Dendritic Spines. Neuron *61*, 247–258.

Ziv, N.E., and Smith, S.J. (1996). Evidence for a role of dendritic filopodia in synaptogenesis and spine formation. Neuron *17*, 91–102.

ANNEX

EHRENERKLÄRUNG – DECLARATION OF HONOR

Ich versichere hiermit, dass ich die vorliegende Arbeit ohne unzulässige Hilfe Dritter und ohne Benutzung anderer als der angegebenen Hilfsmittel angefertigt habe; verwendete fremde und eigene Quellen sind als solche kenntlich gemacht.

Ich habe insbesondere nicht wissentlich:

• Ergebnisse erfunden oder widersprüchlich Ergebnisse verschwiegen,

• statistische Verfahren absichtlich missbraucht, um Daten in ungerechtfertigter Weise zu interpretieren,

• fremde Ergebnisse oder Veröffentlichungen plagiiert,

• fremde Forschungsergebnisse verzerrt wiedergegeben.

Mir ist bekannt, dass Verstöße gegen das Urheberrecht Unterlassungs- und Schadensersatzansprüche des Urhebers sowie eine strafrechtliche Ahndung durch die Strafverfolgungsbehörden begründen kann.

Ich erkläre mich damit einverstanden, dass die Arbeit ggf. mit Mitteln der elektronischen Datenverarbeitung auf Plagiate überprüft werden kann.

Die Arbeit wurde bisher weder im Inland noch im Ausland in gleicher oder ähnlicher Form als Dissertation eingereicht und ist als Ganzes auch noch nicht veröffentlicht.

Magdeburg, 01.10.2018

……

Maura Ferrer Ferrer